MASTER IN BIOLOGY

Role of TLR2 in the induction of inflammation in the context of cutaneous fungal infection

VAN der GUCHT, Marine

Award date:
2024

Awarding institution:
University of Namur

Faculté des Sciences

ROLE OF TLR2 IN THE INDUCTION OF INFLAMMATION IN THE CONTEXT OF CUTANEOUS FUNGAL INFECTION

Mémoire présenté pour l'obtention
du grade académique de master 120 en biochimie et biologie moléculaire et cellulaire

Marine VAN DER GUCHT
Janvier 2024

Université de Namur
FACULTE DES SCIENCES
Secrétariat du Département de Biologie
Rue de Bruxelles 61 - 5000 NAMUR
Téléphone: + 32(0)81.72.44.18 - Téléfax: + 32(0)81.72.44.20
E-mail: joelle.jonet@unamur.be - http://www.unamur.be

Role of TLR2 in the induction of inflammation in the context of cutaneous fungal infection

VAN DER GUCHT Marine

Abstract

Malassezia spp. are commensal fungi, normally colonizing the human skin, which sometimes become involved in skin disorders, like pityriasis versicolor (PV). Dermatophytes are strictly pathogenic fungi responsible for dermatophytosis. During PV or dermatophytosis, filamentous fungal structures named hyphae invade the cornified layer of the epidermis while inflammatory responses are induced in host cells. Models of infection by *Malassezia furfur* or by *Trichophyton benhamiae* on Reconstructed Human Epidermis (RHE) have been described as representative of *in vivo* fungal invasion and skin inflammation. During infection, keratinocytes are the first cell type encountered by developing fungal hyphae and reacts through the secretion of pro-inflammatory factors and antimicrobial peptides as players of innate immunity. However, how keratinocytes perceive the presence of fungi and respond is still unknown. The *Toll-like receptor 2* (TLR2) basally expressed in keratinocytes has been reported being able to recognize fungal motives like phospholipomannan in *Candida albicans*. This work aims to better characterize the precise role of TLR2 expressed by keratinocytes when recognizing *Malassezia* and dermatophyte fungal motives, and how TLR2 induces inflammatory responses during infection.

For this purpose, TLR2$^{-/-}$-N/TERT-keratinocytes have been previously generated in our lab using the CRISPR/Cas9 method. As a first step, the procedures of infection by *M. furfur* and *T. benhamiae* were adapted for RHE made of N/TERT-keratinocytes (N/TERT-RHE). Indeed, weaker barrier function is observed in N/TERT-RHE in comparison with RHE reconstructed with primary keratinocytes (primary RHE), on which the infection procedure was originally established. Unexpectedly, we observed that *M. furfur* does not easily infect N/TERT-RHE in comparison to primary RHE, requiring a longer incubation period and an increased lipid supply. Regarding *T. benhamiae*, the development of infection appeared similar in N/TERT-RHE and in primary RHE. In a second step, RHE reconstructed with unedited TLR2$^{+/+}$-N/TERT-keratinocytes (TLR2$^{+/+}$-RHE) or from TLR2$^{-/-}$-N/TERT-keratinocytes (TLR2$^{-/-}$-RHE) were infected by *T. benhamiae*. No difference was observed in the infection process between TLR2$^{+/+}$- and TLR2$^{-/-}$-RHE. Some decrease in the expression or release of tested markers were sometimes observed but no clear difference was observed in the signaling pathways activated following *T. benhamiae* infection between TLR2$^{+/+}$-RHE and TLR2$^{-/-}$-RHE. Overall, our results suggest that, in addition to TLR2, other receptors also appear involved in the recognition of *T. benhamiae* and in the induction of inflammatory responses.

Mémoire de master 120 en biochimie et biologie moléculaire et cellulaire
Janvier 2024
Promoter: Y. Poumay
Co-promoter: C. Lambert de Rouvroit

Université de Namur
FACULTE DES SCIENCES
Secrétariat du Département de Biologie
Rue de Bruxelles 61 - 5000 NAMUR
Téléphone: + 32(0)81.72.44.18 - Téléfax: + 32(0)81.72.44.20
E-mail: joelle.jonet@unamur.be - http://www.unamur.be

Rôle du TLR2 dans l'induction de l'inflammation dans le contexte d'une infection fongique cutanée

VAN DER GUCHT Marine

Résumé

Les *Malassezia spp.* sont des champignons commensaux, colonisant normalement la peau humaine, qui sont parfois impliqués dans des troubles cutanés, comme le pityriasis versicolor (PV). Les dermatophytes sont des champignons strictement pathogènes responsables de la dermatophytose. Au cours du PV ou de la dermatophytose, des structures fongiques filamenteuses appelées hyphes envahissent la couche cornée de l'épiderme tandis que des réponses inflammatoires sont induites dans les cellules de l'hôte. Des modèles d'infection par *Malassezia furfur* ou par *Trichophyton benhamiae* sur épiderme humain reconstruit (RHE) ont été décrits comme étant représentatifs de l'invasion fongique et de l'inflammation cutanée *in vivo*. Au cours de l'infection, les kératinocytes sont le premier type de cellules rencontrées par les hyphes fongiques en développement et réagissent par la sécrétion de facteurs pro-inflammatoires et de peptides antimicrobiens en tant qu'acteurs de l'immunité innée. Cependant, la manière dont les kératinocytes perçoivent la présence de champignons et y répondent est encore inconnue. Le récepteur Toll-like 2 (TLR2) exprimé de façon basale dans les kératinocytes est capable de reconnaître les motifs fongiques tels que le phospholipomannane de *Candida albicans*. Ce travail vise à mieux caractériser le rôle précis du TLR2 exprimé par les kératinocytes lors de la reconnaissance des motifs fongiques des *Malassezia* et des dermatophytes, et comment le TLR2 induit une réponse inflammatoire au cours de l'infection.

A cette fin, des kératinocytes N/TERT-TLR2$^{-/-}$ ont été générés dans notre laboratoire en utilisant la méthode du CRISPR/Cas9. Dans un premier temps, les procédures d'infection par *M. furfur* et *T. benhamiae* ont été adaptées aux RHE constitués de kératinocytes N/TERT (RHE-N/TERT). En effet, une plus faible fonction de barrière est observée dans les RHE-N/TERT par rapport aux RHE reconstruits avec des kératinocytes primaires (RHE primaires), sur lesquels la procédure d'infection a été établie à l'origine. De manière inattendue, nous avons observé que *M. furfur* n'infecte pas facilement les RHE-N/TERT par rapport aux RHE primaires, nécessitant une période d'incubation plus longue et un apport accru en lipides. En ce qui concerne *T. benhamiae*, le développement de l'infection semblait similaire dans les RHE-N/TERT et dans les RHE primaires. Dans un deuxième temps, des RHE reconstruits avec des kératinocytes N/TERT- TLR2$^{+/+}$ non modifiés (RHE-TLR2$^{+/+}$) ou à partir de kératinocytes N/TERT- TLR2$^{-/-}$ (RHE-TLR2$^{-/-}$) ont été infectés par *T. benhamiae*. Aucune différence n'a été observée dans le processus d'infection entre les RHE-TLR2$^{+/+}$ et les RHE-TLR2$^{-/-}$. Une certaine diminution de l'expression ou de la libération des marqueurs testés a parfois été observée, mais aucune différence claire n'a été observée dans les voies de signalisation activées après l'infection par *T. benhamiae* entre les RHE-TLR2$^{+/+}$ et les RHE-TLR2$^{-/-}$. Dans l'ensemble, nos résultats suggèrent qu'en plus du TLR2, d'autres récepteurs semblent également impliqués dans la reconnaissance de *T. benhamiae* et dans l'induction de réponses inflammatoires.

Mémoire de master 120 en biochimie et biologie moléculaire et cellulaire
Janvier 2024
Promoteur : Y. Poumay
Co-promotrice : C. Lambert de Rouvroit

Acknowledgments

First of all, I'd like to thank my promoter, Professor Yves Poumay, for welcoming me and integrating me into his team for the duration of my master thesis, as well as for his kindness, his availability, his essential help for the research project, his great kindness and the time he devoted to correcting my master thesis.

I would also like to thank my co-promoter, Professor Catherine Lambert de Rouvroit, for her immense kindness, availability and help in advancing this research project.

Many thanks to my two tutors, Emilie Faway and Bastien Tirtiaux, for having integrated me so well into their team, but also for their kindness, their unfailing patience, their invaluable help and above all for the time they devoted to correcting my master thesis and learning the various techniques used in the laboratory.

I'd also like to thank the entire LabCeTi team, as well as the LNR team, for making me feel so welcome in the laboratory, and for their daily good humor, offering an outstanding working atmosphere and conviviality.

I would also like to thank the technologists Kathleen De Swert, Valérie De Glas and Valéry Bielarz for their kindness, availability, and daily help in carrying out my manipulations.

Finally, I'd like to thank my parents and my brother for their unfailing support and encouragement. In particular, I'd like to thank my boyfriend for his emotional and affective support, which was so important throughout the difficult process of writing my master thesis. Finally, I'd like to thank my friend Louise for her support, help and all the fun we've had together over the last three years at university, without whom I'd have given up studying a long time ago.

List of abbreviations

ABC transporter	ATP Binding Cassette transporter
AhR	Aryl hydrocarbon Receptor
AMP	Antimicrobial peptide
ANOVA	Analysis Of Variance
AP-1	Activating protein-1
BCCM	Belgian Coordinated Collections of Microorganisms
BD	β-defensin
BSA	Bovine Serum Albumin
C. albicans	*Candida albicans*
cDNA	Complementary DNA
CFU	Colony-Forming Unit
CLR	C-type Lectin Receptor
CO_2	Carbon dioxide
Cq	Quantification cycle
CTL	Control
D	Day
DAMP	Damage-Associated Molecular Pattern
DNA	Deoxyribonucleic acid
e.g.	exempli gratia
EGFR	Epithelial Growth Factor Receptor
ELISA	Enzyme-Linked Immunosorbent Assay
EphA2	Ephrin type-A receptor 2
ERK	Extracellular signal-regulated kinase
FBS	Fetal Bovine Serum
hBD2	Human β-defensin
HE	Hematoxylin Eosin
hIL-1α	Human Interleukin-1α
hIL-1β	Human Interleukin-1β
HKGS	Human Keratinocyte Growth Supplement
HRP	Horseradish peroxidase
hRPLP0	Human Ribosomal Protein Lateral Stalk Subunit P0
hS100A7	Human S100 calcium binding protein A7
hTERT	Human Telomerase Reverse Transcriptase
i.e.	id est
ICAM1	InterCellular Adhesion Molecule 1
IgE	Immunoglobuline E
IgG	Immunoglobuline G
IKK	Inhibitor of nuclear factor-kappa B kinase
IL	Interleukin
IRAK4	Interleukin1 Receptor Associated Kinase 4
IRF5	Interferon Regulatory factor 5
IκB	Inhibitor of nuclear factor kappa B
JNK	c-Jun N-terminal Kinase

KBM-2	Keratinocyte Basal Medium
KGF	Keratinocyte Growth Factor
KGM-2	Keratinocyte Growth Medium
M. furfur	*Malassezia furfur*
MAPK	Mitogen-Activated Protein Kinase
MgSAP1	Aspartyl protease 1
MgSOD	Manganese-dependent Superoxide Dismutase
MHC	Major Histocompatibility Complex
MyD88	Myeloid Differenciation factor 88
NF-κB	Nuclear Factor-kappa B
N/TERT	Newborn/Telomerase Reverse Transcriptase
O.O.	Olive Oil
p-ERK	Phosphorylated Extracellular signal-regulated kinase
p-IkBα	Phosphorylated Inhibitor of nuclear factor kappa B
p-JNK	Phosphorylated c-Jun N-terminal Kinase
p-P38	Phosphorylated mitogen-activated protein kinase
P16 INK4a	Inhibitor of cyclin-dependent kinase 4
P38	Mitogen-activated protein kinase
PAMP	Pathogen-Associated Molecular Pattern
PAS	Periodic-Acid Schiff
PBS	Phosphate Buffered Saline
PDA	Potato Extract Glucose
pH	Potential of Hydrogen
pRB	Retinoblastoma protein
PRR	Pattern Recognition Receptor
PV	Pityriasis Versicolor
PVDF	Polyvinylidene fluoride
Ref	Reference
RHE	Reconstructed Human Epidermis
RNA	Ribonucleic acid
RPL13A	Ribosomal Protein L 13A
RPM	Revolutions Per Minute
RT-qPCR	Real Time-quantitative Polymerase Chain Reaction
S. cerevisiae	*Saccharomyces cerevisiae*
SB	Stratum Basale
SC	Stratum Corneum
SG	Stratum Granulosum
SS	Stratum Spinosum
STAT6	Signal Transducer and Activator of Transcription 6
T. benhamiae	*Trichophyton benhamiae*
TAB	TAK-Binding Protein
TAK1	Transforming growth factor beta-activated Kinase 1

TEER	Trans-Epithelial Electrical Resistance
TIR	Toll/IL-1R
TIRAP	Tir domain containing Adaptor Protein
TLR	Toll-Like Receptor
TLR2	Toll-Like Receptor 2
TNFα	Tumor Necrosis Factor
TRAF	Tumor necrosis factor receptor-Associated Factor
UV	Ultra-Violet

Table of contents

Table of figures

Table of tables

Table of annexes

1. Introduction

1.1. The human skin

The skin is the largest organ of our body and acts as a barrier to protect the host from environmental aggression, such as pathogens, UV light, chemical and mechanical damages, or from excessive water loss. The skin is also involved in temperature regulation. The skin is made of three overlayed tissues, that are different in structure and functions, named from bottom to the top hypodermis, dermis and epidermis. Epithelial tissues of the skin also include appendages, corresponding to hairs and nails in humans, and glands (sebaceous and sweat). Blood vessels, nerves and nerve endings are also present (Figure 1) [1],[2].

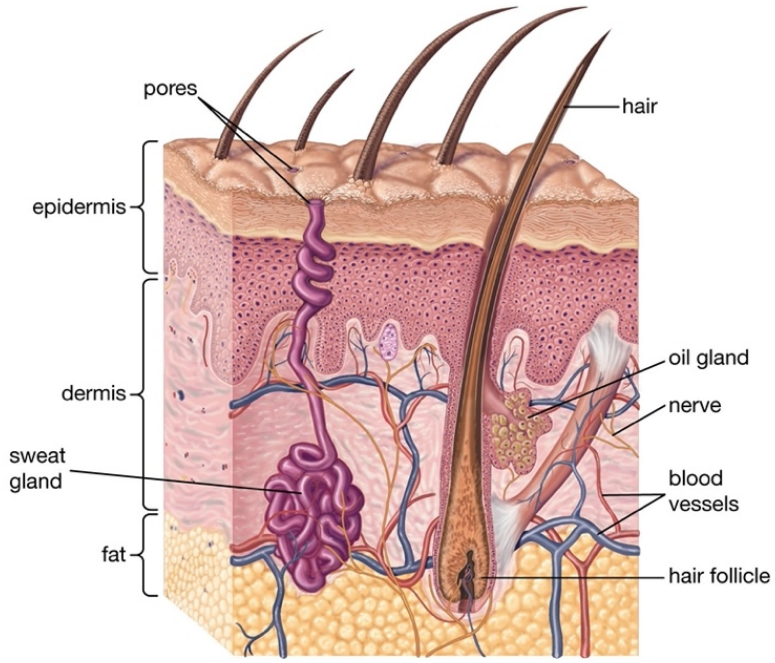

Figure 1: Schematic representation of the skin structure [3]. The skin is composed of three layers: the epidermis, the dermis and the hypodermis (the fat layer). Appendages are the phanera (hair) and the glands.

1.1.1. The hypodermis

The hypodermis is the deepest tissue, mainly made up of loose connective/adipose tissue which forms large pockets that isolate and protect the skin. The hypodermis corresponds to the so-called "subcutaneous fat" involved in thermoregulation, and in protection against external trauma [4],[5].

1.1.2. The dermis

The dermis is located below the epidermis, above the hypodermis. An essential role of the dermis is to provide nutrients to the epidermis, but it also ensures thermoregulation and contributes to eventual healing of the skin. In addition, the dermis provides the skin with support, suppleness, and elasticity. The dermis contains hair follicles with sebaceous and sweat glands, as well as sensory neurons and blood vessels [1]. The sebaceous gland is responsible

for synthesis and secretion of sebum. Sweat glands produce sweat and play an essential role in thermoregulation by secretion of sweat through the skin's pores to cool down body's temperature when necessary (Figure 1) [2],[6]. Blood vessels are also found in the dermis, providing oxygen and nutrients to dermal, as well as epidermal cells (Figure 1) [4]. Blood vessels are also critical in the event of infection, as they enable the transport of immune cells attracted by chemotaxis to inflammatory areas triggered when some infection occurs. Recruited immune cells then take part in the fight against pathogens [7]. Finally, the dermis contains different kinds of nerve endings responsible for the cutaneous sensation of pain, heat and cold (Figure 1) [1]. From a cellular point of view, fibroblasts, which ensure the structural integrity of the dermis by secreting collagen and elastin, are mainly found in the dermis as well as their derivatives such as fibrocytes, and myofibroblasts. Dermal dendritic (antigen-presenting) cells and other immune cells such as macrophages, lymphocytes and mast cells are also found in the dermis [8],[4]. The dermal extracellular matrix is mainly made of type I and type III collagen fibers, providing the skin with tensile strength and mechanical resistance, whilst hyaluronic acid and proteoglycans compose the ground substance [5],[8],[9].

1.1.3. The epidermis

The epidermis is the most superficial layer of the skin and is mainly composed of epithelial cells, named keratinocytes, organized into four different layers, corresponding to different stages of proliferation and differentiation of keratinocytes: the basal, spinous, granular and cornified layers [2],[10]. The basal layer is the deepest layer of the epidermis where keratinocytes are anchored to the basement membrane through hemidesmosomes. In this layer, cubic and undifferentiated keratinocytes follow the cell cycle to ensure proliferation and thereby homeostatic maintenance of the keratinocyte population in the epidermis. Keratinocytes generated in excess at the end of mitosis then push cells upwards to progressively migrate and reach the upper epidermal layers [1],[2],[11]. Indeed, daughter cells move into the spinous layer and initiate the differentiation process called keratinization. Keratinocytes of the spinous layer then harbor a polyhedric morphology with outward projections, allowing contact with neighboring cells through desmosomes [1]. In the granular layer, keratinocytes appear more flat and exhibit keratohyalin granules containing a filaggrin precursor, as well as lamellar bodies containing glycolipids [1]. Keratinocytes in the granular layer also establish intercellular tight junctions that create a barrier between epithelial cells [12]. Finally, keratinocytes reach the cornified layer. This layer is the upper layer of the epidermis, and is composed exclusively of fully keratinized dead keratinocytes, sometimes named corneocytes [1],[2]. These cells have gone through apoptosis and loss of their nucleus, while being filled with keratin intermediate filaments aggregated by filaggrin. Corneocytes are strongly attached to one another through corneodesmosomes and are embedded in a lipid matrix released by lamellar bodies exocytosis [1],[2]. At the epidermal surface, corneocytes will finally detach from the epidermis during a process called desquamation (Figure 2). This loss of keratinocytes is constantly compensated by the proliferation of basal keratinocytes, which then take an average of three weeks to fully differentiate in normal skin [2],[11].

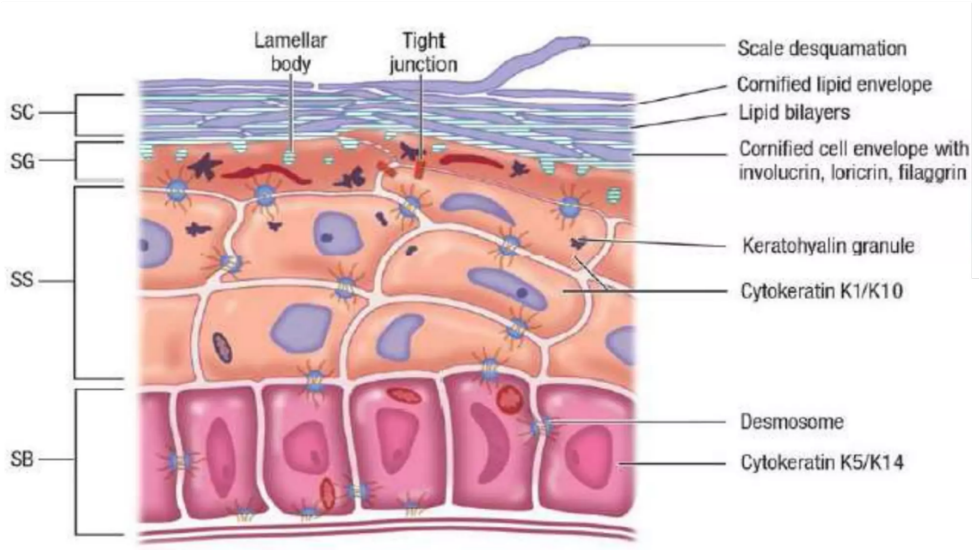

Figure 2: Structure of the epidermis and differentiation of keratinocytes [13]. Basal keratinocyte amplifying cells progressively differentiate through the different layers of the epidermis to the epidermal surface. In the terminal stage, keratinocytes lose their nuclei and flatten out, forming corneocytes. Corneocytes are finally detached from the epidermis during desquamation. SB: basal layer, SS: spinous layer, SG: granular layer, SC: cornified layer.

Each layer is characterized morphologically, indicating its state of differentiation [11]. During their differentiation, keratinocytes produce keratin and basophilic granulations appear in their cytoplasm, which can be identified in the granular layer where the markers of the terminal differentiation of the epidermis appear [2]. Indeed, each layer of the epidermis is characterized by differentiation markers. Basal cells express cytokeratins 5 and 14, while the spinous layer is characterized by cytokeratins 1 and 10 (Figure 2) [14]. As previously mentioned, cells in the granular layer synthesize keratohyalin granules, which are mainly constituted of profilaggrin and loricrin. Finally, in the cornified layer, profilaggrin is transformed into filaggrin. In addition to filaggrin, the cornified layer is made up of cytokeratins 1 and 10, loricrin and involucrin (Figure 2) [15].

Besides keratinocytes, other cell types are found in the epidermis such as melanocytes, Merkel cells and Langerhans cells. Melanocytes, located in the basal layer, produce melanin responsible for skin pigmentation and protection of nuclear DNA against UV radiation [1]. Merkel cells are also found in the basal layer where they act as mechanoreceptors for prolonged light touch, interacting with free nerve endings when they secrete serotonin neurotransmitter [1]. Langerhans cells are located mainly in suprabasal layers of the epidermis and belong to the innate immune system [16]. Indeed, these antigen-presenting dendritic cells exert surveillance inside the epidermis. By expression of major histocompatibility complexes (MHC) class I and II, activated Langerhans cells migrate outward the epidermis to encounter adaptive immune cells in lymph nodes [1].

1.2. The epidermal barrier

The main function of the epidermis is to provide a strong barrier to protect the host from the external environment but also to prevent excessive water loss. Various actors and processes are involved in the establishment of an efficient epidermal barrier.

1.2.1. The physical barrier

The cornified layer of the epidermis is the first layer of the skin to come into contact with external aggressors. For this reason, the cornified layer has an important physical barrier function. Indeed, the cells of the cornified layer, named corneocytes, are surrounded by lipids which are linked to keratin filaments that occupy the intracellular spaces of the corneocyte, allowing these cells to participate in the physical barrier by reinforcing the efficacy of the cornified layer [17],[18]. This layer therefore acts as an outer barrier to prevent the entry of foreign substances and microorganisms, but it further acts as an inner barrier to prevent water loss from the body [19]. Moreover, the presence of tight junctions in the granular layer also contributes to the epidermal barrier function. These junctions form an unbroken intercellular barrier between epithelial cells, allowing them to maintain the separation between tissue spaces and selectively regulating movements of solutes across the epidermis [12].

1.2.2. The immunological barrier

Besides their involvement in physical barrier, keratinocytes also exhibit immunological activities. Indeed, keratinocytes can act as antigen-presenting cells and express only class I histocompatibility surface antigens in the normal state, and certain adhesion molecules such as ICAM1. However, in certain pathological circumstances, they can also express class II antigens like immunocompetent cells [20]. Keratinocytes are also able to respond to the presence of pathogens by secreting pro-inflammatory cytokines (e.g. IL-1, IL-8, IL-6, TNFα) as well as antimicrobial peptides (e.g. BD2, BD3, S100A7) [2]. Indeed, antimicrobial peptides (AMPs) are the main classes of biomolecules involved in skin defense by disrupting bacterial membranes and in the modulation of host immune responses by recruiting immune cells [4],[21]. AMPs can be constitutively expressed or induced as a result of cellular activation responding to an inflammatory context or homeostatic stimulation [4]. Moreover, lipids such as sphingolipids, glucosylceramides and phospholipids, which are the precursors of lipids organized in the cornified layer, exhibit antimicrobial activity [4],[21].

1.2.3. The chemical barrier

As previously mentioned, sebaceous and sweat glands are associated to the epidermis as appendages and produced sweat and sebum which are involved in the formation of a hydrolipidic film. This hydrolipidic film reinforce the barrier function of the cornified layer and make the skin virtually impermeable to water [2]. Indeed, the hydrolipidic film protects the skin from penetration of foreign substances, external aggression and dehydration [22].

1.2.4. The microbiome

The last component of the epidermal barrier is the cutaneous microbiome, which is composed by various commensal microorganisms, including bacteria, viruses and fungi. They colonize the skin surface and appendages shortly after birth and provide a barrier against the colonization

by pathogenic micro-organisms. The microbiome also performs other functions, such as modulating host gene expression, including innate immune response genes and genes involved in cytokine activity, and also promotes homeostatic immunity [4]. Bacteria are the major components of the microbiome, followed respectively by viruses and fungi [4]. The main commensal bacteria found in the microbiome are *Staphylococcus epidermidis* and *Proprionibacterium acnes*. Commensal bacteria can protect the host by competing with other microorganisms for space and nutrients, thereby preventing colonization of the skin by pathogens. However, some commensal bacteria can also directly inhibit the growth of pathogenic strains by secreting antimicrobial agents, such as bacteriocins [4].

The fungal community is not as diverse as the bacterial one within the microbiome, the predominant commensal fungus being *Malassezia spp*. [23], representing more than 90% of the eukaryotic components of the skin microbiome. Being lipophilic yeasts, *Malassezia* are mainly found on sebaceous sites, such as the scalp, face, chest and upper back, and in a lower abundance on the trunk and arms (Figure 3) [4],[24].

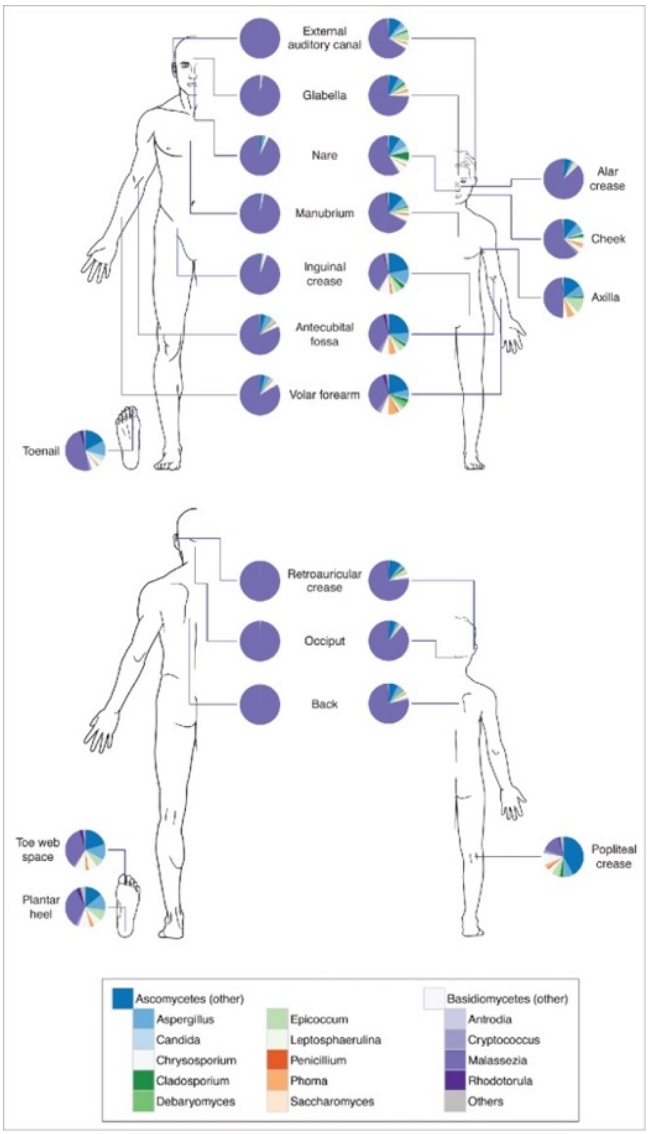

Figure 3: Distribution of fungal communities on various skin sites in adults (left) and children (right) [24]. The predominant fungus in the scalp, face, chest and upper back is *Malassezia spp.* The feet are populated among other by *Aspergillus spp.*, *Cryptococcus spp.*, *Rhodotorula spp.* and *Epicoccum spp.*

Generally, commensal microorganisms colonize the skin without causing disease, some of them being even beneficial to the skin (mutualistic microorganisms). Indeed, hosts have evolved in symbiosis with their commensal microorganisms, resulting in a mutualistic relationship and a hemostatic equilibrium, enabling commensal microorganisms to survive in their host. Such a relationship requires the proper functioning of the host's immune system to prevent commensal microorganisms from over-utilizing the host's resources, while maintaining immune tolerance to innocuous stimuli. Therefore, commensal microorganisms colonizing the host rapidly after birth are able to modulate the innate and adaptive immune system, enabling them to survive without being eliminated by the host [25]. However, in response to changes in the skin microenvironment or dysbiosis, some commensal micro-organisms, such as *Malassezia spp.*, can take advantage of a barrier disruption and may become pathogenic. On the other side, pathogenic micro-organisms, for example dermatophytes, are able to disrupt the epidermal barrier. In both case, proliferation and invasion by these microorganisms lead to skin damages.

1.3. *Malassezia spp.* and associated diseases

1.3.1. *Malassezia spp.* are opportunistic pathogens

Malassezia spp. are basidiomycete yeasts that have been described as budding yeasts [26],[27]. They are yeasts of ovoid, ellipsoid or cylindrical shape and are found in association with warm-blooded vertebrates, taking part in the skin microbiome [26]. To date, twenty species of the genus have been identified. Among them, eleven have been found colonizing humans with some discrepancies in species abundance depending on body sites and countries [24]. In general, *Malassezia globosa* and *Malassezia restricta*, followed by *Malassezia sympodialis* and *Malassezia furfur*, are the most frequently observed species on the human skin. Lacking fatty acid synthase, *Malassezia* are lipophilic, meaning they need an exogenous source of lipids to grow. This is why *Malassezia* develop on our skin in sebum-rich regions as previously mentioned [28]. Although *Malassezia* are mainly found on the skin, these yeasts are also present in smaller quantities in internal organs such as the intestine and the central nervous system [27],[28]. The abundance of *Malassezia* on the skin varies throughout life and is highly related to the sebaceous gland activity. Indeed, *Malassezia* colonization of the skin occurs directly after birth, when the neonatal sebaceous glands are active as a consequence of hormonal stimulation by the mother. Three to six months after birth, the sebaceous glands are dormant and the concentration of *Malassezia* decreases. *Malassezia*'s population increases later in life, with the onset of puberty, due to the activation of sebaceous glands, leading to increased levels of lipid production [24]. Therefore, *Malassezia* are predominant in adults while in children under fourteen years old, *Malassezia* is present but in lower abundance and with a more diverse fungal community (Figure 3) [24].

Malassezia yeasts are surrounded by a thick and multilamellar cell wall representing 26% to 37% of the total cell volume [29]. It allows the fungus to protect itself against osmotic pressure changes but also to interact with its environment and to adhere to cells and tissues. Thus, the integrity and therefore the viability of this fungus is ensured by the stability and rigidity of its cell wall. Although composition of this wall remains poorly studied, it is known being formed around a core of glucans and chitin and being mainly composed of sugars (70%), lipids (15 to 20%), proteins, representing a minor (10%) part [30],[31]. More specifically, it has been demonstrated by a study performed on *M. restricta*, that chitin, chitosan as well as β-(1,3)-glucans and β-(1,6)-glucans are essential components of the cell wall [30].

Malassezia undergoes asexual reproduction by monopolar or unipolar broad-based budding. The bud formed is then separated from the mother cell by a septum and the successive scars generated by the division form a small collar (Figure 4) [26],[32]. Sexual reproduction has never been observed, although genes known to be involved in sexual reproduction have been recently identified [26].

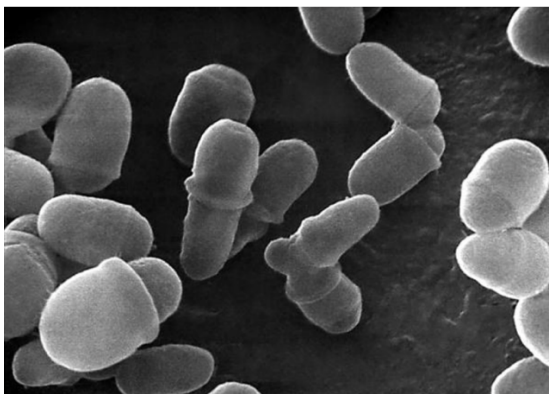

Figure 4: Reproduction of *Malassezia* by budding [32]. The bud formed is separated from the mother cell by a septum and the successive scars generated by the division form a small collar.

Malassezia are dimorphic fungi, which means that they exist in two forms. Indeed, besides their yeast form, as described above, they can also exhibit a mycelial form, i.e. they can exist in the form of ramified and filiform hyphae [33]. The yeast form is predominant and is usually associated with healthy skin, while the mycelial form is observed only in some skin lesions [26]. It is in the 1970s that it was understood that these two morphologies were actually from the same yeast when *in vitro* experiments showed the ability of this yeast to produce hyphae [33],[34]. Hyphae are an important virulence factor of *Malassezia*, since infection by *Malassezia* is caused by the modification of their yeast form into hyphae [35]. However, hyphae also expand to non-lesional skin, promoting the growth of *Malassezia* [27].

1.3.2. Shift from commensal to pathogen and *Malassezia spp.* associated diseases

As previously mentioned, *Malassezia* exist on the skin as a commensal. More recently, *Malassezia* has also been described as a mutualist. Notably, *M. globosa* species has been shown to secrete aspartyl protease 1 (MgSAP1), which hydrolyzes *Staphylococcus aureus* biofilms, protecting the skin from this potentially pathogenic bacteria [36]. However, in some cases, *Malassezia* themselves may become pathogenic and thereby involved in various skin disorders, ranging from non- or mildly inflammatory pathologies, such as pityriasis versicolor or seborrheic dermatitis and dandruff, to more severe inflammatory skin pathologies, such as *Malassezia* folliculitis and atopic dermatitis, explaining why *Malassezia* are described as opportunistic yeasts [37]. Indeed, following changes in the physical and metabolic properties of skin environment, *Malassezia* can shift from commensal to pathogenic state and become implicated in these pathologies [28]. Several host factors drive such dysbiosis, like the host genome, environmental conditions (temperature, humidity and UV), lifestyle, hygiene, or the host immune system [37],[38]. In addition, this shift may result from alterations in the skin's microenvironment, such as sebum production, sweat, skin pH, epidermal barrier integrity, immune responses or variations in the microbiome [39]. Therefore, *Malassezia* can be the direct cause of these pathologies, like in pityriasis versicolor, or they may only be involved in and benefit from changes in the skin environment, as this is likely the case in atopic dermatitis [40].

In addition, *Malassezia* have recently been shown to be associated with Crohn's disease, pancreatic ductal adenocarcinoma, and pulmonary aggravation of cystic fibrosis but won't be investigated as outside of the scope of this study [41]. Interestingly, *Malassezia* can also be involved in systemic infections. For example, it is known that *Malassezia* can colonize and form biofilms on catheters used for parenteral nutrition, leading to bloodstream infections in immunocompromised patients [38].

1.3.2.1. Pityriasis versicolor

Pityriasis versicolor (PV) is a skin disorder characterized by pigmentation defaults and mid-itching. *Malassezia* have been demonstrated as causal agents as hyphae invade the cornified layer of the patient's epidermis [27]. Among all the skin disorders for which *Malassezia* is potentially involved, this is the only one where hyphae have been observed. It has also been shown that this invasion by hyphae is not limited to the injured skin [27]. PV lesions can appear in a variety of hues, ranging from pink or tan to dark brown or even black and is characterized by hypo- or hyperpigmented patches covered with fine scales, which are mainly found on the seborrheic areas of the skin surface, namely the back, chest and neck (Figure 5 a) [27]. In most cases, the lesions typically appear as macules or papules but in more severe instances, they may become confluent. Although some patients experience mild itching, PV is generally asymptomatic, and the main inconvenience for patients is their physical appearance [42]. Histologically, the cornified layer is invaded by *Malassezia* hyphae. Mild to moderate hyperkeratosis and some acanthosis may be observed. Additionally, mild superficial perivascular inflammatory cellular infiltrate may be found in the dermis depending on the extent of the inflammation [27]. This inflammatory infiltrate is mainly composed of lymphocytes but also of histiocytes and sometimes plasma cells (Figure 5 b) [27].

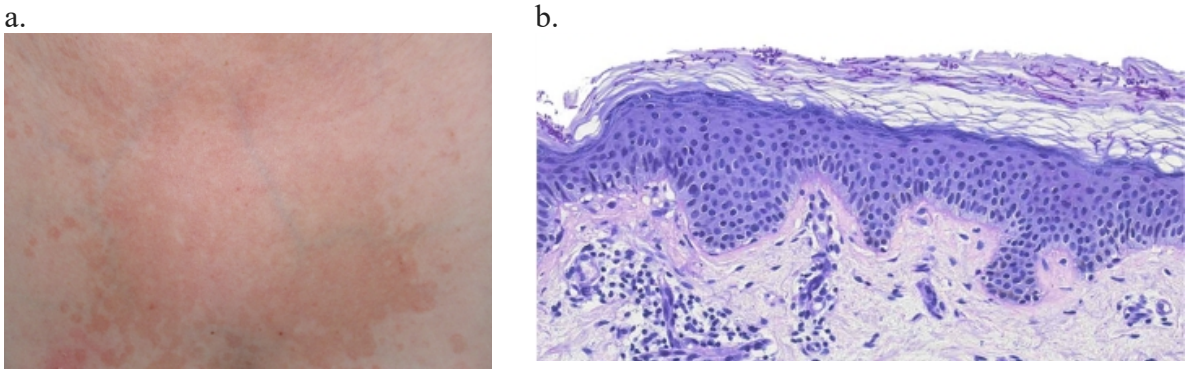

Figure 5: Pityriasis versicolor in a 42-year-old female patient [27]. PV causes hyperpigmented patches covered with fine scales (a). Infiltration of the hyperkeratotic cornified layer by *Malassezia* yeasts and hyphae is observed, as well as a moderate infiltrate of perivascular inflammatory cells in the upper dermis (b).

PV occurs in all age groups, but environmental factors, such as temperature and humidity, the immune status of the patient, as well as genetic predisposition may contribute to the onset of the disease [27],[43],[44]. Indeed, the prevalence of PV is particularly high in tropical and subtropical countries, and immunosuppressed patients are more likely to develop PV [42],[45]. Moreover, certain endogenous factors also favor the development of PV, such as malnutrition, use of oral contraceptives, use of systemic corticosteroids or immunosuppressants, and hyperhidrosis. The application of cream can also encourage the development of lesions [42].

1.3.2.2. Dandruff and seborrheic dermatitis

Dandruff and seborrheic dermatitis are two related pathologies. Dandruff is the less severe form, characterized by non-inflammatory desquamation, while seborrheic dermatitis is the more severe form, characterized by inflammatory desquamation [46]. A study on alterations for the skin microbiome in patients with dandruff and seborrheic dermatitis demonstrated an increase in the amount of *M. restricta* and *M. globosa* in patients with these pathologies, and highlighted the link between *Malassezia* and an increase in itch score and disease severity, suggesting the involvement of this fungus [47].

Dandruff is a frequent but still poorly characterized pathology that affects the scalp. It is mainly characterized by desquamation, while inflammation is minimal or even non-existent, as previously mentioned. *M. globosa* and *M. restricta* have been identified as the predominant species present on the scalp of dandruff sufferers. However, it has never been clearly demonstrated that *Malassezia* is the causative agent of dandruff, but it has been shown that dandruff diminishes after antifungal therapy, suggesting the involvement of *Malassezia* in this pathology [27]. It also seems that in the case of dandruff, the permeability barrier function of the skin is compromised by the irritating effect of free fatty acids and squalene peroxides produced by *Malassezia* lipases due to its nutritional requirements [46]. Indeed, oleic acid, a fatty acid released by *Malassezia* as a result of sebum consumption and degradation, has been shown to induce desquamation in dandruff-sensitive patients. Although the difference between those sensitive to dandruff and those who are not is unclear, there are factors that aggravate dandruff, such as physical factors, nutritional disorders, medication, neurotransmitter abnormalities and immunodeficiency [48].

Seborrheic dermatitis is an inflammatory dermatosis characterized by frequent erythema and scaling with absence of seborrhea (Figure 6) [27],[49]. It is a recurrent pathology that usually affects seborrheic areas of the skin, such as the scalp, eyebrows, paranasal folds, chest, back, axillae, and genitalia [27]. Therefore, the prevalence of seborrheic dermatitis is higher when the sebaceous glands are highly active, i.e. during the first 3 months of life and puberty. Surprisingly, seborrheic dermatitis also affects patients after the age of 50, despite a decrease of sebum excretion. This may be due to a change in sebum composition in these people as a result of degradation of the sebaceous glands in old age, leading to skin dryness, lack of radiance, xerosis, roughness, desquamation and pruritus [50],[51].

Figure 6: Seborrheic dermatitis in the nasolabial folds [27]. Severe seborrheic dermatitis meaning that the disease extends to the parietal region and is associated with strong erythema and scaling.

The specific role of *Malassezia* in seborrheic dermatitis is not yet known. However, this skin disorders is thought to result from an inflammatory reaction to *Malassezia* [52]. Indeed, it seems that the ability of *Malassezia* to modify the local immune response as well as to produce secondary metabolites (indolic metabolites) is involved in the initiation and maintenance of

seborrheic dermatitis [27]. It has also been suggested that *Malassezia*'s involvement in seborrheic dermatitis results from the release of irritant fatty acids derived from the breakdown of sebaceous lipids [53]. Moreover, proteases secreted by *Malassezia* have been shown to promote inflammation [54].

1.3.2.3. Malassezia folliculitis

Although the pathogenesis of *Malassezia* folliculitis is still misunderstood, it is known that it results from a proliferation of *Malassezia* yeasts of the normal skin flora following follicle occlusion or disruption of normal skin flora, such as immunosuppression and the use of antibiotics [55]. It has also been shown that the release of irritant fatty acids from the degradation of sebaceous lipids by *Malassezia* appears to be involved in *Malassezia* folliculitis. [53]. The main symptom of *Malassezia* folliculitis is pruritus and is mainly found in the upper trunk, i.e., shoulders, back and chest, where we can observe greasy and monomorphic follicular papules (Figure 7 a) [27]. The predominance of this pathology is higher in warm and humid regions [27]. Histology reveals dilated and partially destroyed hair follicles containing keratin, debris and sometimes mucin. The affected follicle is also usually encapsulated by a mild to moderate chronic inflammatory cellular infiltrate. Indeed, a high neutrophil amount can be seen in the infundibulum, along with a perifollicular lymphohistiocytic neutrophilic infiltrate [55]. Yeasts are mainly found in the infundibulum of sebaceous glands, where they feed on the lipids contained in sebum [55]. *Malassezia* can be seen as spherical or oval yeasts (Figure 7 b,c). However, hyphae are not observed in this condition [27],[56].

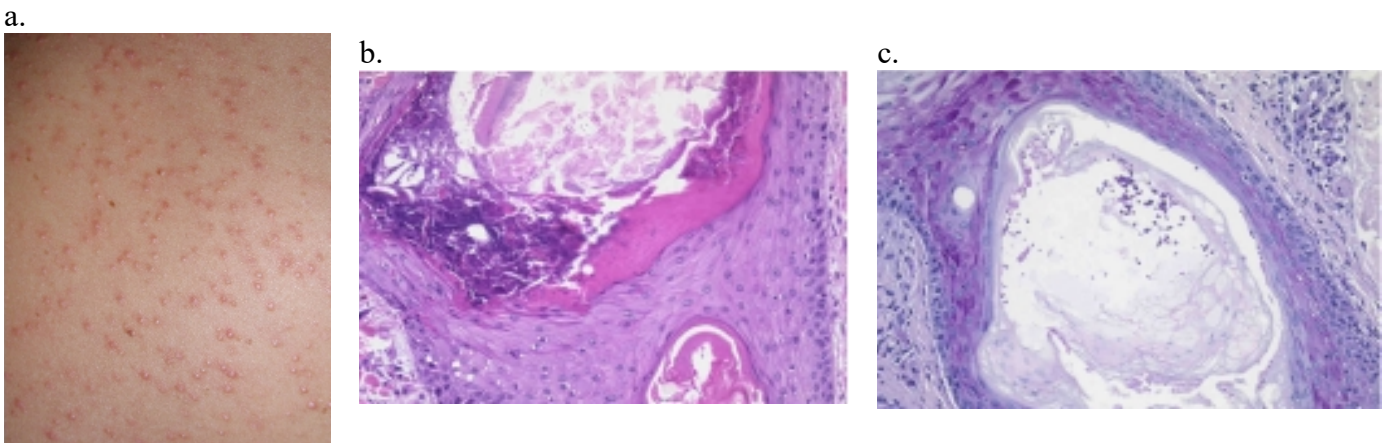

Figure 7: *Malassezia* folliculitis on the back of a 34-year-old man [27]. Greasy and monomorphic follicular papules are observed on the skin of the back (a). Dilated hair follicle filled with keratinous material and basophilic debris. Yeasts are observable within the infundibular lumen adjacent to the site of wall destruction (b). Numerous yeasts are observable within the dilated follicle lumen (c).

1.3.2.4. Atopic dermatitis

Atopic dermatitis is a frequently encountered chronic skin inflammatory disorder. This pathology mainly affecting children, is responsible for a skin eczema causing strong itching. The prevalence of this condition has increased 2 to 3 times over the last 30 years, currently affecting 15-20% of children and 1-3% of adults worldwide [57]. However, the pathogenesis of atopic dermatitis is still not fully understood. Nevertheless, it has been demonstrated that the factors driving dysbiosis are a common chronic pruritic skin condition and a loss of skin barrier integrity, leading to an alteration of the epidermal barrier function and causing a significant

transepidermal water loss, increased pH and changes in the lipid profile, disrupting the *Malassezia* metabolic niche [28],[40],[58],[59]. It has also been suggested that proteases secreted by *Malassezia* promote inflammation in atopic dermatitis [54]. In this condition, *Malassezia* does not appear to be the causative agent but takes advantage of changes in the skin environment. Indeed, the decreased barrier function, associated with a decrease in antimicrobial peptides secretion, favors the proliferation and the invasion of microbes such as *Malassezia* [60],[61]. This yeast can more easily interact with host cells (e.g. keratinocytes, dendritic cells) through membrane surface receptors such as TLR2, as suggested by Glatz M. *et al* in their review, leading to the secretion of pro-inflammatory molecules. Additionally, the increased skin pH favors the release of allergens by *Malassezia* that can also interact with immune cells. Indeed, *Malassezia* induces IgE production through dendritic cells and T cell-mediated B cell activation. These antibodies produced may also contribute to inflammation of the affected skin through mast cells. This inflammation may be maintained by the cross-reaction of autoreactive T cells between fungi and MgSOD (manganese-dependent superoxide dismutase) (Figure 8) [40].

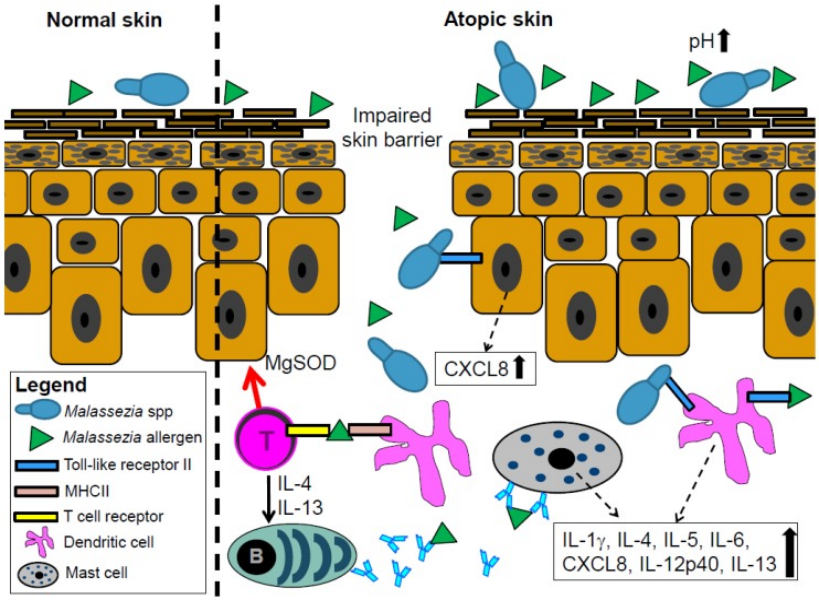

Figure 8: *Malassezia* contribution to skin inflammation in patients with atopic dermatitis [40]. *Malassezia* take advantage of the altered epidermal barrier to infiltrate the skin, where it can interact with TLR2 on keratinocytes and dendritic cells, triggering the release of pro-inflammatory cytokines. *Malassezia*-induced IgE production also contributes to inflammation, which is sustained by the cross-reactivity of autoreactive T cells between *Malassezia* and MgSOD.

1.4. Dermatophytes and associated disease

1.4.1. Dermatophytes are pathogenic fungi

Dermatophytes are part of the phylum *ascomycetes* and are pathogenic filamentous fungi [62],[63],[64]. Dermatophytes are divided into three genus: *Trichophyton, Microsporum* and *Epidermophyton* [65]. In addition, these fungi are classified into three ecological groups based on their natural host specificity: geophilic (rarely pathogenic to humans and animals, but potentially carried by animals), zoophilic (species whose natural host is a specific animal but can be transmitted to other animals, including humans), and anthropophilic (species infecting exclusively humans) [64]. Dermatophytes are keratinophilic fungi, i.e. they are adapted to digest keratin and use it as a source of nutrients [63]. As for *Malassezia spp.*, dermatophyte

cells are surrounded by a cell wall composed of chitin, β-glucans, mannans and galactomannans, serving to give the cell its mechanical strength, shape and rigidity. This cell wall is also involved in adhesion between fungi themselves, and between fungi and host cells [66].

Unlike *Malassezia*, dermatophytes naturally grow as hyphae. These hyphae are composed of interconnected fungal cells aligned and surrounded by an unbroken cell wall. Septa frequently divide these hyphae and are of the same cell wall composition. Additionally, small pores are found on these septa that allow a communication between the cytoplasm of adjacent cell compartments throughout the hyphae [67]. As most fungi, an important feature of dermatophytes is their ability to release spores in the environment. Indeed, when conditions become unfavorable, hyphae lead to the formation and release of spores. Unlike hyphae which are active, spores are dormant unicellular elements characterized by reduced metabolic activity. Spores have high mechanical strength, thanks to their thicker cell wall than hyphae. They also have a high concentration of lipids and glycogen, which function as an energy reserve for possible reactivation. These characteristics enable spores to be physiologically adapted to being dispersed in the environment and to surviving in extreme conditions. Then, when environmental conditions become optimal, the spores reactivate and germinate to give rise to new hyphae. Finally, hyphae develop, become filamentous, septate and branch out to form the mycelium. Two types of spores can be produced by hyphae: conidia and arthroconidia [67]. Conidia are formed by lateral or terminal budding of the hypha while arthroconidia are formed by fragmentation of hyphae (Figure 9 a,b) [66].

a. b.

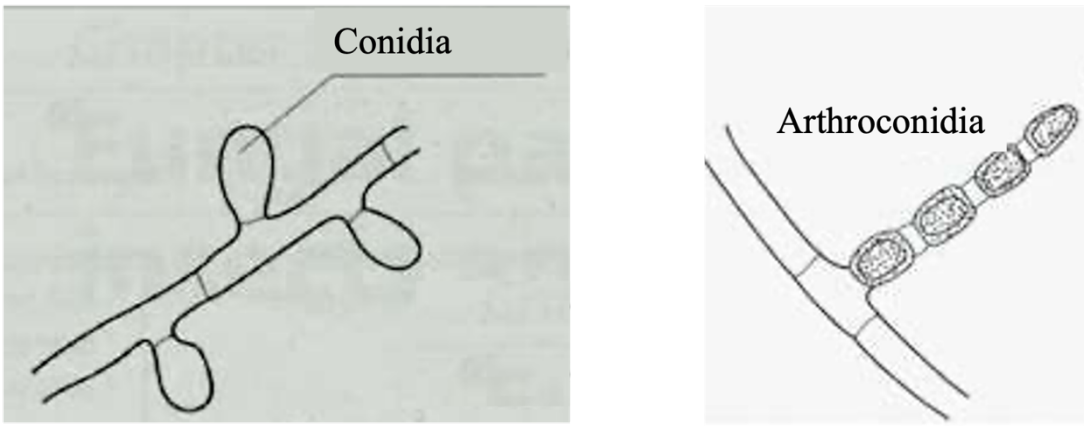

Figure 9: Formation of conidia (a) and arthroconidia (b) in dermatophytes [68]. Conidia are formed by lateral or terminal budding of the hypha while arthroconidia are formed by fragmentation of hyphae.

1.4.2. Dermatophytosis

The incidence of dermatophytosis in humans is high, estimated between 20 and 25% of the world's population, and continuously increasing, making it a public health problem [66],[69]. Indeed, dermatophytes are exclusively pathogenic fungi, responsible for dermatophytosis, more commonly known as ringworm or tinea, which is a superficial infection of the keratinized structures of the host, namely skin, hair and nails [66]. Dermatophyte contamination occurs through direct contact with an infected patient or animal. However, as spores remain infectious for more than a year in the environment, humans can also be contaminated by skin contact with contaminated objects [66].

Dermatophytosis can take on different forms, depending on the area of the body affected: tinea cruris (Figure 10 a), mannuum (Figure 10 b), pedis (Figure 10 c), unguium (Figure 10 d) and corporis (Figure 10 e). In most cases, dermatophyte infection remains superficial and limited to the cornified layer of the epidermis, as dermatophytes are unable to invade deeper tissues or organs in immunocompetent hosts [63]. Histologically, hyphae invading the cornified layer of the epidermis are observed (Figure 10 f) [66],[70].

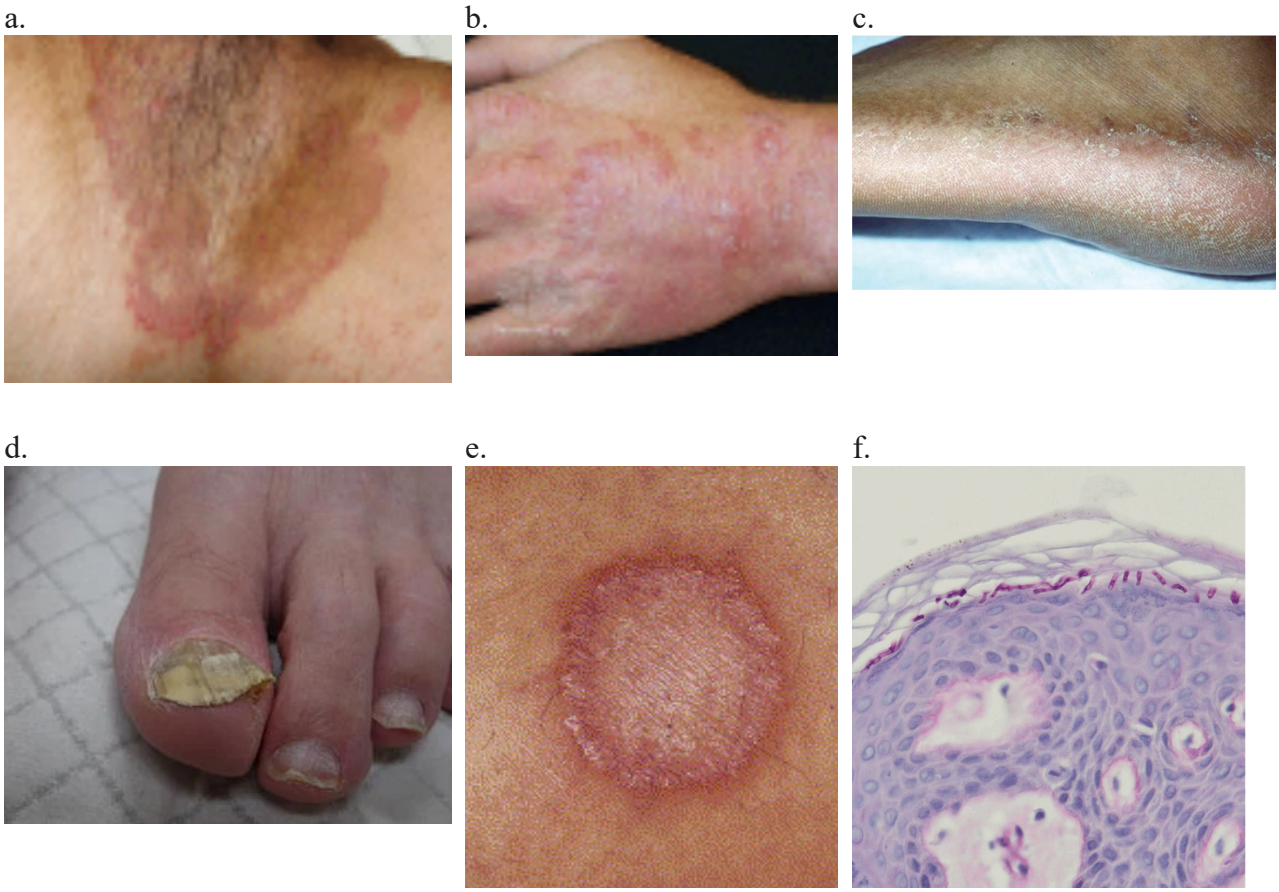

Figure 10: Clinical forms and histology of dermatophytosis. Tinea cruris (a) [71], manuum (b) [72], pedis (c) [73], unguium (d) [74] and corporis (e) [75]. Histology shows hyphae invading the cornified layer of the epidermis (f) [70].

The infection cycle of dermatophytes occurs in several stages. Firstly, polysaccharides and proteins expressed on the cell wall surface, as well as proteases released by the fungus, enable the spores to adhere to the host epidermis. Secondly, favorable conditions allow spores to reactivate their metabolism and thus enable hyphal growth through a process called germination [66]. The third stage of infection, called invasion, consists in the invasion of the cornified layer by hyphae [66]. The hyphae invade the cornified layer of the epidermis, degrading keratin into small peptides and amino acids but also corneodesmosomes and the lipid matrix. After four days of infection, tight junctions are altered and the integrity of the epidermal barrier is lost. Keratinocytes detect the presence of fungus and exhibit enhanced expression and release of proinflammatory cytokines and antimicrobial peptides, leading to activation of the immune system (Figure 11) [66]. Finally, new spores are produced from these hyphae and released in the environment to infect surrounding tissues or individuals [66].

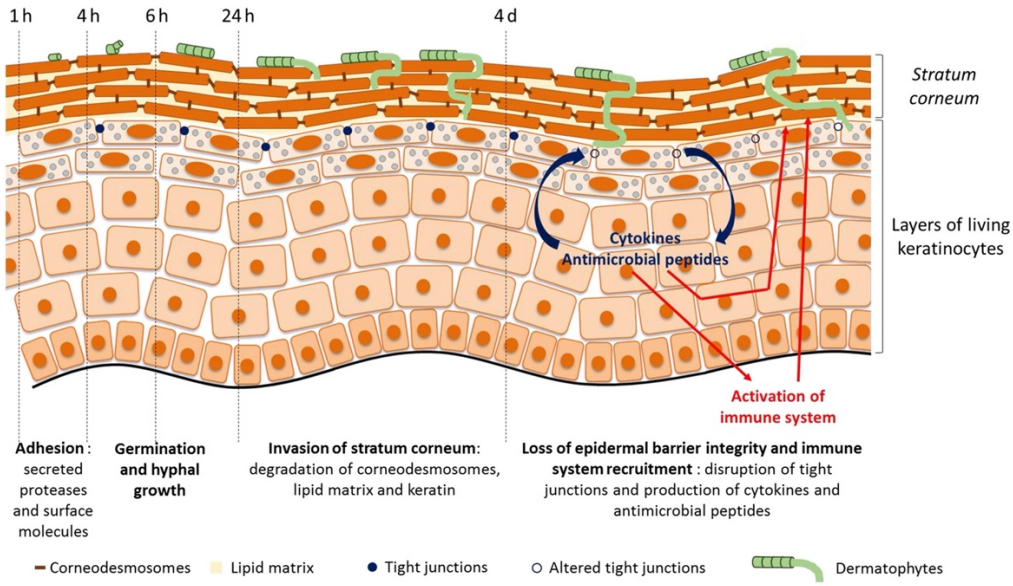

Figure 11: Different stages in dermatophyte infection of the epidermis [66]. Dermatophyte spores first adhere to the epidermis thanks to their surface molecules and the secretion of proteases. During germination, the spores reactivate their metabolism and the hyphae grow. The hyphae then invade the cornified layer (stratum corneum) of the epidermis, degrading corneodesmosomes, the lipid matrix and keratin. After four days of infection, tight junctions are altered and the integrity of the epidermal barrier is lost. Keratinocytes detect the presence of fungus and exhibit enhanced expression and release of proinflammatory cytokines and antimicrobial peptides, leading to activation of the immune system.

1.5. Anti-fungal treatments and resistance

Many antifungal agents are available for treating fungal infections. They are classified into two classes: fungistatic, i.e. agents that inhibit the development and reproduction of the fungus without killing it (e.g. azoles, 5-flucytosine) and fungicidal, i.e. the agents that destroy the fungus (e.g. amphotericin B, echinocandins, terbinafine). These antifungals can be administered by different means, either topically (cream, shampoo) or orally (pills) and have different mechanisms of action. Some antifungal agents disrupt the cell membrane, causing a loss of integrity and leading to the death of the fungus, as in the case of amphotericin B, azoles, echinocandins and terbinafine. Other antifungals block protein synthesis acting at RNA level, and also block protein DNA synthesis, as in the case of 5-flucytosine [76],[77].

Nevertheless, despite the availability of numerous antifungal treatments, the emergence of *Malassezia* and dermatophytes resistant strains is constantly increasing. Emerging resistance to azole antifungals has been demonstrated *in vitro* in *Malassezia furfur* [78]. This resistance could be due to overexpression of efflux pump genes, but also to the fact that *M. furfur* is capable of forming biofilms, which could contribute to reduced sensitivity to azole antifungals [38]. Concerning dermatophytes, several mechanisms of azole resistance have been suggested. Firstly, *Trichophyton rubrum* has been shown to overexpress genes encoding ABC transporters, drug efflux pumps that expel antifungal agents. A mutation in the gene coding for 14-α-lanosterol, a precursor in ergosterol synthesis, which is an essential component of the fungal membrane, could also be involved in azole resistance [79]. Moreover, mutations in the squalene epoxidase gene, an enzyme also involved in ergosterol synthesis, have been shown to be a mechanism of resistance to terbinafine in dermatophytes [75]. Finally, it has been shown that many proteins are secreted by dermatophytes in response to environmental stress and drug exposure in order to adapt to stress. It has then been suggested that this adaptation to stress

stabilizes the fungus in the presence of drugs and enables it to develop greater resistance mechanisms, although this link has yet to be clearly described [79],[80]. Furthermore, the stress generated by the application of a non-inhibitory dose of antifungal drugs could stimulate stress-compensatory responses by the fungus, leading to increased expression of genes involved in cellular detoxification, drug expulsion and signaling pathways, which could participate in drug resistance [79],[81]. However, in addition to these resistances, other problems are associated with antifungal treatments. Oral antifungal agents, such as azoles, have side effects such as hepatotoxicity and drug interactions [82]. Moreover, since antifungal treatments are long-term, it is common for patients not to respect the duration of treatment, and therefore not to be cured. In view of these problems, further research is needed to develop more suitable antifungal treatments.

1.6. Infection and inflammatory responses

Therefore, fungi can adhere to their substrate by different means. In addition, keratinocytes detect the presence of fungi in the environment via surface receptors, leading to the induction of an inflammatory response.

1.6.1. Mechanisms by which cells perceive the presence of fungi

Fungi secrete various enzymes that can be recognized by host cells, notably keratinocytes, promoting host inflammation. As a lipo-dependant yeast, *Malassezia* secrete lipases and phospholipases, that degrade sebum and are essential for its metabolism. However, this may lead to the release of unsaturated fatty acids, known to trigger host inflammatory responses [37]. Dermatophytes secrete proteases which are involved in the adhesion and invasion of the fungus in the cornified layer of the epidermis [83].

Furthermore, these fungi can interact with host cells through the secretion of molecules. For example, *Malassezia* secrete indoles that activate the host intracellular aryl hydrocarbon receptor (AhR). As a result, *Malassezia*-secreted indoles could alter the skin homeostasis [37].

Finally, fungi can also interact with host cells by producing extracellular vesicles that interact with host cells to notably trigger the secretion of pro-inflammatory mediators, thus modulating the host innate immune responses [84],[85].

On the other hand, keratinocytes can recognize fungi by capturing fungal motives present in the environment through cell surface receptors, notably Toll-Like Receptors (TLRs), such as TLR2, and C-type lectin receptors (CLRs), such as dectin-1, expressed by keratinocytes and which recognize carbohydrates present in the fungal cell wall [86],[87]. Recognition of fungi by these receptors enables the initiation of an appropriate antifungal immune response. In addition to these receptors, other receptors may be involved in the recognition of fungi. Indeed, studies carried out on *Candida albicans* have demonstrated the involvement of receptors such as E-cadherin, Ephrin type-A receptor 2 (EphA2) or Epithelial Growth Factor Receptor (EGFR) in the antifungal response [86],[87]. However, the recognition of *Malassezia* and dermatophytes by these receptors has not yet been proven.

TLRs are a group of PRRs (Pattern Recognition Receptors). They are involved in triggering innate immune responses, but also influence future adaptive responses [88]. Some TLRs (TLRs 1 to 6 and TLR9) are notably expressed at the plasma membrane of keratinocytes and play a

crucial role in the recognition of pathogen-associated molecular patterns (PAMPs) as well as physiological endogenous ligands, triggering specific signaling pathways and leading to the release of inflammatory mediators (pro-inflammatory cytokines, chemokines and antimicrobial peptides) and in the initiation of the innate immune response [88],[89],[90],[91],[92],[93]. The structure of TLRs comprises an N-terminal extracellular domain made up of leucine-rich repeats which selectively recognizes PAMPs and DAMPs (damage-associated molecular patterns), and a cytoplasmic domain, named the Toll/IL-1R region (TIR), due to its homology with the signaling domain of the interleukin-1 receptor, which is responsible for signal transduction [88],[94]. Ten different TLRs have been identified in humans [88]. Nevertheless, the ligands of only five of them are known, namely TLR2, TLR3, TLR4, TLR5 and TLR9 [88]. However, TLR2 is currently the only TLR known to recognize only fungal motives.

1.7. Overview of TLR2 signaling pathways

TLR2 is a type 1 transmembrane protein expressed on various cell types, including immune, endothelial and epithelial cells, and is constitutively expressed by keratinocytes [90],[95]. It has been shown that TLR2 plays a dual role in infection processes [96],[97]: while TLR2 triggers a strong pro-inflammatory response, protecting the organism by eliminating the pathogen, this TLR2-induced inflammation can eventually cause tissue damage and impair the healing process [98],[99],[100]. Additionally, TLR2 also acts as a bridge between the innate and adaptive immune systems, as it is also capable of activating the acquired immune response [101].

TLR2 is able to recognize a wide variety of ligands, including DAMPs and PAMPs [94]. Notably, it is able to recognize microbial structures belonging to yeasts and fungi, found in the fungal cell wall [90],[95]. Upon ligand binding, TLR2 heterodimerizes with other receptors, such as TLR1, TLR6 or Dectin-1. Following heterodimerization, the adaptor protein MyD88 (myeloid differentiation factor 88) is recruited through intracellular TIR domains for the activation of downstream signaling pathways [88],[94]. Three different pathways involved in TLR2 signaling are known: the MAPK pathway, the IκB pathway, and the IRF5 pathway. All three pathways induce the production of pro-inflammatory cytokines and factors that control inflammation and modulate cell survival and proliferation (Figure 12) [94].

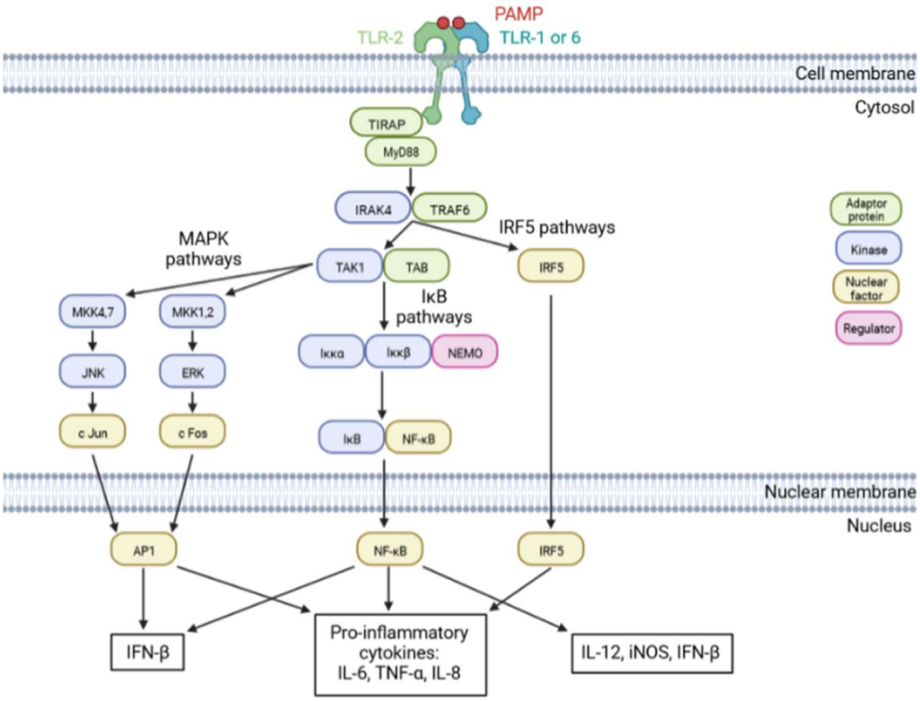

Figure 12: TLR2 signaling (Master thesis of E. Denil). Following recognition and binding of the PAMP by TLR2, TLR2 heterodimerizes with TLR1 or 6. Ligand binding triggers the recruitment of the TIRAP and MyD88 adaptor proteins, which interact with the TIR domain of the receptor. This interaction activates the IRAK4 kinase, enabling the recruitment of the TRAF6 adaptor protein. Activated TRAF6 enables activation of the IRF5 pathway and the TAK1/TAB complex, stimulating activation of the MAPK and IKK pathways. Activation of these pathways leads to nuclear translocation of the transcription factors AP-1, NF-κB and IRF5, resulting in the production of pro-inflammatory cytokines and antimicrobial peptides.

1.8. TLR2 in the context of cutaneous fungal infection

It is well-established that TLR2 can recognize fungal components and is constitutively expressed at the cell surface of keratinocytes. Therefore, one could hypothesize that this receptor likely plays major roles in keratinocyte-fungus interactions during skin infection. In 2008, Baroni A. *et al.* showed an mRNA overexpression of β-defensin 2 and IL-8 by keratinocytes grown as monolayer after exposure to *M. furfur*. Using TLR2 blocking antibody, they showed that these responses were TLR2-dependent [88]. Even though informative, this study was rather incomplete and, to the best of our knowledge, no other studies on the roles of TLR2 expressed by keratinocytes during *Malassezia* infection have been published since then. Similarly, one study demonstrated an overexpression of proteins involved in signaling pathways activated upon TLR2 stimulation in a keratinocyte cell line (HaCaT cells) infected with *Trichophyton rubrum* and *Microsporum canis* [102]. Others have investigated the roles of TLR2 expressed by other cell types found in the skin, such as monocytes. Indeed, Celestrino G. *et al.* demonstrated that blocking TLR2 impairs phagocytosis of *T. rubrum* conidia by monocytes [90]. They also observed a production of pro-inflammatory cytokines, such as IL-1β, IL-6, IL-10 and TNF-α, following stimulation of monocytes with fungal conidia [90]. Additionally, an overexpression of TLR2 in inflammatory granulocytes and monocytes has also been demonstrated in mice after infection with *T. mentagrophytes* [103].

Although suggesting a role of TLR2 in recognition of *Malassezia* and dermatophytes, these aforementioned studies, based on keratinocytes cultured as monolayers, did not reproduce all stages of fungal infections due to the lack of keratinocytes differentiation and the establishment of an epidermal barrier function. Although some studies have been performed *in vivo* on mice [103], they do not allow to specifically capture the roles of TLR2 expressed by keratinocytes, as measured inflammatory responses are due to keratinocytes as well as immune cells. However, since keratinocytes are the first cells to encounter fungi during skin infection, it is indeed reasonable to hypothesize that they play major roles in the establishment of an innate immunity through the secretion of inflammatory molecules such as interleukins and antimicrobial peptides. Reconstructed human epidermis (RHE) is a three-dimensional tissue constituted of differentiated keratinocytes that harbor a structure that is highly similar to the *in vivo* epidermis [104],[105]. RHE exhibit four typical epidermal layers, including the cornified layer which is known to be invaded by *Malassezia* and dermatophytes hyphae (Figure 13). This *in vitro* model thus appears as a valuable tool to specifically study keratinocytes involvement during fungal infection.

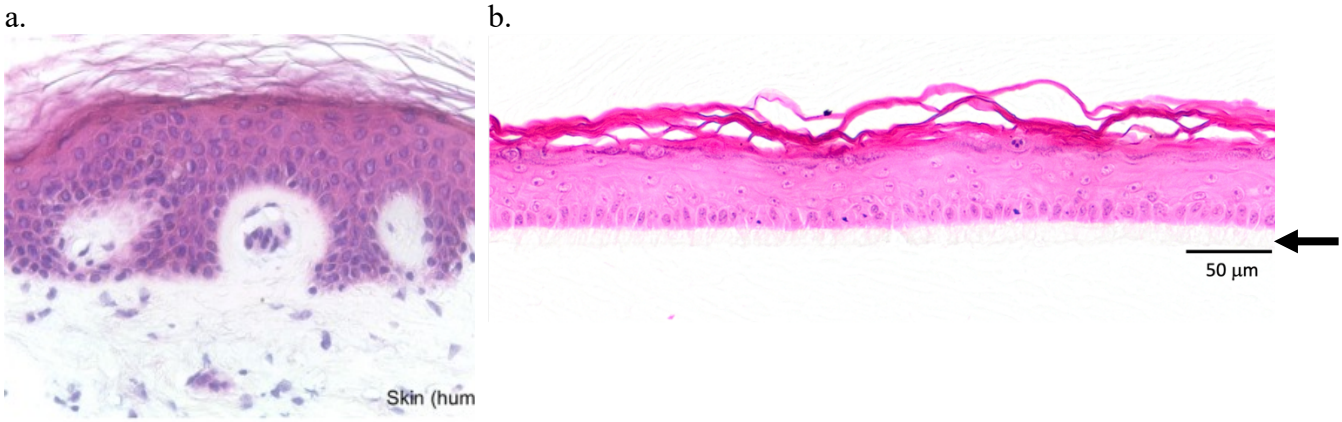

Figure 13: Morphology of *in vivo* human epidermis and *in vitro* reconstructed human epidermis [106]. Both tissues have been stained with HE (hematoxylin eosin). The reconstructed human epidermis includes all the epidermal layers found on *in vivo* human epidermis (a). The arrow represents the polycarbonate filter (b).

RHE have already been successfully infected by *M. furfur* and *T. rubrum* in our lab (Master Thesis of B. Tirtiaux) [107],[108]. Fungal proliferation and invasion, associated to mRNA overexpression and secretion of several pro-inflammatory cytokines and AMPs by keratinocytes has been demonstrated. Furthermore, TLR2 overexpression by keratinocytes has been observed following infection by these fungi, suggesting a possible involvement of this receptor in specific recognition of *M. furfur* and *T. rubrum*. To assess the role of TLR2, immortalized N/TERT keratinocyte cell lines deleted for the *TLR2* gene have been generated using the CRISPR Cas 9 method (Master Thesis of E. Denil). RHE were then produced using these TLR2$^{-/-}$ N/TERT keratinocytes and infected by *T. rubrum*. The absence of TLR2 resulted in a slight decrease in inflammatory responses measured during *T. rubrum* infection (Master Thesis of E. Denil). These preliminary results suggest an involvement of TLR2 in the establishment of inflammation during dermatophytes infection.

The immortalized N/TERT cell line is used in this work as its ability to survive to numerous passages is required to delete genes using the CRISPR/Cas9 method. N/TERT cells were generated by transferring the catalytic subunit of telomerase (hTERT) gene into primary human keratinocytes and spontaneously losing the pRB/p16 INK4a cell cycle control mechanism. Reactivation of telomerase prevents telomere shortening and thus cell senescence. However,

telomerase reactivation is not sufficient to immortalize keratinocytes. Indeed, Dickson M. *et al* demonstrated that keratinocytes also need to lose the pRB/p16 INK4a cell cycle control mechanism to become immortal [109]. As well as primary keratinocytes, N/TERT keratinocytes was shown to exhibit normal epidermal stratification and differentiation properties. Moreover, N/TERT cells faithfully recapitulate primary keratinocytes in terms of tight junction organization and functional barrier formation, in contrast to HaCaT cells, a spontaneously immortalized human keratinocyte line widely used in monolayer models [110],[111]. The immortalized N/TERT cell line is thus used in this work due to its ability to produce fully differentiated RHE [111].

1.9. Objectives

The clinical signs caused by infection by *Malassezia* or dermatophytes are due to degradation of the epidermal tissue by the fungus, but they are also and above all due to the inflammation generated by the infection. However, how keratinocytes are able to sense the presence of these fungi and generate an inflammatory response is still unknown. Even though data from our lab and from the literature suggest that TLR2 likely plays a role in the establishment of inflammatory responses during cutaneous fungal infection, this remains to be demonstrated. Thus, this work aims to depict the specific role of TLR2 in these keratinocytes-induced inflammatory responses during infection by *Malassezia* and dermatophytes.

In this work, the zoophilic species of dermatophyte, *Trichophyton benhamiae*, will be used as this species is known to cause more inflammatory lesions *in vivo*. On the other hand, *Malassezia furfur* is the species used as it is one of the most frequently observed species and can infect RHE. To specifically assess the involvement of TLR2, immortalized N/TERT keratinocytes have previously been deleted for the *TLR2* gene using CRISPR/Cas 9. The use of this cell line, in comparison to non-edited cells, should provide new insights in the involvement of TLR2 during infection by either *T. benhamiae* or *M. furfur*. Firstly, RHE infection by *M. furfur* and *T. benhamiae* should be adapted to N/TERT-RHE. As they exhibit a weaker barrier function, the size of the inoculum and/or the duration of infection should be adapted to maintain an infection limited to the cornified layer of RHE. Secondly, the relevance of TLR2 in this context will be investigated by comparing inflammatory responses (e.g. RT-qPCR, ELISA), as well as TLR2 activation pathways (e.g. immunofluorescence, Western-blot) between $TLR2^{+/+}$- and $TLR2^{-/-}$-RHE.

2. Materials and methods

2.1. Cell culture

2.1.1. N/TERT keratinocytes Reconstructed Human Epidermis

Reconstructed Human Epidermis (RHE) are produced following the method published by De Vuyst E. *et al* and Poumay Y. *et al.* [104],[105]. N/TERT keratinocytes, stored in liquid nitrogen, are first thawed and seeded on a T175 flask in Keratinocyte Basal Medium (KBM-2, Lonza Clonetics Ref CC-3103) supplemented with Keratinocyte Growth Medium (KGM-2, Lonza Clonetics Ref CC-4152) and a mix of antibiotics (streptomycin 50 mg/mL, Sigma Ref S9137-25G and penicillin 50,000 U/mL, Millipore Ref S161-25Mu) for at least seven hours at 37°C and 5% CO_2. Medium is then replaced by EpiLife medium (Gibco Ref MEP1500CA), supplemented with Human Keratinocyte Growth Supplement (HKGS, Gibco Ref S-001-K), as well as the same mix of streptomycin and penicillin. Medium is changed ever two days until keratinocytes reach a 80% confluency. Keratinocytes are harvested using trypsin (Sigma Ref T9201) for 5 minutes. Activity of trypsin is then blocked using a 2% Fetal Bovine Serum (FBS) solution (Sigma Ref F7524). Cells are counted using Cyto Smart counter (Corning Ref 6749) with trypan blue exclusion to assess cell viability. A 300,000 cells suspension in EpiLife medium supplemented with HKGS and 1.5 mM Ca^{2+} is then seeded in cell culture insert (Millicell Ref PIHP01250). These inserts are placed in six-well plates containing 2.5 mL of the same medium and cells are incubated at 37°C for 48 to 72 hours (37°C, 5% CO_2) to allow cell adhesion to the polycarbonate membrane of the insert. Afterwards, keratinocytes are exposed to the air-liquid interface by removing the remaining media in cell culture inserts, promoting keratinocyte differentiation. Simultaneously, the medium below the insert is replaced by 1.5 mL of pre-warmed EpiLife medium supplemented with HKGS, 1.5 mM Ca^{2+}, Keratinocyte Growth Factor (KGF, 10 ng/mL, Amsbio Ref ams-942-100) and vitamin C (50 µg/mL, Sigma Ref 49752-10g). This medium is renewed every two days until fully differentiated RHE are obtained 11 days after this air-liquid interface step. RHE are then ready for infection by either *Malassezia furfur* or *Trichophyton benhamiae*.

2.1.2. *Malassezia* yeasts

Malassezia furfur CBS 7019 strain has been obtained from the Belgian Coordinated Collections of Microorganisms (BCCM/IHEM collection of biomedical fungi and yeasts). This strain has been isolated from a 15-year-old patient diagnosed with pityriasis versicolor. *M. furfur* is grown on mDixon agar, composed of 36g/L malt extract (Carl Roth Ref AE68.1), 10 g/L oxbile (Carl Roth Ref 7595.1), 10 g/L peptone (VWR BDH Chemicals Ref 84610.0500), 2 mL/L glycerol (Merck KGaA Ref 1.04092.1000), 10 mL/L tween 60 (Carl Roth Ref 9694.2) and 20 g/L agar (Fisher Bioreagents Ref BP1423-2). *M. furfur* is grown for four days at 28.5°C prior infection on RHE.

2.1.3. Dermatophytes

2.1.3.1. Culture and production of dermatophyte spores

Trichophyton benhamiae IHEM 20163 strain has been obtained from the Belgian Coordinated Collections of Microorganisms and isolated from an immunocompetent patient diagnosed with tinea corporis. Unicellular spores are required to infect RHE and are therefore isolated following a protocol developed previously by Faway E. *et al*. [112]. Dermatophytes are grown

on Sabouraud agar, composed of 2% glucose (VWR BDH Chemicals Ref 24369.290), 1% peptone (VWR BDH Chemicals Ref 84610.0500) and 2% agar (Fisher Bioreagents Ref BP1423-2). After three days of growth at 28.5°C, fungal material is collected, cut into small pieces and suspended in sterile PBS. This fungal suspension is spread on Potato Extract Glucose (PDA) agar, composed of 26,5 g/L PDA (Carl Roth Ref CP74.1) and 2% agar (Fisher Bioreagents Ref BP1423-2). PDA plates are then incubated for 10 days at 30°C and 12% CO_2 to promote spore production. Fungal material is recovered from PDA and suspended in sterile PBS. To isolate unicellular spores from hyphae, the suspension is shaken for four hours at 4°C and is filtered through three layers of sterile Miracloth paper (EMD Millipore Ref 475855-1R). The spore suspension obtained is stored for up to three months at 4°C.

To measure spore density in the suspension, serial dilutions are performed in PBS and seeded onto Sabouraud agar. The plates are incubated for three days at 28.5°C and Colony-Forming Units (CFUs) are counted under a phase-contrast microscope.

2.2. Infection models on Reconstructed Human Epidermis

2.2.1. RHE infection by *Malassezia furfur*

After four days of growth on mDixon, *M. furfur* yeasts are collected and suspended in sterile water. To dissociate aggregates, a 45-second sonication is performed at 4°C and is repeated three times. Yeasts are then counted using a Thoma cell counting chamber and the inoculum is prepared in sterile water. To provide a source of lipids to *M. furfur*, 100 µL of sterile olive oil (Carrefour Bio, extra virgin olive oil Ref 223859290) are added, prior infection, on RHE for one hour at 37°C. The air-liquid interface is then re-established and RHE are placed in EpiLife medium supplemented with HKGS, 1.5 mM Ca^{2+}, KGF and vitamin C. A 200 µl volume of the inoculum is applied onto RHE for four hours at 37°C to let yeast cells adhere to the tissue. For controls, the same volume of sterile water is added on olive oil pre-treated RHE. The remaining suspension is finally removed to expose keratinocytes to the air- liquid interface again. Infected and control RHE are placed at 37°C and 5% CO_2 for several days, depending on the duration of infection tested. During the infection process, infected and control RHE are recovered and stored at -80°C for RNA extraction or fixed in formalin (VWR Ref 90240-5000) for morphological analysis.

2.2.2. RHE infection by *Trichophyton benhamiae*

An inoculum of 30 CFU of *T. benhamiae* suspended in 200 µl of PBS is used to infect RHE. In practice, RHE are placed in a 24-well plate containing 500 µL of EpiLife supplemented with HKGS, 1.5 mM Ca^{2+}, KGF and vitamin C. The inoculum is added topically on each RHE for four hours at 37°C and 5% CO_2 to let spores adhere to the tissue. The remaining PBS is then removed from RHE surface, and three PBS washes are performed to eliminate non-adherent spores. Infected and control RHE are then incubated at 37°C and 5% CO_2 for up to four days. The medium is renewed every day during the infection process, and the medium collected is stored at -20°C for ELISA. Infected and control RHE are recovered and stored at -80°C for RNA and protein extraction or fixed in formalin for morphological analysis.

2.3. Assessment of the epidermal barrier integrity

To assess the epidermal barrier integrity, the trans-epithelial electrical resistance (TEER) of RHE is measured prior and during infection, using an electrode probe connected to a Volt-Ohm meter (Millicell ERS probes Ref MERSSTX01, Millicell ERS-2 Ref MERS00002). Practically, RHE are placed in a 6-well plate containing 4.5 mL of EpiLife and 500 µL of EpiLife are added topically onto RHE. Electrodes are placed on either side of the tissue, allowing the current to flow through the RHE. The electrical resistance is then measured and the higher is the value, the more difficult it is for the current to cross the RHE, demonstrating an efficient epidermal barrier.

2.4. Histology

RHE are fixed in a 4% formaldehyde solution (VWR Ref 90240-5000) at room temperature for at least 24 hours. After fixation, RHE are dehydrated by three successive 10-minute baths of absolute methanol. RHE and the polycarbonate filter are then detached from the plastic insert by slightly shaking the insert in toluol. The tissue is then placed between two foams inserted in an annotated cassette that undergoes three successive 10-minute baths of toluol. Finally, RHE are incubated at 60°C in liquid paraffin for at least one hour before being embedded in solid paraffin. Histological sections of 6µm thickness are then prepared using a microtome. Once dried, slides are deparaffinized in successive baths of toluol and methanol before being rehydrated in water baths before staining.

2.4.1. Periodic-Acid Schiff (PAS) staining

An α-amylase (0.001g/mL, Sigma Ref A3176-1MU) pre-treatment for one hour at 37°C is required to digest the glycogen that is surprisingly present in RHE. PAS staining is then performed with a 20-minute bath in 1% periodic acid (VWR BDH Chemicals Ref 294604D), followed by a 20-minute bath in a Schiff solution (ROTH Fisher Ref x900) and finally a 5-minute bath in sulfite solution composed of 1N HCl and 10% sodium bisulfite. Tissues are then counterstained with hemalum for 10 seconds and dehydrated in successive 3-minute baths in absolute isopropanol and toluol before mounting the slides with Dpx (BDH Ref 36029).

2.4.2. Immunofluorescence

Different conditions were tested:

	With unmasking	**Without unmasking**
Unmasking	20 min at 95°C in 0,1 M citrate buffer pH 6	/
Saturation	30 min in 1% PBS-BSA	30 min in 1% PBS-BSA - 0,02% Triton

Before saturation, the unmasked tissues are rinsed in PBS. They then undergo three 2-minute baths in 0,1 M glycine and are rinsed three times in PBS. Finally, the tissues are circled with a hydrophobic marker. After saturation, primary antibody (Mouse IgG2a anti- human CD282 TLR2, 0,5 mg/mL, BioLegend Ref 309702) diluted in the corresponding saturation solution is added to the tissues. Three dilutions were tested: 1/40, 1/200 and 1/1000. A control without primary antibody is also performed. Slides are incubated overnight in a humidity chamber at 4°C. After three 5-minute rinses in the corresponding saturation solution, the secondary

antibody (Alexa Fluor 488 goat anti-mouse IgG, Invitrogen Ref A11001) diluted 1/200 in the saturation solution is added to the tissues and slides are incubated in a humidity chamber for 45 minutes at room temperature. After rinsing in the corresponding saturation solution, the tissues are incubated in a humid chamber for 15 minutes at room temperature in Hoechst diluted 1/100 in PBS to mark the nuclei. The slides are finally mounted in Mowiol after final rinses in the corresponding saturation solution. Slides are stored at 4°C and protected from light.

2.5. Keratinocyte responses

2.5.1. RT-qPCR

To extract total RNA from RHE, RHE are mechanically lysed in 50 µl of Trizol (Ambion Ref 15596018) using a grinder (Genetics Ref NG:010262038). 950 µl of Trizol are then added to reach a total volume of 1 mL and samples are incubated for 5 minutes at room temperature. 200 µl of chloroform (VWR BDH Chemicals Ref 22715.293) are added to the lysate and samples are incubated for 3 minutes at room temperature. A 15-minute centrifugation at 12,000g and 4°C is performed to isolate the aqueous phase from others. The aqueous phase is collected and mixed with the same volume of 70% ethanol (Fisher Scientific Ref BP2818-212). Total RNA is then purified by using the RNeasy Mini Kit (Qiagen Ref 74106), and DNase treatment was applied (Qiagen Ref 79256) following manufacturer's instructions. The concentration of extracted RNA is then measured using a spectrophotometer (Thermo Scientific NanoDrop 1000).

RNA is retro-transcribed into cDNA using Superscript III Reverse Transcriptase Kit (Invitrogen, 18080-044).

For quantitative PCR, a 15 µl mix containing SybrGreen (1X, Takyon Ref UF-NSMT-B0701) and 300 nM of forward and reverse primers is prepared. The sequences of primers used are listed in table 1. Then, 5 µl of 1:20 cDNA is added to the mix for a total volume of 20 µl. qPCR is run using Lightcycler96 (Roche LightCycler 96 Ref FW11862). After pre-incubation of 600 seconds at 95°C, 45 amplification cycles of 10 seconds at 95°C, 10 seconds at 60°C and 10 seconds at 72°C are performed. A melting step is then performed to assess primer specificity. The relative expression of the amplified genes is then calculated using the ΔΔCq method by the formula: $2^{-\Delta\Delta Cq}$.

Table 1 : Primers used to amplify targeted genes.

Genes	Primer F 5' -> 3'	Primer R 3' -> 5'	Company
hRPLPO (reference gene)	ATCAACGGGTACAAACGAGTC	CAGATGGATCAGCCAAGAAGG	Eurogentec
hIL-1α	AACCAGTGCTGCTGAAGGAGAT	TGGTCTCACTACCTGTGATGGTTT	Sigma
hIL-1β	TCCCCAGCCCTTTTGTTGA	TTAGAACCAAATGTGGCCGTG	Eurogentec
hS100A7	ACGTGATGACAAGATTGAGAAGC	GCGAGGTAATTTGTGCCCTTT	Eurogentec
hβ-defensin 2	ATCAGCCATGAGGGTCTTGT	GAGACCACAGGTGCCAATTT	Eurogentec

2.5.2. ELISA

The DuoSet ELISA Development kits Human IL-1α/IL-1F1 (R&D Systems Ref DY200) and Human IL-1β/IL-1F2 (R&D Systems Ref DY201-05) are used according to the manufacturer's instructions.

2.5.3. Western blot

2.5.3.1. Protein extraction

Proteins are extracted from control and infected RHE stored at -80°C. Firstly, the tissue is cut from the plastic insert, placed in lysis buffer, and then heated to boiling for 5 minutes in order to detach cells from the polycarbonate membrane and to lyse them. To recover all the cells, their detachment from the filter is helped by scraping with a tip, and the samples are again heated to boiling for 2 minutes. After centrifugation at 10,000 RPM for 5 minutes at 4°C, the supernatant containing protein extract is collected and stored at -20°C until use.

2.5.3.2. Protein concentration

Protein concentration is determined by the Pierce method, using the Ionic Detergent Compatibility Reagent kit (ThermoScientific Ref 22660 + 22663). Samples are first diluted 1:4 in lysis buffer. Bovine Serum Albumin standards (BSA, Sigma Ref A8806-1G) are then prepared to establish a standard curve. Five standards are prepared: 4 mg/mL, 2 mg/mL, 1 mg/mL, 0.5 mg/mL and 0.25 mg/mL. The revelation solution is finally prepared: 1:20 ionic detergent inhibitor (50 mg/mL) is added to the Pierce solution. 5 µL of each sample and standard are deposited in duplicate in a 96-well plate. A lysis buffer blank is also prepared. 75 µL of revelation solution are added to each well and the plate is incubated for 10 minutes in the dark at room temperature. Optical density is read at 660 nm using a spectrophotometer (Molecular Devices, VERSA max microplate reader). Protein concentration is obtained using the standard curve formula.

2.5.3.3. Protein analysis

10% running gel and 4% stacking gel are used in this study. 25 µg of sample are loaded into the stacking gel, after being heated to boiling for 5 minutes, then cooled on ice and rapidly centrifuged. A ladder (PageRuler Prestained Protein Ladder, ThermoScientific Ref 26616) is loaded into the first well. Migration is started at 120 Volts for 1h30. After migration, the gel is collected, and the stacking gel is cut off and discarded. The gel is soaked in transfer buffer, as well as the Whatman papers. The PVDF Transfer membrane (ThermoScientific Ref 88518) is soaked in methanol (Fisher Chemical Ref M/4000/PC17) before being immersed in the transfer buffer. The assembly is then placed in the transfer tank with a magnetic chip and a cooling block for cooling the structure. Transfer is started at 100 Volts for 40 minutes, with agitation and refrigeration. Once the proteins have been transferred to the membrane, the latter is recovered and saturated for 30 minutes at room temperature under agitation with non-fat dry milk (5%, Santa Cruz Biotechnology Ref Sc-2325) diluted in PBS-Tween-20, which is the saturation solution. Primary antibody (Table 2) diluted in the saturation solution is added and incubated overnight at 4°C with agitation. After rinsing three times for 10-minutes with PBS-Tween-20, the secondary antibody (Table 2) diluted in the saturation solution is added and

incubated for 1 hour at room temperature with agitation. After rinsing three times for 10-minutes, the proteins are revealed: the membrane is incubated for 1 minute in the revealing solution (Luminescence substrate, Roche Diagnostics Ref 11500694001+ Starting solution 1:100 Roche Diagnostics Ref 11500694001) and is revealed using the ImageQuant LAS 4000 mini.

Table 2 : Information and references of the antibodies used.

Antibody type	Target	Source	Dilution	Molecular weight of target	Reference
Primary antibody	RPL13A (reference gene)	Rabbit	1/1000	23 kD	Cell Signaling 2765S
	STAT6 (reference gene)	Rabbit	1/1000	110 kD	Cell Signaling 9362S
	P38	Rabbit	1/1000	43 kD	Cell Signaling 9212L
	p-P38	Rabbit	1/1000	43 kD	Cell Signaling 9211S
	TLR2	Mouse	1/1000	95 kD	Proteintech 66645-1-Ig
	IκBα	Rabbit	1/1000	39 kD	Cell Signaling 4812
	p-IκBα	Rabbit	1/1000	39 kD	Cell Signaling 2859
	ERK 1/2	Rabbit	1/1000	42/44 kD	Cell Signaling 9102
	p-ERK 1/2	Mouse	1/1000	42/44 kD	Cell Signaling 9106
	MyD88	Rabbit	1/1000	33 kD	Cell Signaling 4283
	JNK	Rabbit	1/1000	46/54 kD	Cell Signaling 9252
	p-JNK	Mouse	1/1000	46/54 kD	Cell Signaling 9255
HRP-linked secondary antibody	Rabbit IgG	Goat	1/1000	/	Cell Signaling 7074S
	Mouse IgG	Horse	1/1000	/	Cell Signaling 7076S

2.6. Assessment of RNA integrity

The Qubit RNA IQ Assay kits (Invitrogen Ref Q33221, Q33222) are used according to the manufacturer's instructions.

2.7. Statistical analyses

Statistical analyses are performed using two-way ANOVA on Sigma Plot.

3. Results

3.1. Adaptation of *M. furfur* infection on N/TERT-RHE

First, the infection protocol by *M. furfur* CBS 7019 needs to be adapted on unedited N/TERT-RHE, due to the weaker barrier function of N/TERT-RHE in comparison with RHE made of primary keratinocytes, on which the infection procedure was originally established (B. Tirtiaux, manuscript in preparation). As very little RHE invasion by *M. furfur* hyphae had been observed when RHE had been infected with five different inocula and recovered on day four (D4) post-infection (Annex 1), we hypothesized that *Malassezia* might need more time to infect N/TERT keratinocytes. RHE were exposed for one hour to olive oil, to provide a source of lipids to promote *Malassezia* growth, and were then infected on D0 by topical application of the inoculum suspended in water. Five inocula were topically applied on olive oil pre-treated RHE: 10^3, 10^4, 10^5, 10^6 and 10^7 *M. furfur* yeasts. Four hours after infection, the remaining suspension was removed to eliminate non-adherent fungi and to expose keratinocytes to the air-liquid interface again. Infected RHE were then maintained in culture up to eight days after infection. Non-infected control RHE (CTL) as well as an olive oil control RHE (CTL O.O., RHE pre-treated for one hour with olive oil and exposed for four hours to sterile water) were also performed to evaluate the potential impact of olive oil on epidermal construction.

To monitor epidermal invasion by *M. furfur* hyphae, histological analysis with Periodic-acid Schiff (PAS) staining was performed. Overall, *M. furfur* hyphae invasion within the cornified layer on day six (D6) and day eight (D8) of infection appears higher than on D4 (Figure 14 a). Nevertheless, no differences are observed between the different inocula tested. Furthermore, both controls appear similar (Figure 14 a). Therefore, these results suggest that *Malassezia* seem to need more time to invade N/TERT-RHE. However, RHE invasion by *M. furfur* hyphae remains weak when compared to invasion of RHE made of primary keratinocytes (Annex 3).

The trans-epithelial electrical resistance (TEER) of infected and control RHE was assessed during infection to give an indication of the integrity of the epidermal barrier. An increase of TEER values is observed for the non-infected control RHE (CTL) over time, suggesting that the epidermal barrier strengthens overtime. However, the TEER of the olive oil control (CTL O.O.) shows a tendency to decrease on D4 and then gradually increases, suggesting that the addition of olive oil seems to alter the barrier integrity within the first four days of infection. The TEER of infected RHE also decreases on D4 and then stabilizes. This trend is observed for all inocula tested and no clear differences are observed between them (Figure 14 b).

a.

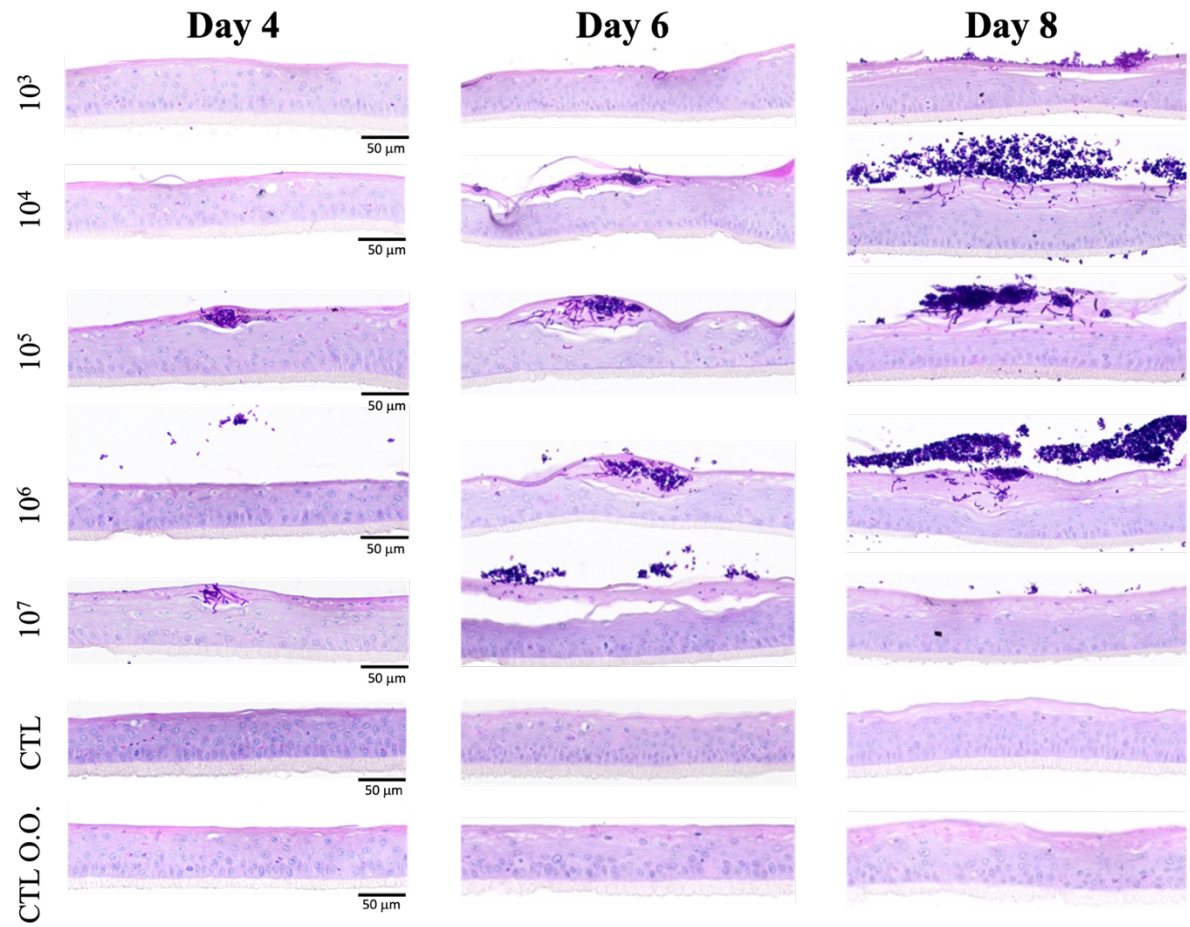

b.

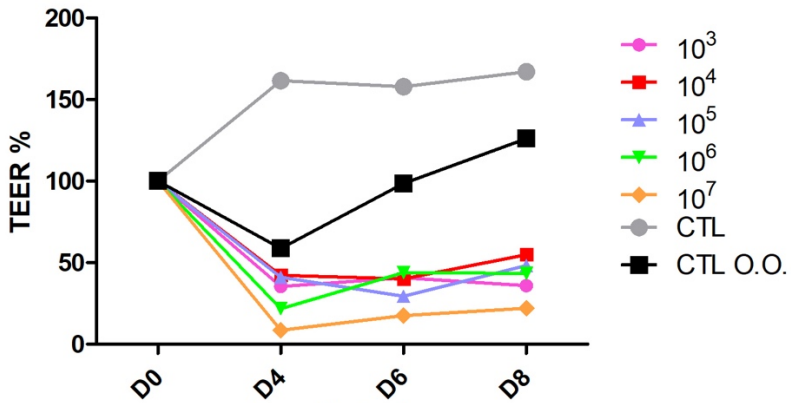

Figure 14: *M. furfur* hyphae invade more RHE by increasing the duration of infection. a. Periodic-Acid Schiff staining with α-amylase treatment and followed by a counterstaining with hemalum, of histological sections of control RHE and RHE infected by *M. furfur*. Unedited NTERT-RHE were exposed one hour to olive oil to provide a source of lipid to *Malassezia* and were infected with different inocula of *M. furfur*: 10^3,10^4,10^5,10^6 and 10^7 *M. furfur* yeasts. RHE were then recovered on days four (D4), six (D6) and eight (D8) after infection. A non-infected control RHE (CTL) as well as an olive oil control RHE (CTL O.O., RHE pre-treated for one hour with olive oil and exposed for four hours to sterile water) were performed to evaluate the impact of olive oil on RHE morphology. n=1. b. Assessment of the transepithelial electrical resistance (TEER) of RHE. TEER was measured before infection (D0) and then at days four (D4), six (D6) and eight (D8) after infection. TEER values were transformed into percentages. n=1.

Simultaneously, the inflammatory responses of keratinocytes during RHE infection with *M. furfur* were analyzed by RT-qPCR, measuring the expression of the pro-inflammatory cytokines IL-1α and IL-1β, and of the antimicrobial peptide β-defensin 2. These inflammatory factors were chosen because highest overexpression following infection with *M. furfur* was obtained for these factors (Annex 2). The expression of inflammatory factors between the uninfected control (CTL) and the olive oil control (CTL O.O.) is broadly similar, suggesting that the addition of olive oil to RHE does not impact keratinocyte inflammatory responses. All these inflammatory factors appear overexpressed compared to controls, regardless of the inoculum. However, the expression of these factors seems slightly increased on D6 and D8 post-infection compared with D4 for almost all tested inocula (Figure 15). Furthermore, the inflammatory responses obtained are weaker than those observed in RHE made of primary keratinocytes infected with *M. furfur* (Annex 4). These results suggest that N/TERT keratinocytes seem to be able to detect *M. furfur* motives and induce inflammatory responses during infection.

Taking these results altogether, increasing the inoculum does not seem to induce greater invasion of RHE by *Malassezi*a hyphae. Nevertheless, *Malassezia* hyphae seem to need more time to infect N/TERT-RHE as compared to primary RHE. As no strong differences were observed when increasing the inoculum, we decided to keep 10^4 *M. furfur* yeasts as inoculum for future infections, given that invasion of the cornified layer of RHE was observed, as well as strong inflammatory responses. However, the duration of infection was increased up to six days post-infection, as cellular responses were higher on D6 than on D4 but were similar at D8 compared to D6.

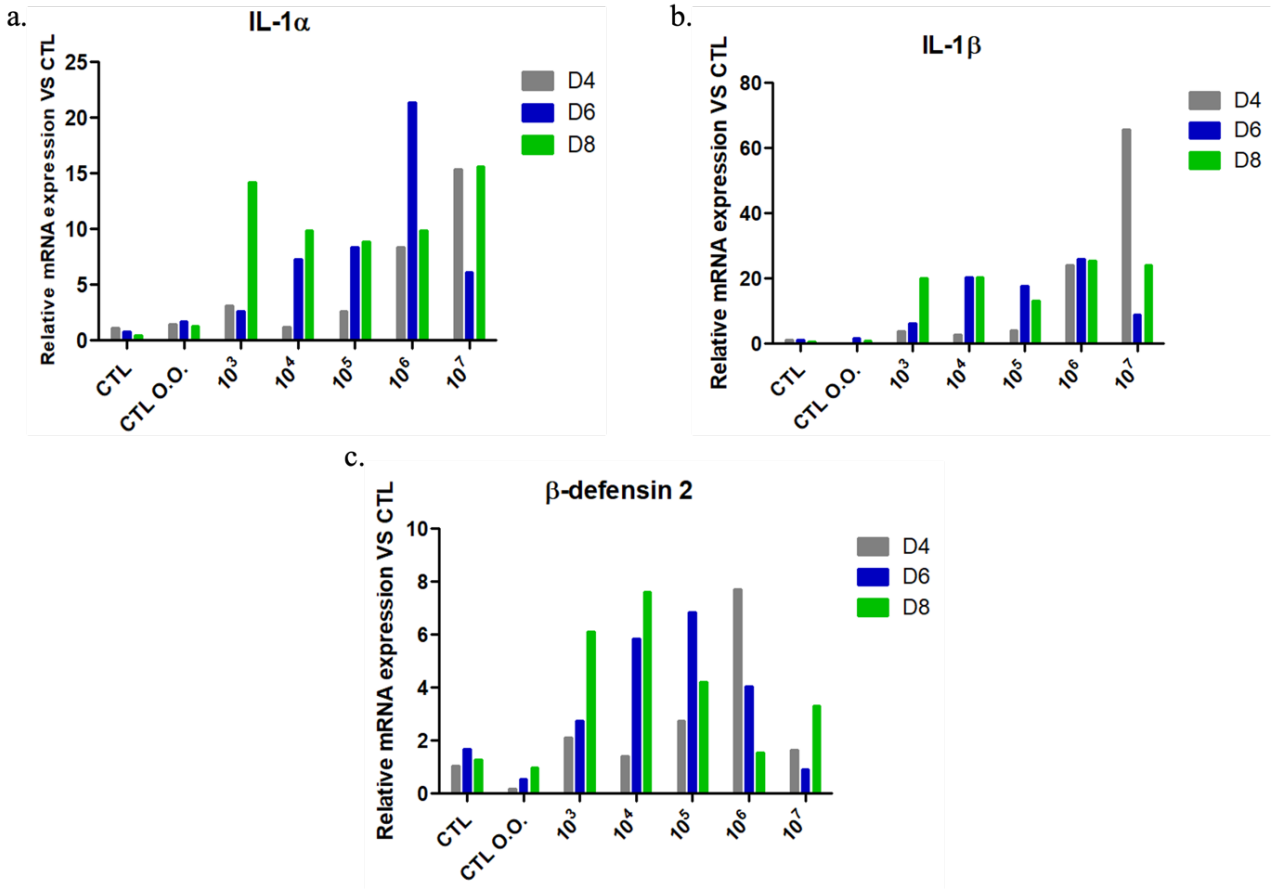

Figure 15: N/TERT keratinocytes can detect the presence of *M. furfur* and induce inflammatory responses during *M. furfur* infection. Unedited N/TERT-RHE pre-treated with olive oil were infected with different inocula of *M. furfur*: 10^3,10^4,10^5,10^6 and 10^7 *M. furfur* yeasts and were recovered on days four (D4), six (D6) and eight (D8) post-infection. A non-infected control RHE (CTL) as well as an olive oil control RHE (CTL O.O., RHE pre-treated for one hour with olive oil and exposed for four hours to sterile water) were also performed to evaluate the impact of olive oil on inflammatory responses. Total RNA was extracted and pro-inflammatory cytokines (a) IL-1α (b) IL-1β, and antimicrobial peptide (c) β-defensin 2 gene expression was analyzed by RT-qPCR. Gene expression was normalized to RPLP0 reference gene and relatively to non-infected control RHE (CTL). The expression of inflammatory factors by the olive oil control (CTL O.O.) on each day after infection was measured relatively to non-infected control (CTL) on the same day and set arbitrarily at 1. The expression of the inflammatory factors by the non-infected control (CTL) on days six (D6) and eight (D8) was measured relatively to non-infected control (CTL) on day four (D4) and set arbitrarily at 1. n=1.

3.1.1. Analysis of the effect of the addition of olive oil over the course of infection

Since RHE invasion by *M. furfur* hyphae remains weak when compared to invasion of RHE made of primary keratinocytes (Annex 3), we hypothesized that *Malassezia* could consume the entire lipid source, provided by olive oil, during the first four days of infection. This lack of lipids could indeed explain why *M. furfur* do not invade the tissue much beyond four days post-infection, even with increased inocula. For this reason, another infection in which olive oil was added over the course of the infection was performed. Practically, RHE were infected on the eighth day after the air-liquid interface, as opposed to the usual eleventh day, for practical reasons. RHE pre-treated with olive oil were infected with 10^4 *M. furfur* yeasts and 40 µL of olive oil was then added on the surface of RHE on D3 after infection and RHE were maintained

in culture until D6. For this experiment, an additional control has also been performed to assess the impact of the addition of olive oil on D3 on an uninfected olive oil pre-treated RHE (CTL O.O. D0+D3). More invasion of the cornified layer of the RHE by *M. furfur* is observed on D6 after infection compared with D4 for both tested conditions. However, no obvious difference is observed on D6 following the addition of olive oil (Infected RHE O.O. D0+D3) compared to the infected RHE where olive oil was not added (Infected RHE O.O. D0) (Figure 16 a). It is important to note that infected RHE on which olive oil has been added (Infected RHE O.O. D0+D3) has a less attractive morphology than RHE infected without olive oil addition (Infected RHE O.O. D0). Nevertheless, the controls show that the addition of olive oil on D3 after infection does not impact tissue morphology (Figure 16 a).

The TEER of infected and control RHE was also assessed during infection to obtain an indication of the integrity of the epidermal barrier. An increase of TEER is observed for the non-infected control (CTL) over time, suggesting a strengthened epidermal barrier. This observation is not surprising, given that the infection was initiated earlier than usual. TEER therefore began to be measured earlier when RHE were not fully differentiated, which explains why TEER values increase sharply over time, the time required for RHE to become fully differentiated. However, a difference between the non-infected control and the controls exposed to olive oil is observed. Moreover, differences are observed between the olive oil control (CTL O.O. D0) and the resupplied olive oil control (CTL O.O. D0+D3) on D6 of infection. Indeed, the TEER of the olive oil control increases on D6 while the TEER of the resupplied olive oil control decreases, suggesting that the addition of olive oil has an impact on the epidermal barrier integrity (Figure 16 b). Finally, the difference on D6 of infection is also observed between the infected RHE without olive oil resupply (Infected RHE O.O. D0) and the infected RHE with olive oil resupply (Infected RHE O.O. D0+D3). Indeed, the TEER of the infected RHE O.O. D0+D3 seems to continue to decrease on D6, while the TEER of the infected RHE O.O. D0 stabilizes (Figure 16 b), as described previously (Figure 14 b). These results suggest that the addition of olive oil during infection on the infected RHE allow *Malassezia* hyphae to further disrupt the epidermal barrier, as a decrease of 63% is obtained between infected RHE without and with addition of olive oil.

a.

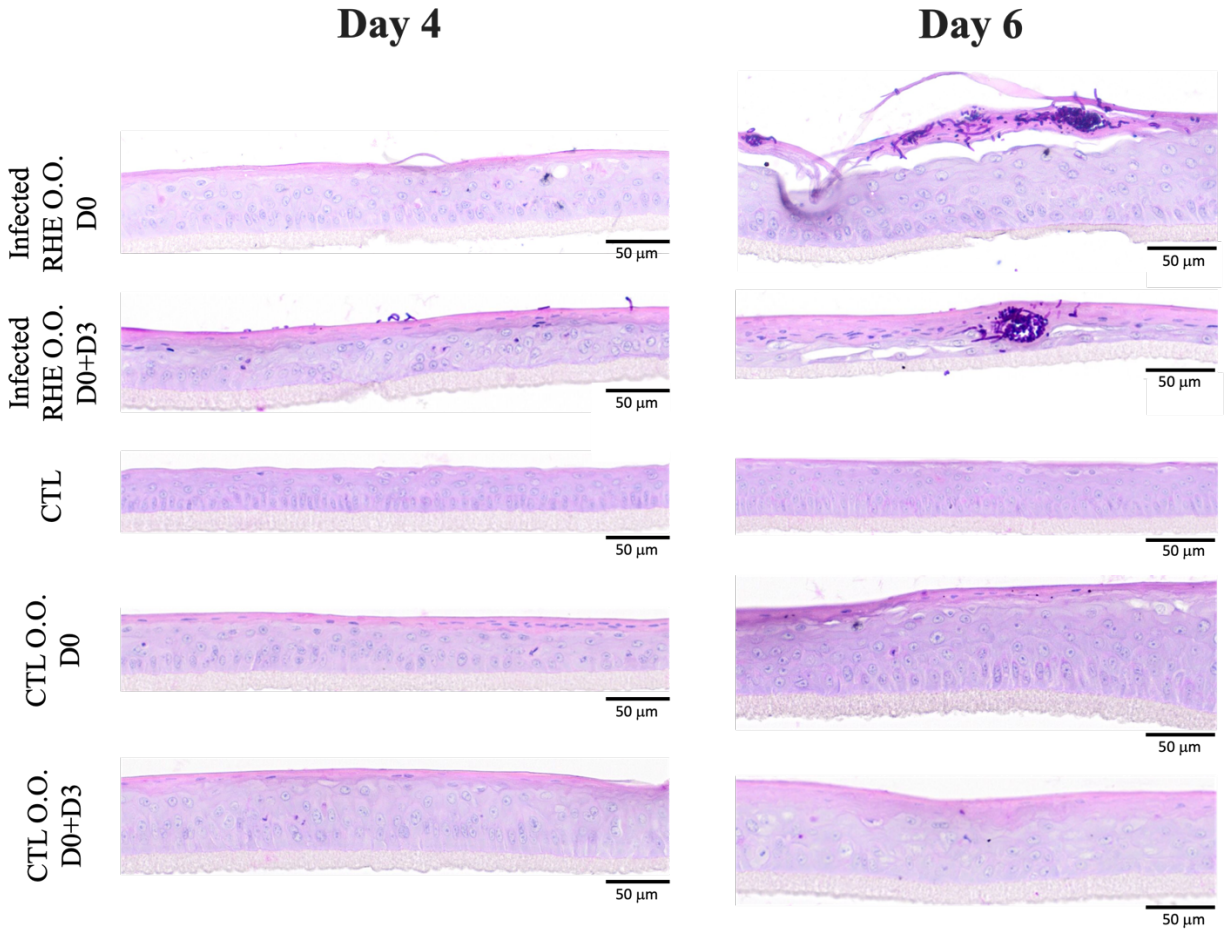

b.

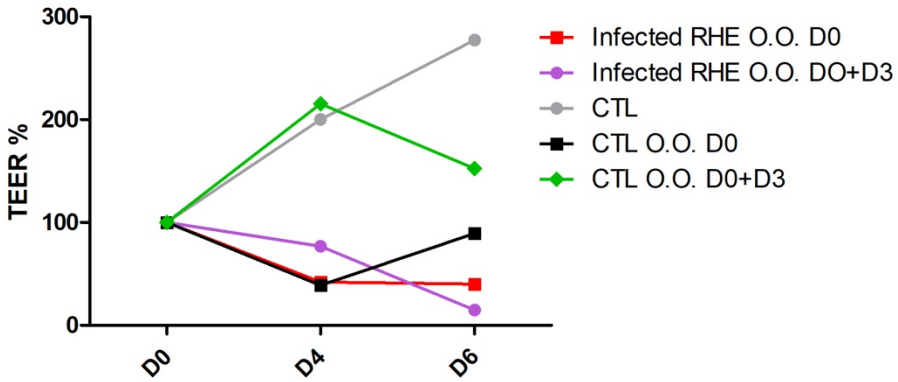

Figure 16: The addition of olive oil does not lead to stronger invasion of the cornified layer of RHE following infection by *M. furfur*. a. Periodic-Acid Schiff staining with α-amylase treatment and followed by a counterstaining with hemalum, of histological sections of RHE infected by *M. furfur*. Unedited N/TERT-RHE were infected with 10^4 *M. furfur* yeasts. Olive oil was added (Infected RHE O.O. D0+D3) or not (Infected RHE O.O. D0) on RHE on day three (D3) after infection and RHE were recovered on days four (D4) and six (D6) post-infection. Different non-infected controls were performed: a non-exposed to olive oil control (CTL), an olive oil control (CTL O.O. D0, RHE exposed to olive oil only one hour before infection) and a resupplied olive oil control (CTL O.O. D0+D3, RHE exposed to olive oil one hour before infection and on which olive oil was also added on D3 after infection) to evaluate the impact of olive oil on RHE morphology. n=1. b. Assessment of the transepithelial electrical resistance (TEER) of RHE. TEER was measured before infection (D0) and then at days four (D4) and six (D6) of infection. TEER values were transformed into percentages. n=1.

Simultaneously, the inflammatory responses of keratinocytes during RHE infection were analyzed by RT-qPCR, measuring the expression of the pro-inflammatory cytokines IL-1α and IL-1β, and of the antimicrobial peptide β-defensin 2. It should be noted that a higher expression of inflammatory factors by infected RHE is observed on D6 of infection, compared to D4 (Figure 17). These results concur with the histology, where a stronger invasion was observed (Figure 16 a). Interestingly, the expression of IL-1α and IL-1β is much higher following the addition of olive oil (Infected RHE O.O. D0+D3) compared to infected RHE where olive oil was not resupplied (Infected RHE O.O. D0) (Figure 17). Expression of β-defensin 2 appears unchanged. Nevertheless, the expression of inflammatory factors appears to be increased in controls exposed to olive oil compared with unexposed controls, suggesting that the addition of olive oil alters inflammatory responses induced by keratinocytes (Figure 17).

Altogether, these results suggest that keratinocytes can detect the presence of *Malassezia* motives. Nevertheless, *Malassezia* seem to need the addition of olive oil during infection to induce stronger inflammatory responses by N/TERT keratinocytes.

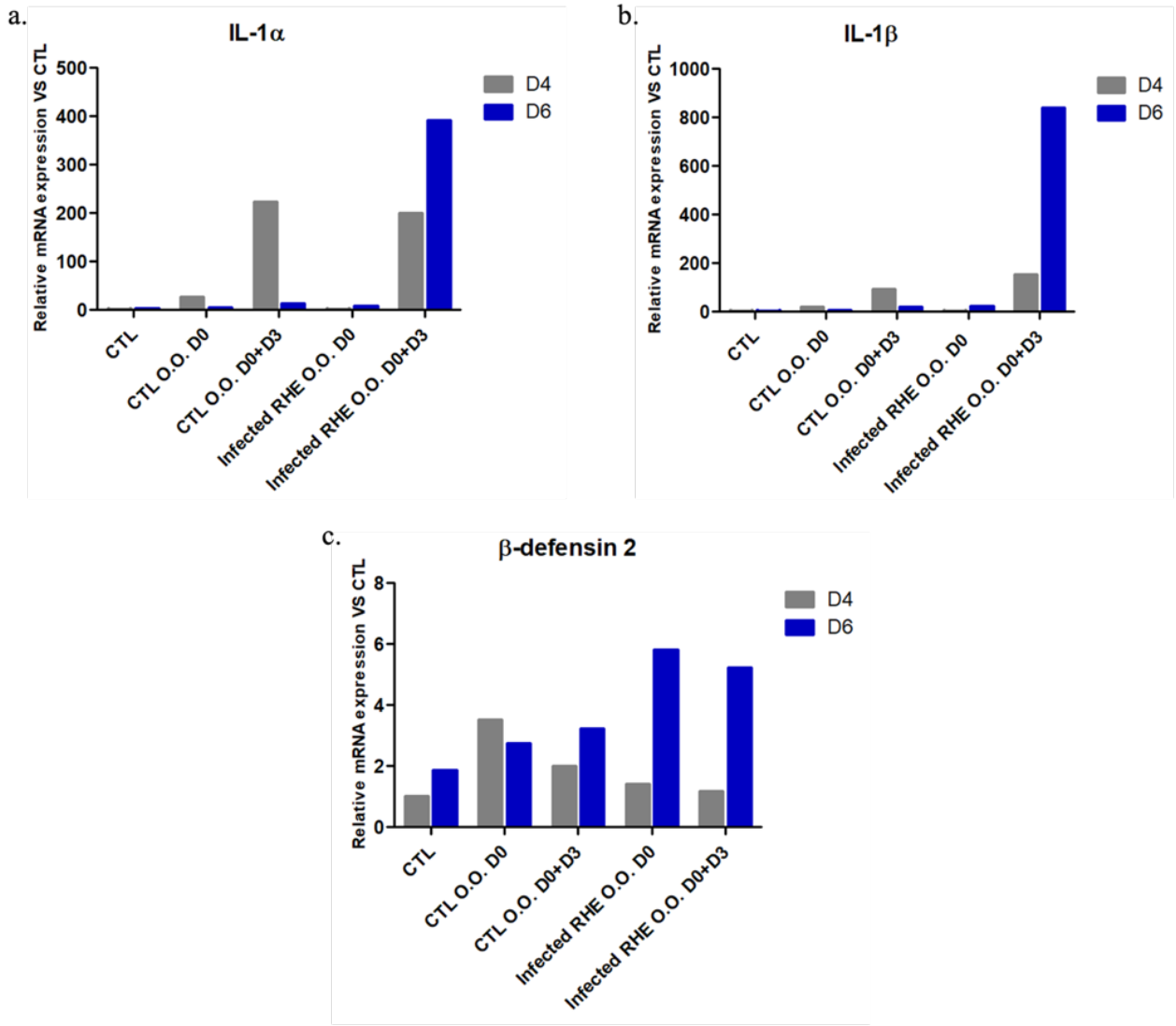

Figure 17: The addition of olive oil during *M. furfur* infection induces stronger inflammatory responses by N/TERT keratinocytes. Unedited N/TERT-RHE pre-treated with olive oil were infected with 10^4 *M. furfur* yeasts. Olive oil was added (Infected RHE O.O. D0+D3) or not (Infected RHE O.O. D0) on day three (D3) after infection and RHE were recovered on day four (D4) and day six (D6) post-infection. Different non-infected controls were performed: a non-exposed to olive oil control (CTL), an olive oil control (CTL O.O. D0, RHE exposed to olive oil only one hour before infection) and a resupplied olive oil control (CTL O.O. D0+D3, RHE exposed to olive oil one hour before infection and on which olive oil was also added on D3 after infection) to evaluate the impact of olive oil on inflammatory responses. Total RNA was extracted and pro-inflammatory cytokines (a) IL-1α (b) IL-1β, and antimicrobial peptide (c) β-defensin 2 gene expression was analyzed by RT-qPCR. Gene expression was normalized to RPLP0 reference gene and relatively to non-infected and non-exposed to olive oil control RHE (CTL). The expression of inflammatory factors by the olive oil controls (CTL O.O. D0 and D0+D3) on each day after infection was measured relatively to non-exposed to olive oil control (CTL) on the corresponding day and set arbitrarily at 1. The expression of the inflammatory factors by the control non-exposed to olive oil (CTL) on day six (D6) was relativized to control non-exposed to olive oil (CTL) on day four (D4) and set arbitrarily at 1. n=1.

3.2. Adaptation of *T. benhamiae* infection on N/TERT-RHE

A first infection by *T. benhamiae* IHEM 20163 was carried out to adapt the infection protocol on N/TERT-RHE because of the weaker barrier function of N/TERT-RHE in comparison with RHE made of primary keratinocytes, on which the infection procedure was originally established [108]. To proceed, RHE were constructed using N/TERT keratinocytes. RHE were infected on D0 by topical application of 30 CFU of *T. benhamiae* suspended in PBS. Four hours after infection, three PBS washes were performed to eliminate non-adherent spores and to expose keratinocytes to the air-liquid interface again. Infected RHE were then maintained in culture for four additional days. It is interesting to note that the inoculum was checked, to make sure that the infection observed is due to the correct inoculum (Annex 5). A non-infected control RHE, as well as a PBS control RHE, on which PBS without spores was topically applied on D0 and which underwent PBS washes, were also maintained in culture for four days. Infected and control RHE were recovered every day of the infection process to analyze the development of the infection.

Interestingly, PAS staining of infected RHE show that tissue invasion is not observed until the third day of infection, where invasion appears limited to the cornified layer of the epidermis, whereas the entire tissue is invaded by *T. benhamiae* hyphae on D4 (Figure 18 a). Moreover, no difference in tissue morphology is observed between the non-infected control RHE (CTL-PBS) and the PBS control RHE (CTL+PBS) (Figure 18 a). It is important to note that the results of one assay showed differences from the other two, where invasion by *T. benhamiae* hyphae appeared to be limited to the cornified layer on D4 of infection (Annex 6). Moreover, the number of spores in the inoculum used was far from the theoretical inoculum of 30 CFU (50% error) compared with the other two assays (Annex 5).

The TEER of the uninfected as well as the PBS-treated control increases similarly over time, suggesting a strengthened epidermal barrier and demonstrating that the temporary loss of the air-liquid interface and the PBS washes do not alter the epidermal barrier. On the other hand, the TEER of infected RHE decreases from D3 of infection, suggesting that invasion by *T. benhamiae* hyphae disrupts the epidermal barrier (Figure 18 b). Additionally, slight variability is observed on D4 of infection. This could be explained by the fact that one assay exhibited a delayed invasion of the cornified layer when compared to the two others (Annex 6).

a.

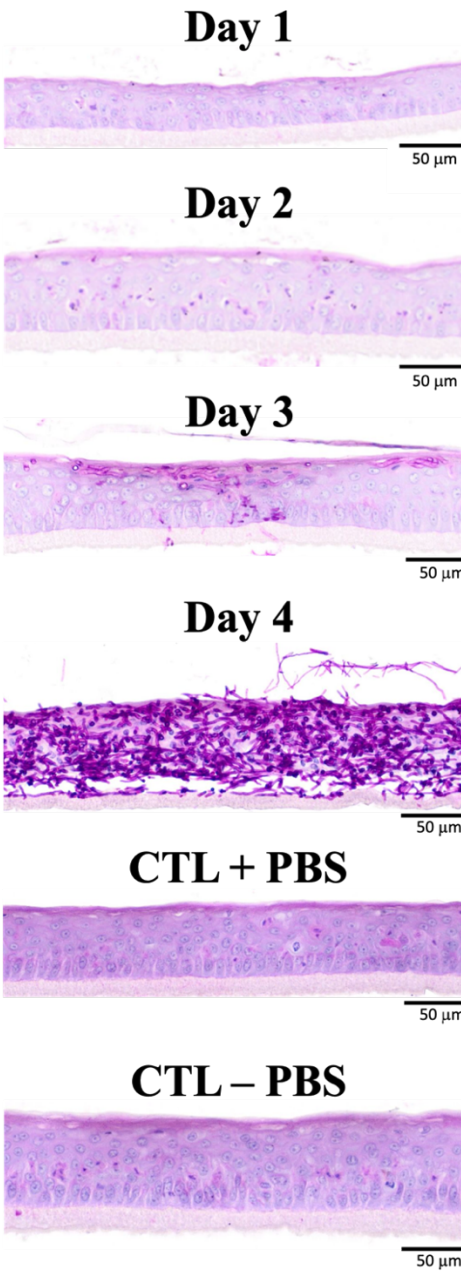

b.

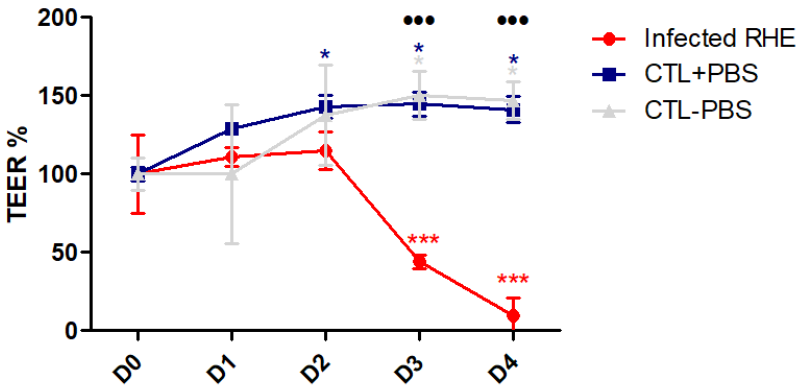

Figure 18: *T. benhamiae* hyphae invade RHE from the third day of infection. a. Periodic-Acid Schiff staining with α-amylase treatment and followed by a counterstaining with hemalum, of histological sections of RHE infected by *T. benhamiae*. Unedited N/TERT-RHE were infected with 30 CFU of *T. benhamiae* and recovered each day after infection until day four (D4). A non-infected control RHE (CTL-PBS), as well as a PBS control RHE (CTL+PBS), on which PBS without spores was topically applied on D0 and which underwent PBS washes were performed to evaluate the impact of PBS on RHE morphology. Representative pictures of one of three independent experiments. b. Assessment of the transepithelial electrical resistance (TEER) of RHE. TEER was measured before infection (D0) and then every day after infection until day four (D1 to D4). TEER values were transformed into percentages. n=3, Mean ± SD; ANOVA 2; colored asterisks show differences with D0 for each condition, dots show differences between both controls (CTL+PBS and CTL-PBS) and infected RHE.

Finally, inflammatory responses of keratinocytes following RHE infection by *T. benhamiae* were assessed. RNA was extracted from control and infected RHE on each day until D4 of infection and the expression of two pro-inflammatory cytokines (IL-1α and IL-1β) and two antimicrobial peptides (β-defensin-2 and S100A7) was assessed by RT-qPCR (Figure 19). These inflammatory factors were selected as they have already been shown to be overexpressed by keratinocytes following infection of N/TERT-RHE by *T. rubrum* (Master thesis of E. Denil). Overexpression of S100A7 has also been demonstrated following infection of N/TERT-RHE by *M. furfur* (Annex 2). Strong overexpression of IL-1α is observed as soon as D3 of infection, while the three other factors appear significantly overexpressed on D4 of infection (Figure 19). Low variabilities are observed between the two controls, suggesting that the topical application of PBS to infect RHE has no impact on the inflammatory responses of keratinocytes.

Taken together, these results suggest that keratinocytes detect the presence of fungal elements and induce high inflammatory responses during *T. benhamiae* infection. Therefore, the use of an inoculum containing 30 CFU of *T. benhamiae* seems appropriate to induce an infection in RHE and a four-day infection period were maintained for future experiments.

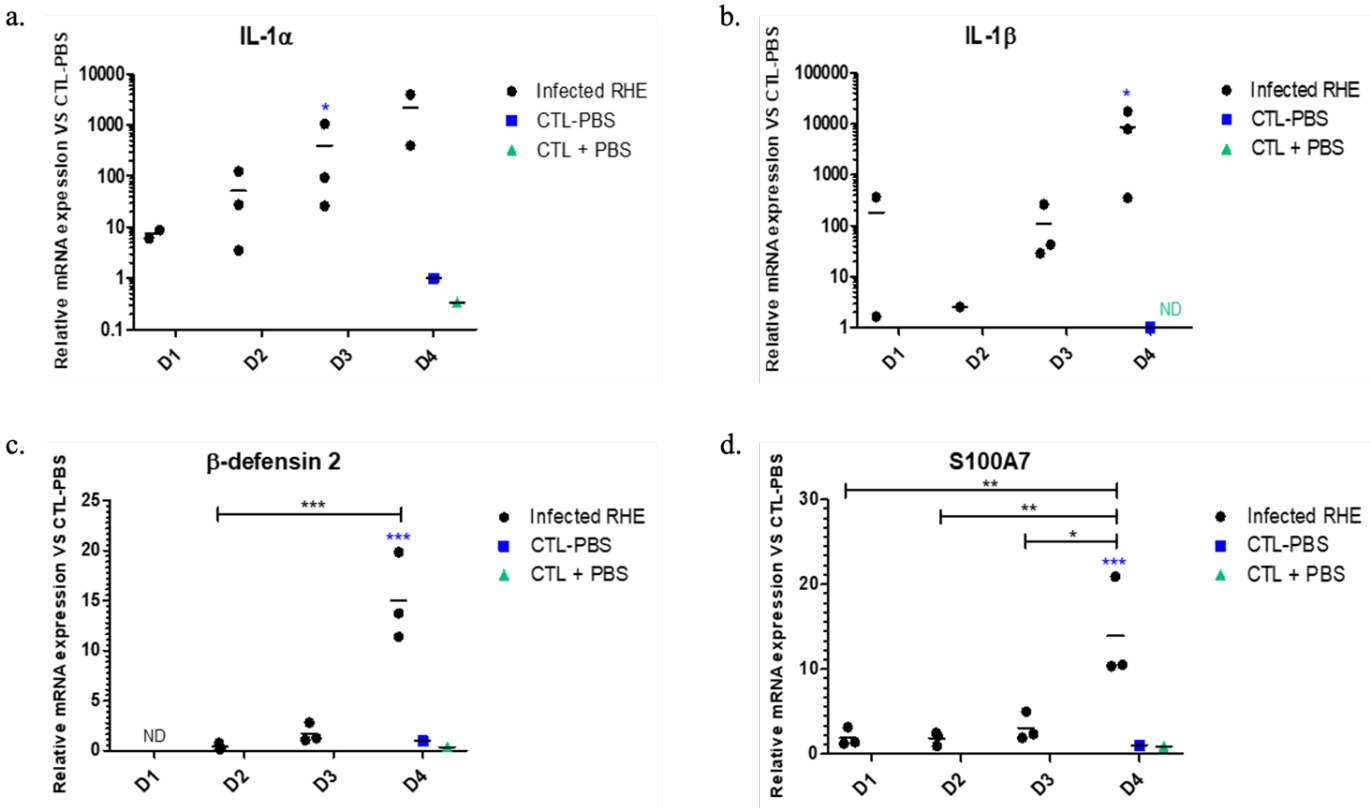

Figure 19: N/TERT keratinocytes can detect the presence of fungal elements and induce inflammatory responses during *T. benhamiae* infection. Unedited N/TERT-RHE were infected with 30 CFU of *T. benhamiae* and recovered each day during the four days following infection (D1 to D4). A non-infected control RHE (CTL-PBS), as well as a PBS control RHE (CTL+PBS), on which PBS without spores was topically applied on D0 and which underwent PBS washes were performed to evaluate the impact of PBS on inflammatory responses. Total RNA was extracted and the expression of pro-inflammatory cytokines (a) IL-1α and (b) IL-1β, as well as antimicrobial peptides (c) β-defensin-2 and (d) S100A7 gene expression was analyzed by RT-qPCR. Gene expression of infected and PBS control RHE was normalized to RPLP0 reference gene and relatively to non-infected control RHE (CTL-PBS) recovered on D4 of infection. The expression of β-defensin-2 on D1 by infected RHE, as well as the expression of IL-1β by the PBS control (CTL+PBS) were not detected (ND, Cq>45). Colored asterisks show differences between non-infected control RHE (CTL-PBS) and infected RHE. Black asterisks show differences between days of infection for infected RHE. IL-1α D1: n=2, D2: n=3, D3: n=3, D4: n=2. IL-1β D1: n=2, D2: n=1, D3: n=3, D4: n=3. β-defensin 2: n=3, S100A7: n=3, Mean; ANOVA 2.

3.3. Comparison of infection on TLR2 $^{+/+}$ RHE and TLR2 $^{-/-}$ RHE

To specifically study the involvement of TLR2 expressed by keratinocytes in measured cellular responses during *T. benhamiae* infection, TLR2$^{+/+}$- and TLR2$^{-/-}$- RHE were infected with 30 CFU of *T. benhamiae* and were recovered on D3 and D4 after infection for analysis, as the first two days did not show invasion and strong inflammatory responses. Non-infected TLR2$^{+/+}$- and TLR2$^{-/-}$- RHE, not exposed to PBS and recovered on D4, were used as controls. These controls were not exposed to PBS, as the lack of impact of PBS addition on tissue morphology, barrier integrity and inflammatory responses has been confirmed previously, as described above.

No difference in RHE morphology is observed between non-infected control TLR2$^{+/+}$- and TLR2$^{-/-}$- RHE, both being well differentiated and constructed (Figure 20 a). Infected RHE did not show difference in dermatophyte invasion between TLR2$^{+/+}$- and TLR2$^{-/-}$- RHE (Figure 20 a). As described above, dermatophyte invasion appears to be limited to the cornified layer on D3 of infection, while invading the entire RHE thickness on D4 (Figure 20 a). It should be noted that the inoculum was also checked for each infection, demonstrating that the three replicates were similar (Annex 7).

A similar increase in TEER is observed for TLR2$^{+/+}$- and TLR2$^{-/-}$- controls over time, suggesting a reinforcement of the epidermal barrier, and indicating that the absence of TLR2 does not alter the barrier function, although high variability is observed for the TLR2$^{+/+}$ control (Figure 20 b). The TEER of infected RHE decreases significantly during infection in both conditions, becoming very low on D4, suggesting that invasion by *T. benhamiae* hyphae disrupts the epidermal barrier. Interestingly, no significant differences are observed between TLR2$^{+/+}$- and TLR2$^{-/-}$-RHE, both in non-infected control, and during infection (Figure 20 b).

a.

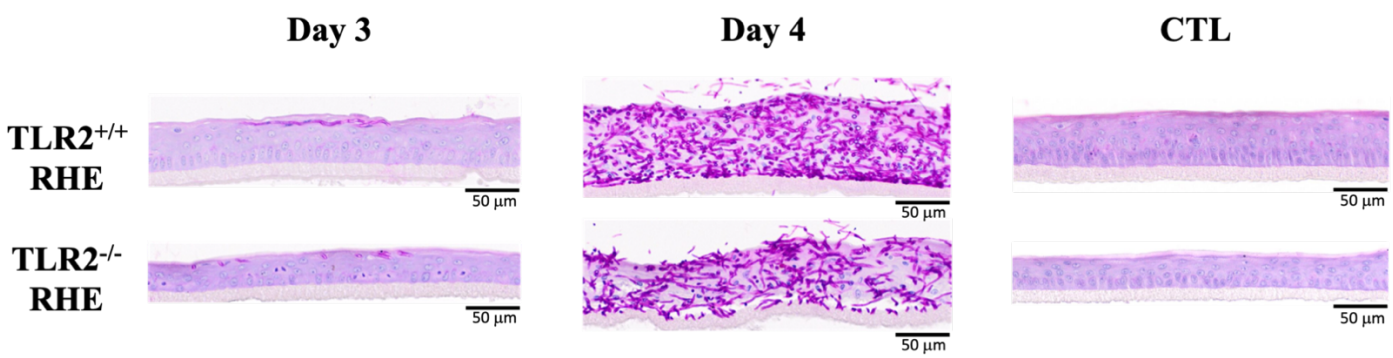

b.

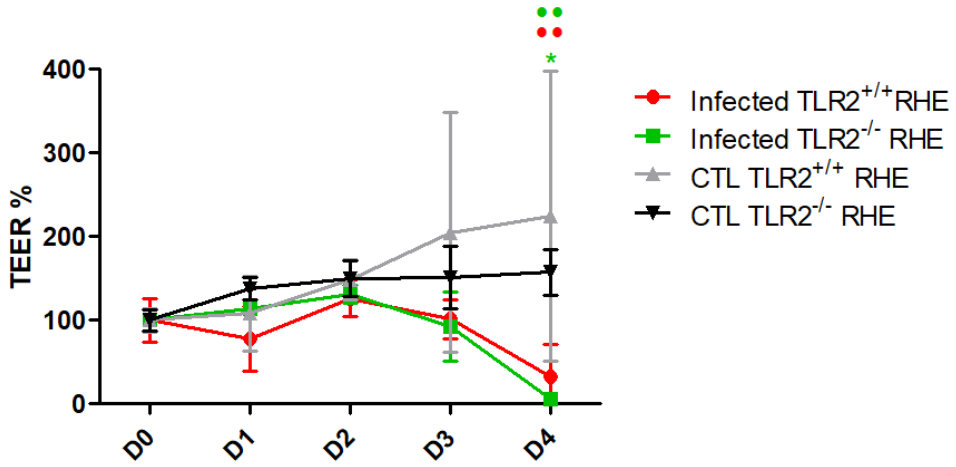

Figure 20: *T. benhamiae* invade TLR2$^{+/+}$- and TLR2$^{-/-}$- RHE. a. Periodic-Acid Schiff staining with α-amylase treatment and followed by a counterstaining with hemalum, of histological sections of TLR2 $^{+/+}$- and TLR2 $^{-/-}$-N/TERT-RHE infected by *T. benhamiae*. Non-infected TLR2$^{+/+}$ RHE (CTL TLR2$^{+/+}$ RHE) and TLR2$^{-/-}$ RHE (CTL TLR2$^{-/-}$ RHE), not exposed to PBS and recovered on day four (D4), were used as controls. RHE were infected with 30 CFU of *T. benhamiae* and recovered on days three (D3) and four (D4) after infection. Representative pictures of three independent experiments. b. Assessment of the transepithelial electrical resistance (TEER) of RHE. TEER was measured before infection (D0) and then every day after infection until day four (D1 to D4). TEER values were transformed into percentages. n=3, Mean ± SD; ANOVA 2; asterisk shows differences between D2 and D4 for infected TLR2$^{-/-}$ RHE, dots show differences between control and infected RHE on D4 of infection.

Inflammatory responses of keratinocytes during RHE infection were also assessed by RT-qPCR. RNA was extracted on D3 and D4 post-infection and the expression of pro-inflammatory cytokines (IL-1α and IL-1β) and antimicrobial peptides (β-defensin-2 and S100A7) was investigated (Figure 21 a). Strong overexpression of IL-1α and IL-1β is observed on D4 of infection, while β-defensin 2 and S100A7 are overexpressed as soon as on D3 of infection (Figure 21 a). Interestingly, no statistical differences in the expression of all genes tested is measured between TLR2$^{+/+}$- and TLR2$^{-/-}$- infected RHE, although inflammatory factors tend to be more overexpressed by TLR2$^{+/+}$ RHE than TLR2$^{-/-}$ RHE. Nevertheless, a large variability is observed in infected TLR2$^{+/+}$ RHE for each inflammatory factor. Furthermore, no significant difference is observed between TLR2$^{+/+}$- and TLR2$^{-/-}$- controls for IL-1α, IL-1β and S100A7, whereas this is the case for β-defensin 2 (Figure 21 a). An ELISA assay confirmed the significant release in infected RHE on D4, regardless of the expression of TLR2 (Figure 21 b). Interestingly, IL-1α, but not IL-1β, seems to be less released by infected TLR2$^{-/-}$ RHE than TLR2$^{+/+}$ RHE (Figure 21 b).

Taken together, these results demonstrate that N/TERT keratinocytes recognize *T. benhamiae* and induce inflammatory responses over the course of infection. Additionally, even in the absence of statistical differences, some decrease in inflammatory markers expression or release are measured in absence of TLR2. However, keratinocyte responses remain sometimes high even in the absence of TLR2, suggesting that in addition to the partial involvement of TLR2, other receptors also appear to be involved in the recognition of *T. benhamaie* and in the induction of inflammatory responses.

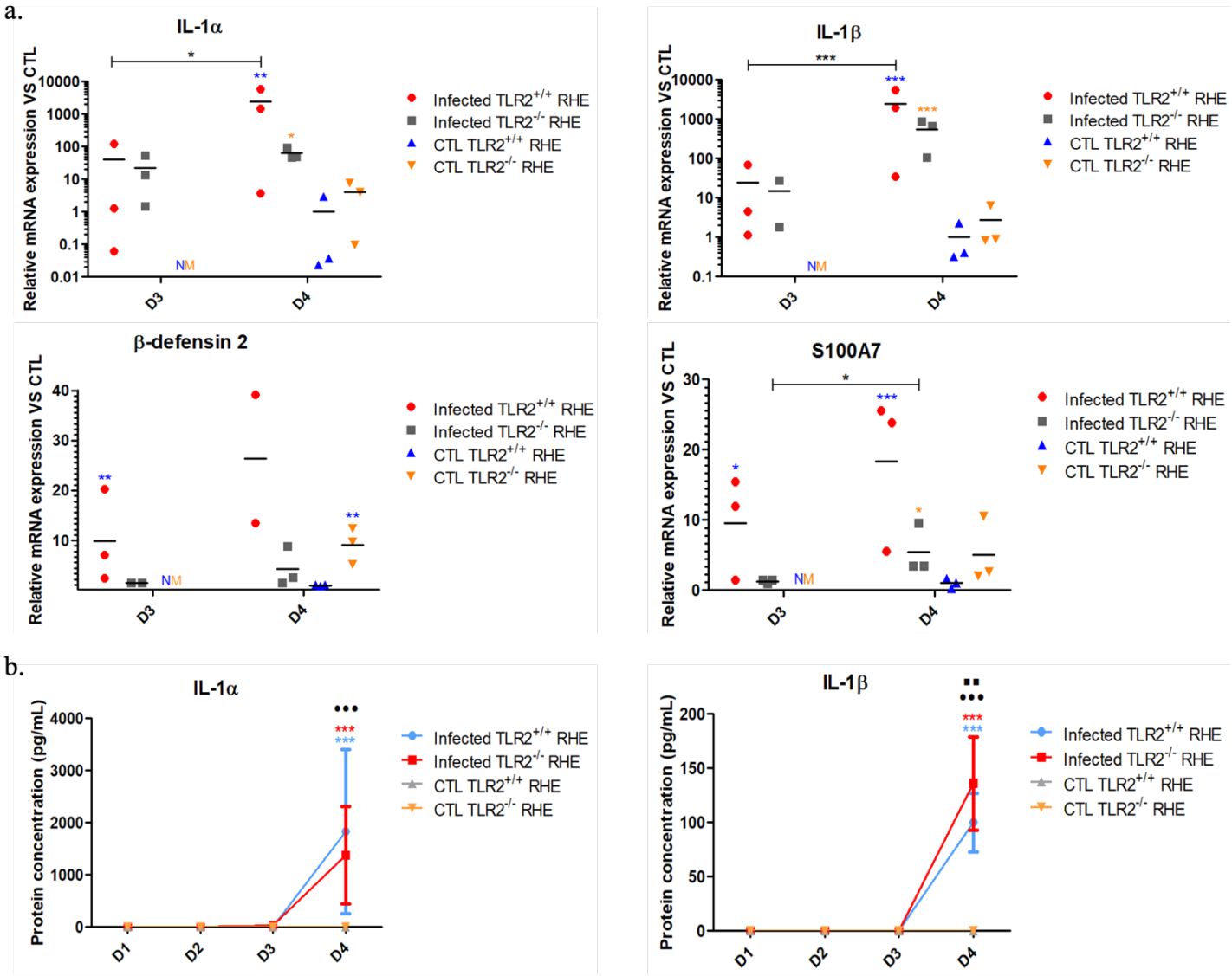

Figure 21: Infection of TLR2$^{+/+}$- and TLR2$^{-/-}$-RHE by *T. benhamiae* induces N/TERT keratinocyte responses. a. Relative mRNA expression of pro-inflammatory cytokines and antimicrobial peptides by keratinocytes. TLR2 $^{+/+}$- and TLR2 $^{-/-}$-N/TERT-RHE were infected with 30 CFU of *T. benhamiae* and recovered on days three (D3) and four (D4) post-infection. Non-infected TLR2$^{+/+}$ RHE (CTL TLR2$^{+/+}$ RHE) and TLR2$^{-/-}$ RHE (CTL TLR2$^{-/-}$ RHE), not exposed to PBS and recovered on day four (D4), were used as controls. Total RNA was extracted and pro-inflammatory cytokines (IL-1α, IL-1β) and antimicrobial peptides (β -defensin-2, S100A7) gene expression was analyzed by RT-qPCR. Gene expression was normalized to RPLP0 reference gene and relatively to non-infected control RHE. The expression of inflammatory factors by the TLR2$^{-/-}$ control was measured relatively to the TLR2$^{+/+}$ control set arbitrarily at 1. Colored asterisks show differences between non-infected control RHE and infected RHE. Black asterisks show differences between days of infection for infected RHE. IL-1β and β-defensin 2 infected TLR2$^{-/-}$ RHE D3: n=2, β-defensin 2 infected TLR2$^{+/+}$ RHE D4: n=2, others: n=3. IL-1α and S100A7: n=3 Mean; ANOVA 2. b. Assessment of pro-inflammatory cytokine secretion by ELISA. TLR2 $^{+/+}$- and TLR2 $^{-/-}$-N/TERT-RHE were infected with 30 CFU of *T. benhamiae*. Culture medium from infected and control RHE was recovered daily until the fourth day of infection (D1 to D4). Colored asterisks show differences between day one (D1) and day four (D4) of infection for infected RHE, dots show differences between control and infected RHE on day four (D4) of infection, square shows differences between infected TLR2$^{+/+}$- and TLR2$^{-/-}$-RHE within D4 of infection. n=3, Mean ± SD; ANOVA 2.

3.3.1. Identification of activated signaling pathways

To identify signaling pathways activated in keratinocytes following *T. benhamiae* infection, potentially induced downstream of TLR2 activation, Western blotting was performed to label proteins already reported in the literature to be involved in TLR2 signaling (Figure 22). Proteins were extracted from $TLR2^{+/+}$- and $TLR2^{-/-}$-RHE infected with *T. benhamiae* on day three (D3) and day four (D4) post-infection. Non-infected $TLR2^{+/+}$ RHE and $TLR2^{-/-}$ RHE, not exposed to PBS and recovered on D4, were used as controls. The RPL13A was used as loading control. Four signaling proteins were labeled, i.e. JNK, P38, ERK and IκBα, as well as the adaptor protein MyD88. JNK, P38 and ERK are involved in the MAPK pathway, while IκBα is involved in the IκB pathway, both of which are known to be recruited after TLR2 activation. MyD88 is the adaptor protein required for activation of these pathways.

Looking at $TLR2^{+/+}$ RHE, more intense signals are observed for phosphorylated form of P38 in infected epidermis than in control ones. Total and phosphorylated forms of IκBα are also found more abundant in infected RHE on D3 than in control RHE (Figure 22). These observations suggest that signaling pathways depending on P38 and IκBα may be activated following *T. benhamiae* infection. In $TLR2^{-/-}$ RHE, a similar profile is observed for P38 and IκBα, for which the phosphorylated form appears more abundant on D3 post-infection than in control RHE (Figure 22). Surprisingly, the abundance of phosphorylated P38 and IκBα appears higher for $TLR2^{-/-}$ RHE compared to $TLR2^{+/+}$ RHE on D3 of infection, with no apparent change in abundance on D4. In addition, the phosphorylation of JNK and ERK are also more important in infected $TLR2^{-/-}$ RHE than in control $TLR2^{-/-}$ RHE, suggesting an activation of both these signaling pathways in response to the infection (Figure 22). Unexpectedly, these observations therefore suggest a recruitment of more signaling pathways in $TLR2^{-/-}$ RHE than in $TLR2^{+/+}$ RHE during infection by *T. benhamiae*.

MyD88 appears to be strongly present in each condition (Figure 22). Its presence seems normal, given that this protein is constantly present in the cell and not only when TLR2 is activated. It is also interesting to note that no difference was observed in protein abundance between $TLR2^{+/+}$- and $TLR2^{-/-}$- RHE. Note that we also attempted to analyze the protein concentration of TLR2 in these RHE, but the Western blot analysis did not exhibit any signal (data not shown).

Interestingly, overall protein abundance appears to be lower in infected RHE recovered on D4 post-infection than in infected RHE recovered on D3, as weaker bands are observed on D4 of infection compared with D3 (Figure 22). This observation can be linked to tissue histology which showed that the tissue is completely invaded by *T. benhamiae* hyphae on D4 post-infection (Figure 20 a). We can therefore hypothesize that all the cells died or are dying following invasion of the tissue, and proteins were no longer synthesized.

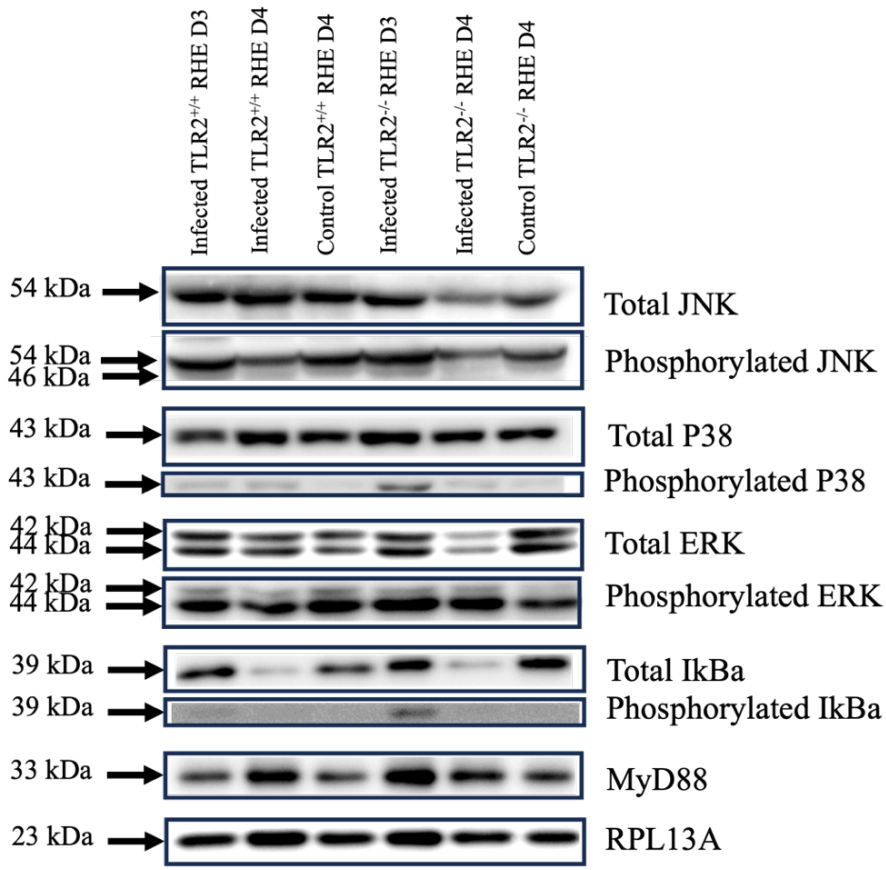

Figure 22: The MAPK and IκB pathways are activated following *T. benhamiae* infection. Proteins were extracted from TLR2$^{+/+}$ RHE and TLR2$^{-/-}$ RHE infected by *T. benhamiae* and recovered on the third (D3) and fourth (D4) days after infection. Non-infected TLR2$^{+/+}$ RHE and TLR2$^{-/-}$ RHE, not exposed to PBS and recovered on day four (D4), were used as controls. The total and phosphorylated forms of four proteins were studied: JNK, P38, ERK and IκBα. MyD88 abundance was also analyzed. RPL13A was used as loading control. P38, p-P38, ERK, p-ERK, IκBα, p-IκBα, JNK: n=3. P-JNK, MyD88: n=2.

3.4. Assessment of RNA integrity for RT-qPCR

In all RT-qPCR performed during this work, many samples had abnormally high Cq values for all genes tested, including the housekeeping gene RPLP0. These high Cq values could explain the high fold changes calculated for many genes and conditions. We hypothesized that the RNA used for RT-qPCR may have been degraded during the extraction procedure. To test this, RNA integrity of several RHE infected with either *M. furfur* (*M.f.*) or *T. benhamiae* (*T.b.*) was assessed using Qubit RNA IQ Assay kits. Samples were chosen based on the Cq values of the *RPLP0* gene: normal Cq values are considered as below 20 while abnormal ones are above 20. These kits measure the amount of small and large RNA with a ratio ranging from one to ten. A score of 1 means that the RNA is highly degraded while a score of 10 demonstrates that the RNA is very well preserved. The score of each RNA tested, regardless of the Cq value of the *RPLP0* gene, is between 7.4 and 9.1 (Figure 23). These results demonstrate that the integrity of all the tested RNAs is high and that they are not degraded.

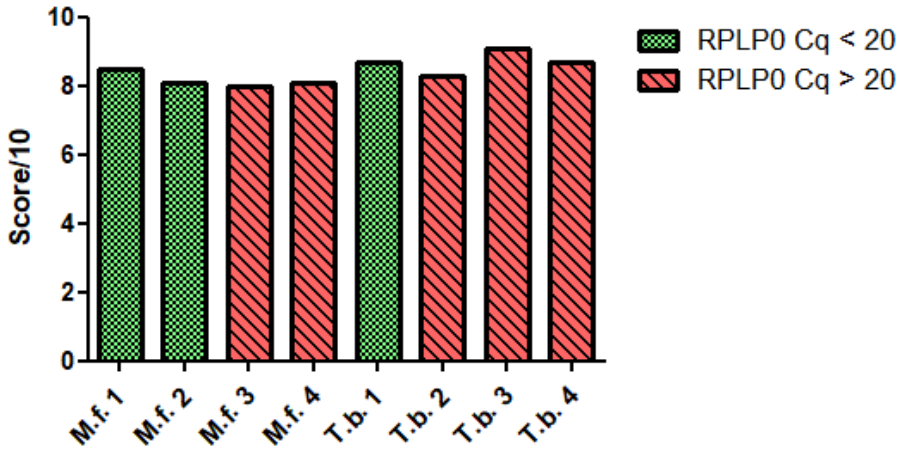

Figure 23: RNA with high RPLPO Cq values have good integrity. RNA integrity of several RHE infected with either *M. furfur* (*M.f.*) or *T. benhamiae* (*T.b.*) was assessed. Samples were chosen based on the Cq values of the *RPLP0* gene: normal Cq values are considered as below 20 while abnormal ones are above 20. The score is out of ten and is calculated on the basis of the ratio between the percentage of small RNA and the percentage of large RNA present. The higher is the percentage of small RNA present, the lower is the score, meaning that the RNA is degraded.

4. Discussion

In this work, we investigated the interactions of two types of fungi, namely *Malassezia* yeasts and filamentous dermatophytes, with keratinocytes. On one hand, *Malassezia* are commensal fungi (yeasts) belonging to our skin microbiome, sometimes involved in pathological conditions. On the other hand, dermatophytes are strictly pathogenic filamentous fungi responsible for dermatophytosis, which is a cutaneous infection of the keratinized structures of the host, namely hairs, nails and epidermal cornified layer. During infection, both fungi produce hyphae that invade the cornified layer of the epidermis, leading to various clinical signs. As keratinocytes are the first cells to encounter these fungi during infection, it is reasonable to hypothesize that they play major roles in the establishment of an innate immune response through the secretion of inflammatory molecules. However, how keratinocytes can sense the presence of such fungi and generate an inflammatory response is still unknown. The *Toll-like receptor 2* (TLR2), basally expressed in keratinocytes, is one innate immunity receptor that has been reported able to recognize certain fungal motives, such as phospholipomannan in *C. albicans* or β-glucan in *S. cerevisiae* [95]. Previous studies in our laboratory have demonstrated that reconstructed human epidermis (RHE) produced using cultured primary keratinocytes exhibit overexpression of pro-inflammatory cytokines, of AMPs and of TLR2 when infected by either *M. furfur* or *T. rubrum* (Master Thesis of B. Tirtiaux, 2020) [107],[108]. Even though data from our lab and from the literature suggest that TLR2 likely plays a role in the establishment of inflammatory responses during cutaneous fungal infection, this remains to be demonstrated. Taking advantage of previously developed infection models on RHE, the goal of this work was to investigate the potential roles of TLR2 expressed by keratinocytes in fungal recognition and in the induction of subsequent inflammatory responses.

To achieve this goal, RHE reconstructed with either non-edited $TLR2^{+/+}$ N/TERT keratinocytes ($TLR2^{+/+}$-RHE) or invalidated $TLR2^{-/-}$ N/TERT keratinocytes ($TLR2^{-/-}$-RHE), previously produced in our lab by the CRISPR/Cas9 method (Master Thesis of E. Denil, 2022), were used to perform infections. However, while infection models have been initially developed using RHE made of primary keratinocytes (primary RHE), the invalidation of TLR2-encoding gene had to be performed on an immortalized cell-line because of the elevated number of passages required for the selection of the edited-genotype. The immortalized cell-line, named N/TERT keratinocytes, has already been used in our lab to produce knock-outs and had been chosen because of its ability to produce fully differentiated RHE [111]. Even if N/TERT-RHE appear like primary RHE, they exhibit weaker barrier function. Therefore, the first step of this work was to test and adapt the infection protocols previously described (B. Tirtiaux, manuscript in preparation),[108].

An inoculum of 10^4 *M. furfur* yeasts topically applied on an olive oil pre-treated RHE was found to allow a strong hyphal invasion within the cornified layer of primary RHE in the four days following infection (Master Thesis of B. Tirtiaux, 2020). To induce infection in N/TERT-RHE, different inocula of *M. furfur* were tested and infected tissues were recovered after four, six, and eight days. Histologically, slightly more hyphae invading the cornified layer were observed on the sixth and eighth days of infection than on the fourth day. Nevertheless, weaker invasion of N/TERT-RHE is observed compared to primary RHE infected with *M. furfur*, which is surprising due to the weaker epidermal barrier of N/TERT-RHE. The TEER of infected RHE dropped compared to uninfected controls, but unlike histology, no difference was observed between days six and eight compared to day four of infection, TEER dropping on day four but then stabilized until day eight. These results suggest that there appears to be no disruption of

epidermal barrier integrity beyond four days of infection. Nevertheless, the TEER measurement technique has its limitations, with variability observed. Indeed, the variability observed between TEER measurements can stem from various factors, such as the lack of reproducibility in electrode placement, temperature variations and the generally extended period of time between measurements [114]. Therefore, in order to reduce this variability, other techniques could be used to test the integrity of the epidermal barrier, such as the Lucifer Yellow test [107]. No differences in invasion and TEER values were observed between the different inocula tested. Surprisingly, the TEER of the olive oil control has shown a tendency to decrease on the fourth day and then gradually increased, suggesting that the addition of olive oil could somehow alter the barrier integrity within the initial four days of infection. This result is surprising, as no difference was obtained between the uninfected control and the olive oil control in infection trials on primary RHE (B. Tirtiaux, manuscript in preparation). However, this difference may be explained by the fact that only one trial was carried out herein, thus the experiment should be repeated to determine if this observation persists. In addition, this difference may occur because the RHE were constructed with different cells (primary and immortalized keratinocytes). Interestingly, in non-infected control RHE, the addition of olive oil did not appear to have any impact on the epidermal morphology, nor on inflammatory responses. Indeed, simultaneously, the inflammatory responses of keratinocytes were analyzed during RHE infection. The inflammatory cytokines and AMP seemed to be overexpressed on day four of infection, whereas the expression of these inflammatory factors was slightly increased on day six and day eight post-infection compared with day four, which is consistent with histology. Nevertheless, the inflammatory responses detected are weaker than those reported with primary keratinocytes infected with *M. furfur* (Master Thesis of B. Tirtiaux, 2020). Besides, no difference was observed in the expression of inflammatory factors between inocula of the different sizes. Altogether, these results suggest that increasing the fungal load in inoculum does not seem to induce greater invasion of RHE by *Malassezi*a hyphae. Moreover, *Malassezia* hyphae seem to need more time to infect N/TERT-RHE as compared to primary RHE. The inoculum of 10^4 *M. furfur* yeasts was therefore chosen since it is sufficient for hyphal invasion and to induce host inflammatory responses. However, the duration of infection was increased up to six days post-infection, as cellular responses were higher on day six than on day four but were similar on day eight compared with day six.

Since no clear difference in epidermal invasion by *M. furfur* was observed with a longer infection period and RHE invasion remains weak when compared to invasion of RHE made of primary keratinocytes, we hypothesized that *Malassezia* might consume the entire lipid source during the first four days of infection. Indeed, since RHE lacks natural sebum, the olive oil pretreatment, performed just before infection, is the only lipid supply available to sustain *Malassezia* growth. The limited availability of lipids could therefore explain why *Malassezia* do not invade the tissue much beyond four days post-infection, even with increased inoculum. To test this hypothesis, olive oil was added again on the third day after infection and RHE were maintained in culture up to the sixth day of infection. Histological analyses had shown that the addition of olive oil on the third day was not affecting the morphology of the tissue. In infected epidermis, fungal hyphae slightly invade the cornified layer, with no difference after additional application of olive oil. The TEER values for infected RHE coincide with the histological results since a decrease in TEER is observed during infection, compared to the uninfected control, meaning that the epidermal barrier appears to be disrupted by *Malassezia* hyphae during infection. However, the re-exposure of uninfected control RHE to olive oil on the third day seems to alter the barrier function as revealed by a decrease in TEER value. The inflammatory responses of infected RHE were also analyzed: interestingly, the expression of IL-1α and IL-1β appeared much higher, following the addition of olive oil on the third day of

infection compared to infected RHE in which only the olive oil pretreatment was performed. The expression of β-defensin 2 appeared unchanged depending on olive oil application on the third day. However, the exposure of uninfected RHE to olive oil on the third day induces overexpression of IL-1α, IL-1β and β-defensin 2, suggesting that the inflammatory responses induced by keratinocytes may be due to the presence of olive oil on RHE and not to the infection by *M. furfur*. This observation may therefore distort our results, which must be interpreted with hindsight. Moreover, it is important to keep in mind that the Cq values of RPLP0 (the reference gene) obtained by RT-qPCR were abnormally high. The relative expression of the inflammatory factors being relativized with the Cq values of RPLP0, the latter therefore modified the expression of the inflammatory factors upwards, thus distorting the real relative expressions that we should have obtained. We therefore hypothesized that these abnormally high values could be due to eventual RNA degradation. To test this hypothesis, we assessed the integrity of RNA extracted from *M. furfur* infected RHE. Interestingly, RNA with high RPLP0 Cq values had very good integrity, thus rejecting our initial hypothesis. Another hypothesis for this problem could be an error made by the experimenter during reverse transcription and RT-qPCR. To test this possibility, these experiments need to be repeated, eventually by a different experimenter, but with the same samples. The RT-qPCR results should therefore be considered cautiously.

Surprisingly, *M. furfur* proliferates less well on N/TERT-RHE than on primary RHE (Master Thesis of B. Tirtiaux, 2020). N/TERT-RHE cannot be easily infected with *M. furfur* CBS 7019 and further testing is required. Firstly, perhaps these low infections are due to the strain of *M. furfur* used. It would therefore be interesting to test other *Malassezia* strains, such as CBS6000, which can produce hyphae to invade RHE, as previously tested (B. Tirtiaux, manuscript in preparation). We could also try to weaken the integrity of the epidermal barrier by treatment with TH2 cytokines (IL-4/IL-13), which would likely help *Malassezia* hyphae to invade the cornified layer of the epidermis. IL-4 and IL-13 are already known to be released in atopic dermatitis and to alter the epidermal barrier [113]. As *Malassezia* are known to be involved in atopic dermatitis, it is interesting to use the treatment with TH2 cytokines on N/TERT-RHE to mimic the *in vivo* mechanisms of epidermal barrier alteration. Furthermore, given that *Malassezia* can secrete molecules (indoles) and enzymes (lipases, proteases) that can interact with host cells, we can hypothesize that these molecules and enzymes are less effective when invading the epidermis reconstructed with N/TERT keratinocytes [37]. We can also hypothesize that the immortalization of human keratinocytes could result in a mutation in the genome of these cells that might interfere with their ability to recognize fungal patterns. Finally, the model could be improved by testing another source of fatty acids, such as olive oil from Sigma with a standardized composition, or synthetic sebum, which would reduce the impact of lipid addition on the barrier function of RHE as well as keratinocyte responses. Anyway, altogether, our results show that an inoculum of 10^4 *M. furfur* yeasts, with a re-application of olive oil after three days, allows the production of hyphae and the invasion of the cornified layer of N/TERT-RHE in six days, while inducing host inflammatory responses. This procedure of infection will thus be used to compare infection development and inflammatory responses on N/TERT TLR2$^{+/+}$- and TLR2$^{-/-}$ - RHE to identify the specific role of TLR2 in *Malassezia* recognition and in the induction of inflammatory responses by keratinocytes.

T. benhamiae infection on RHE were also performed. To test the infection procedure previously set-up on primary RHE [108], N/TERT-RHE were infected with 30 CFU of *T. benhamiae* suspended in PBS and recovered during the four days following infection. A non-infected control RHE, as well a PBS control RHE, on which PBS without spores was topically applied

on D0 and which underwent PBS washes, were also performed to evaluate if the PBS alters tissue morphology and the induction of inflammatory responses. Firstly, histological analyses showed the invasion of *T. benhamiae* hyphae limited to the cornified layer of RHE on the third day of infection while all layers were invaded on day four. Simultaneously, the barrier integrity decreased, as shown with the measurement of TEER. Values were particularly low on day four, synonymous with a complete breakdown of the epidermal barrier. However, it is important to mention that the results of one assay showed differences compared to the two others. Indeed, in this assay, invasion by *T. benhamiae* hyphae appeared to be limited to the cornified layer on the fourth day of infection. This variability was also observed in TEER values, which is consistent because weaker invasion leads to weaker disruption of the epidermal barrier. This infection should thus be repeated to reduce variability between replicates. As observed previously (Master Thesis of E. Denil), the addition of PBS did not alter the tissue morphology nor the epidermal barrier integrity. RT-qPCR analysis showed a strong overexpression of inflammatory factors, mainly IL-1α and IL-1β, from the third day of infection compared with non-infected RHE, suggesting that N/TERT keratinocytes induce inflammatory responses following invasion of the cornified layer of RHE by *T. benhamiae* hyphae. Noteworthy, the tested factors were even more overexpressed on the fourth day of infection. Altogether, these results show that the inoculum of 30 CFU of *T. benhamiae* and a four-day infection are a suitable procedure to infect N/TERT-RHE. However, on the four day following RHE infection, the epidermal tissue is completely invaded by *T. benhamiae* hyphae, which is different from *in vivo* lesion where fungal invasion is restricted to the cornified layer [66]. The third day of infection therefore seems more physiological since hyphae are limited to the cornified layer of the RHE at this time.

Once the infection parameters were set-up, we sought to study the relevance of TLR2 in the induction of inflammatory responses, measured by RT-qPCR. $TLR2^{+/+}$- and $TLR2^{-/-}$-RHE were simultaneously infected with 30 CFU of *T. benhamiae* and RHE were recovered on the third and fourth days of infection, as the first two days did not show invasion and strong inflammatory responses. Histological analyses showed invasion by *T. benhamiae* hyphae limited to the cornified layer on the third day of infection in both $TLR2^{+/+}$- and $TLR2^{-/-}$ -RHE, before invading the entire tissue on the fourth day. These results remain relevant to those previously obtained following infection of N/TERT $TLR2^{+/+}$- and $TLR2^{-/-}$ -RHE *by T. rubrum*, as the same invasion profile was observed (Master Thesis of E. Denil). A similar decrease of TEER values was observed for $TLR2^{-/-}$- and $TLR2^{+/+}$-RHE infected with *T. benhamiae*. Noteworthy, no difference in TEER values was observed between non-infected $TLR2^{+/+}$ - and $TLR2^{-/-}$ -RHE, indicating that the absence of TLR2 does not alter the barrier function.

Inflammatory responses, namely overexpression of inflammatory markers, appeared slightly reduced in $TLR2^{-/-}$ RHE in comparison with $TLR2^{+/+}$ RHE. Moreover, IL-1α, but not IL-1β, seemed to be less released by infected $TLR2^{-/-}$ RHE than $TLR2^{+/+}$ RHE, even if no statistically significant difference was determined, due to variability in responses. Indeed, a large variability was observed in infected $TLR2^{+/+}$ RHE for each inflammatory factor. This variability for IL-1α, IL-1β and β-defensin-2 expression in $TLR2^{+/+}$ RHE is due to one of the three replicates assay showing a higher relative expression than the other two replicates on the third day, and conversely, a lower relative expression on the fourth day. This variability was also observed on the fourth day in the protein concentration of IL-1α and IL-1β released and is also due to one of the three replicates with a lower concentration than the other two. Nevertheless, this is not the same borderline replicate as the RT-qPCR results. It would therefore be necessary to repeat these assays to reduce the variability between the replicates. It should also be noted that only

two replicates could be carried out for β-defensin 2, so a third assay is required to confirm these observations. Moreover, a third assay needs to be performed for IL-1β and β-defensin 2 expression by TLR2$^{-/-}$ RHE on the third day of infection to statistically validate the results obtained. Finally, it is important to note that the Cq values of RPLP0 obtained by RT-qPCR were abnormally high, such as during infection with *M. furfur*, explaining why we obtained very high values of relative expression of inflammatory factors amplified. However, the RNA integrity test also confirmed that RNA with high RPLP0 Cq value used for RT-qPCR were not degraded. To confirm these results, RT-qPCRs need to be repeated to obtain average RPLP0 Cq values and thus more reliable relative expressions of inflammatory factors.

TLR2 signaling pathways activated following *T. benhamiae* infection on N/TERT TLR2$^{+/+}$- and TLR2$^{-/-}$-RHE were assessed. The total and phosphorylated forms of four proteins known to be involved in the TLR2 signaling pathway were studied by Western blot: JNK, P38, ERK and IκBα. MyD88, a major adaptor protein of several TLR pathways, was also analyzed. More intense signals were observed for the phosphorylated form of P38 as well as total and phosphorylated forms of IκBα in infected TLR2$^{+/+}$ RHE than in control ones, suggesting that signaling pathways depending on P38 and IκBα may be activated following *T. benhamiae* infection. These results seem consistent with the literature which attests that IκBα is activated in the signaling pathway following stimulation of TLR2 and that P38 is overexpressed following infection by *Trichophyton rubrum* and *Microsporum canis* in another keratinocyte cell line (HaCaT cells) [94],[102]. A similar profile was observed for phosphorylate P38 and IκBα in TLR2$^{-/-}$ RHE on day three of infection compared with control RHE. Surprisingly, the abundance of phosphorylated P38 and IκBα appeared higher for TLR2$^{-/-}$ RHE compared to TLR2$^{+/+}$ RHE on day three of infection. In addition, the phosphorylation of JNK and ERK were also more important in infected TLR2$^{-/-}$ RHE than in control TLR2$^{-/-}$ RHE, suggesting an activation of both these signaling pathways in response to the infection, which is surprising in view of the literature, which suggests activation of these signaling pathways following TLR2 activation [94],[102]. Unexpectedly, these observations suggest a recruitment of more signaling pathways in TLR2$^{-/-}$ RHE than in TLR2$^{+/+}$ RHE during infection by *T. benhamiae*. Therefore, we can hypothesize that in addition to TLR2, other receptors may be involved in *T. benhamiae* recognition and signaling pathways induction. It is also possible that other, still unknown, signaling pathways can be involved in TLR2 signaling.

MyD88 appeared to be strongly present in each condition, meaning that this adaptor protein seems to be recruited following infection by *T. benhamiae*, in accordance with the literature [94],[115]. Its presence seems normal, given that this protein is constantly present in the cell and not only when TLR2 is activated. It is also interesting to note that no difference was observed in protein abundance between infected TLR2$^{+/+}$- and TLR2$^{-/-}$-RHE. However, Western blot is a semi-quantitative method, meaning that results are only evidence of the strong presence or absence of the protein, but give no information on the exact quantity. To refine these results, it might be interesting to quantify the intensity of the bands. This was not done in this work due to lack of time. However, this approach also has its limitations, depending on the zones selected and background. Furthermore, it should be noted that in this work, we studied protein abundance in the whole RHE tissues, whereas it is unlikely that all keratinocytes in the RHE respond simultaneously to infection, given that some are further away from the infection for example, and this could therefore dilute any possible effects on protein abundance and eventual phosphorylation. Finally, it is also possible that other, still unknown, signaling pathways can be involved in TLR2 signaling and that other receptors may be involved in addition to TLR2. Interestingly, protein abundance appeared to be lower in infected RHE

recovered on day four after infection than in infected RHE recovered on day three. This observation can be linked to tissue histology which showed that the tissue is completely invaded by *T. benhamiae* hyphae on day four post-infection. We can therefore hypothesize that all the cells died or are dying following invasion of the tissue, explaining that proteins were no longer synthesized. Finally, we can note that we also attempted to analyze the protein concentration of TLR2 in $TLR2^{+/+}$- and $TLR2^{-/-}$-RHE, but the Western blot analysis did not demonstrate any signal. Therefore, two hypotheses can be proposed to explain our observations. Firstly, it could be a technical problem. Thus, it might be interesting to test other anti-TLR2 antibodies to test if we get a better signal. Secondly, the absence of signal could mean that TLR2 may not be activated in the conditions tested.

To conclude, no difference was observed in the infection development between $TLR2^{+/+}$- and $TLR2^{-/-}$-RHE. However, even in the absence of statistical differences, some decrease in the expression or release of tested markers was sometimes observed between $TLR2^{+/+}$- and $TLR2^{-/-}$-RHE, which had also been demonstrated previously following infection with *T. rubrum* (Master Thesis of E. Denil, 2022). Indeed, we demonstrated that *T. benhamiae* infected and invaded both N/TERT $TLR2^{+/+}$- and N/TERT $TLR2^{-/-}$-RHE, and that an inflammatory response was also elicited by both types of N/TERT keratinocytes following *T. benhamiae* infection, suggesting the partial involvement of TLR2 but also the involvement of other receptors.

Indeed, since we obtained no difference between $TLR2^{+/+}$- and $TLR2^{-/-}$- RHE, and since RT-qPCR results are difficult to interpret due to RPLP0 Cq problems, we can hypothesize that the lack of difference between $TLR2^{+/+}$- and $TLR2^{-/-}$- RHE could be due to the involvement of a receptor other than TLR2 in the recognition of *T. benhamiae* and in the induction of inflammatory responses. Indeed, it has been demonstrated in the literature that TLR2 is capable of dimerizing with other Toll-like receptors but also with dectin-1. Dectin-1 is a receptor belonging to the lectin family which recognizes β-glucans and can interact with TLR receptors to detect pathogens. Nevertheless, dectin-1 can also form homodimers and act independently of TLR2 to recognize fungal motives. Dectin-1 could be an interesting target as it has already been shown in the literature to be involved in the induction of inflammatory responses following *T. rubrum* infection [90]. Dectin-1 expression has also been shown to promote NF-κB activation via TLR-mediated signaling. Finally, dectin-1 has been shown to act synergistically with TLRs in regulating cytokine production, notably interleukin-12 and TNFα [116]. This information therefore suggests a major involvement of dectin-1 in the induction of inflammatory responses as well as its potential involvement in dimerization with TLR2 to induce inflammatory responses. To test this target, we could generate double knock-out for *TLR2* and *dectin-1* genes in N/TERT-RHE. Nevertheless, other receptors known to dimerize with TLR2, such as TLR1 and TLR6, could also be investigated [94]. Moreover, as previously mentioned, *Malassezia* and dermatophytes can secrete molecules and enzymes that are implicated in inflammatory responses [37],[83],[84],[85]. It would therefore be interesting to study exactly how these molecules are perceived by keratinocytes and what role they play in measured responses. Finally, it would be interesting to determine the exact position of TLR2 on keratinocytes. To do that, a TLR2 immunostaining could be carried out. It is interesting to note that TLR2 immunofluorescence has already been achieved but did not give any relevant results, as the signal was very diffuse throughout the RHE, and no difference was observed between $TLR2^{+/+}$- and $TLR2^{-/-}$-RHE (Annex 9). Therefore, we could try to fine-tune this technique by testing other anti-TLR2 antibodies for example. Moreover, fluorescent strains of *M. furfur* and *T. benhamiae* could also be used to study interactions between the fungus and keratinocytes, and to see if *Malassezia* and dermatophytes co-localize with TLR2. Finally,

fluorescence could also be used to determine if TLR2 is associated with another receptor such as TLR1, TLR6 or dectin-1, as explained above, by labelling these receptors with different fluorochromes. A better understanding of how keratinocytes interact with fungi could offer new therapeutic strategies against these fungal infection, in view of the emergence of resistant strains to current treatments [38],[75],[78],[79],[80],[81].

Supplementary data

Annex 1: Periodic-Acid Schiff (PAS) staining with α-amylase treatment of histological sections of N/TERT-RHE infected with *M. furfur*. Unedited N/TERT-RHE were infected with different inocula of *M. furfur*: (a) 1,000, (b) 10,000, (c) 50 000, (d) 100,000 and (e) 1,000,000. RHE were then recovered on day four of infection, histologically processed, and stained with Periodic-Acid Shiff (PAS). Two pictures of the histological sections were taken per condition. Arrows show fungal material.

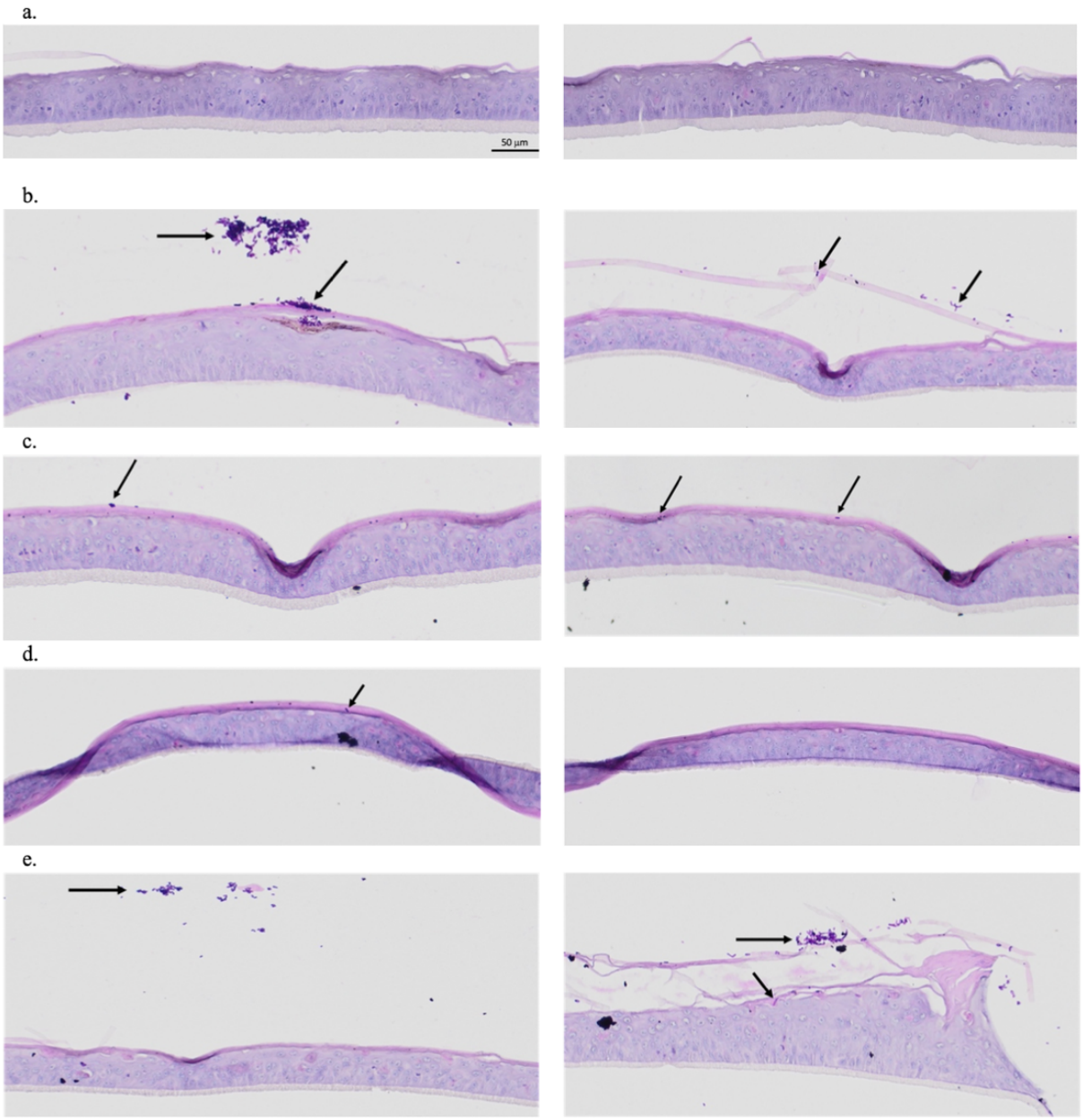

Annex 2: Relative mRNA expression of pro-inflammatory cytokines and antimicrobial peptides by N/TERT-RHE infected with *M. furfur*. Unedited N/TERT-RHE were infected with different inocula of *M. furfur*: 1,000; 10,000; 50 000; 100,000 and 1,000,000. Infected RHE were recovered on day four of infection. Total RNA from infected and control RHE was extracted and pro-inflammatory cytokines (a) TNFα, (c) IL-1α, (e) IL-1β and antimicrobial peptides (b) β-defensin 2 (BD2), (d) β-defensin 3 (BD3), (f) S100A7 were amplified by RT-qPCR. Gene expression was normalized to RPLP0 reference gene and compared to non-infected control RHE which have undergone olive oil pretreatment. Expression of inflammatory markers for the 1,000,000 inoculum could not be determined (Cq>45) and was then noted ND, for non-determined, in graphs. n=1.

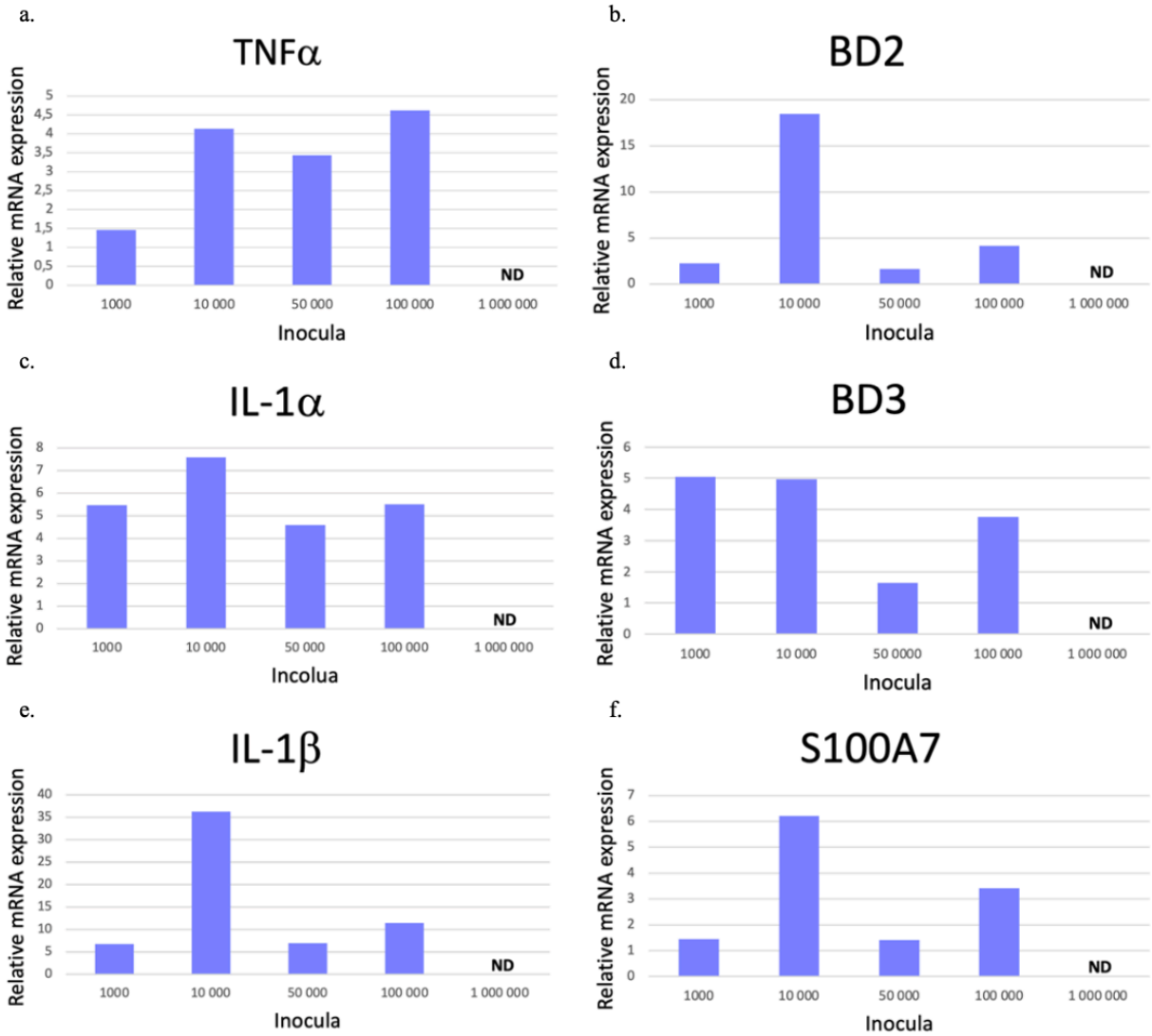

Annex 3: Periodic-Acid Schiff (PAS) staining with α-amylase treatment of histological sections of HEKa-RHE infected with *M. furfur*. HEKa (primary keratinocytes) RHE were infected with 10,000 *M. furfur* yeasts. RHE were then recovered on day four of infection, histologically processed and stained with Periodic-Acid Shiff (PAS). Arrows show fungal material.

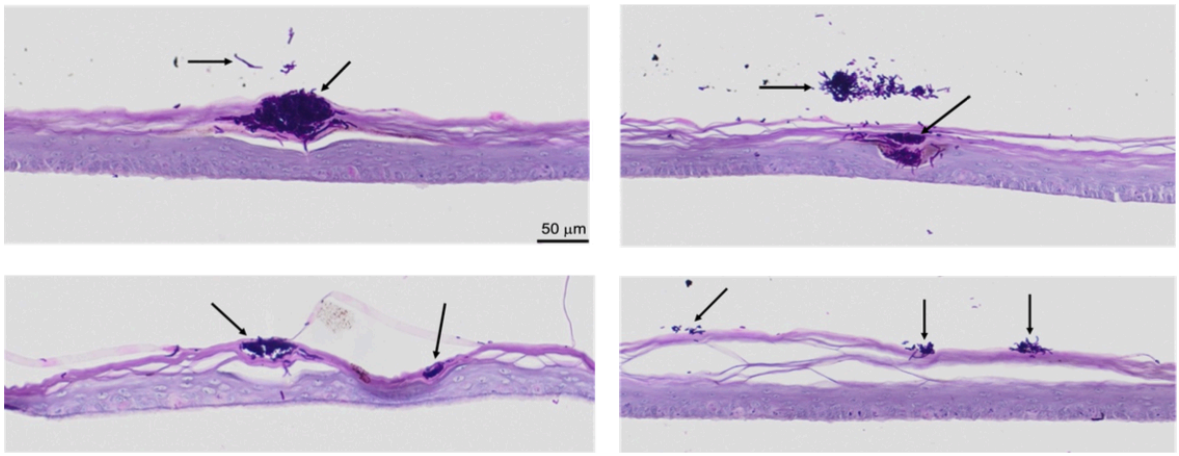

Annex 4: Relative mRNA expression of pro-inflammatory cytokines, antimicrobial peptides and TLR2 by HEKa-RHE infected with *M. furfur*. HEKa (primary keratinocytes) RHE was infected with 10,000 *M. furfur* yeasts. Infected RHE was recovered on day four of infection. Total RNA from infected and control RHE was extracted and pro-inflammatory cytokines (TNFα, IL-1α, IL-1β), antimicrobial peptides (BD2, BD3, S100A7) and TLR2 were amplified by RT-qPCR. Gene expression was normalized to RPLP0 reference gene and compared to non-infected control RHE which have undergone olive oil pretreatment. n=1.

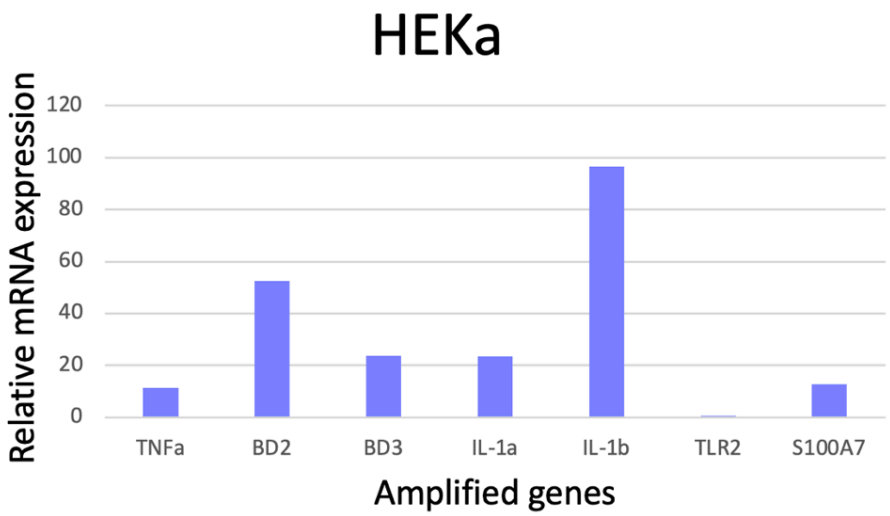

Annex 5: Inoculum verification of *T. benhamiae* infection to adapt infection on N/TERT-RHE. The inoculum was seeded on Sabouraud plate and CFUs were counted after 3 days of incubation.

Replicates	Theoretical inoculum	Real inoculum	Error percentage
n1	30 CFU	35 CFU	17 %
n2	30 CFU	45 CFU	50 %
n3	30 CFU	31 CFU	3 %

Annex 6: Periodic-Acid Schiff (PAS) staining with α-amylase treatment of histological sections of N/TERT-RHE infected by *T. benhamiae*. Unedited N/TERT-RHE were infected with 30 CFU of *T. benhamiae* and recovered each day after infection until day four. Representative pictures of two of three independent experiments (n2 and n3).

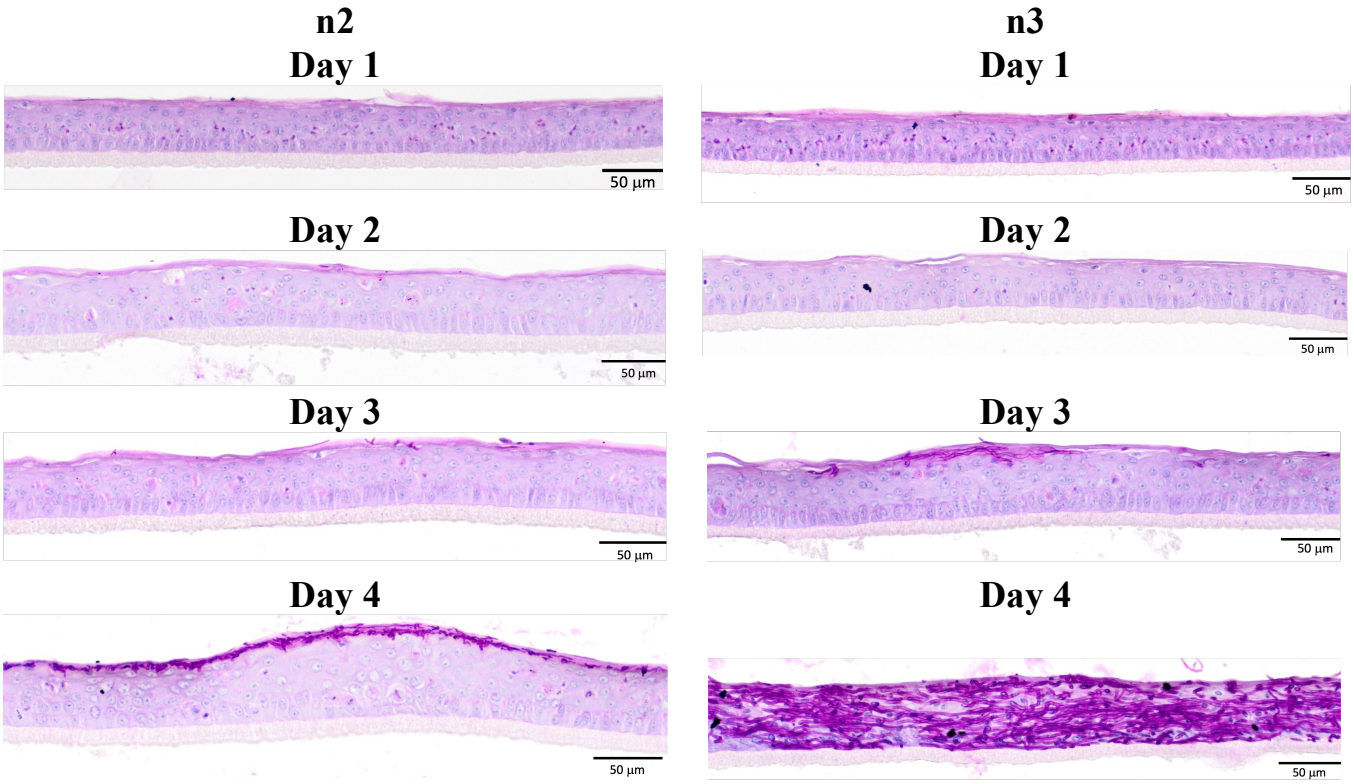

Annex 7: Inoculum verification of *T. benhamiae* infection to compare infection between N/TERT TLR2$^{+/+}$ RHE and N/TERT TLR2$^{-/-}$ RHE. The inoculum was seeded on Sabouraud plate and CFUs were counted after 3 days of incubation.

Replicates	Theoretical inoculum	Real inoculum	Error percentage
n1	30 CFU	17 CFU	43 %
n2	30 CFU	32 CFU	7 %
n3	30 CFU	22 CFU	27 %

Annex 8: Western blot analysis of protein abundance. Proteins were extracted from N/TERT TLR2$^{+/+}$ RHE and N/TERT TLR2$^{-/-}$ RHE infected with *T. benhamiae* and recovered on the third (D3) and fourth day (D4) after infection. The total and phosphorylated forms of four proteins were studied: P38, ERK, IκBα and JNK. The abundance of MyD88 was also analyzed. STAT 6 and RPL13A are loading controls. Representative images of three independent tests (n1, n2, n3). A: Infected TLR2$^{+/+}$ RHE D3, B: Infected TLR2$^{+/+}$ RHE D4, C: Control TLR2$^{+/+}$ RHE D4, D: Infected TLR2$^{-/-}$ RHE D3, E: Infected TLR2$^{-/-}$ RHE D4, F: Control TLR2$^{-/-}$ RHE D4.

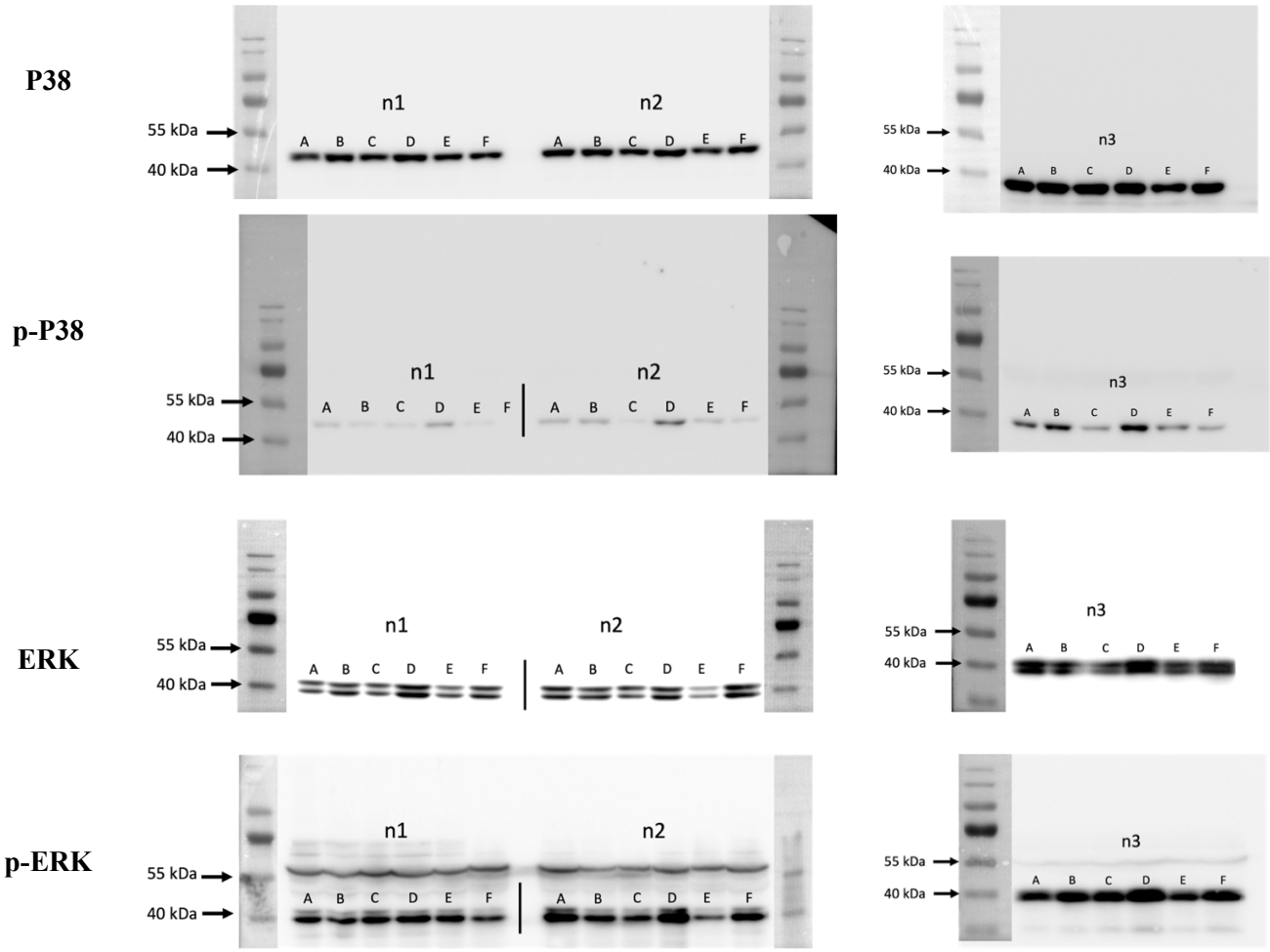

IκBα

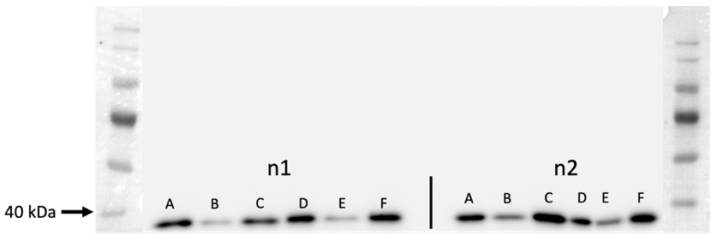

p-IκBα

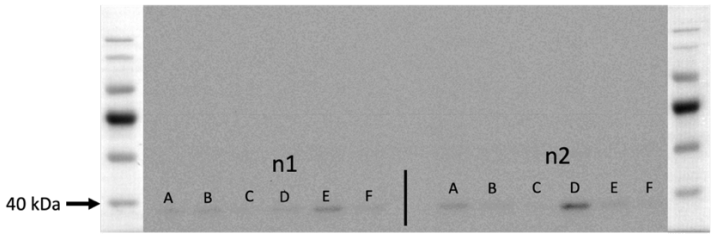

JNK

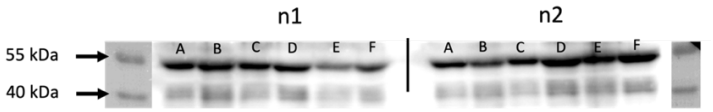

p-JNK

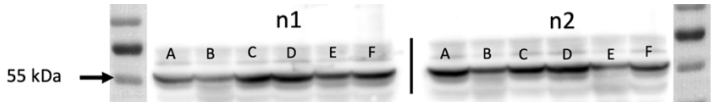

MyD88

STAT 6

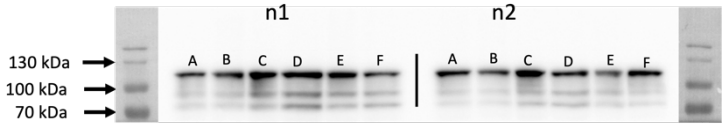

RPL13A

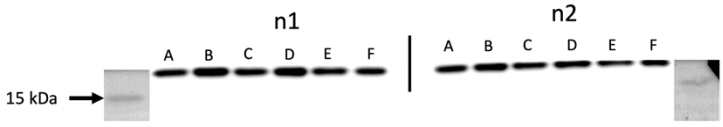

Annex 9: TLR2 immunolabeling. Labeling was performed on N/TERT TLR2$^{+/+}$ RHE and N/TERT TLR2$^{-/-}$ RHE. Two conditions were tested: with and without demasking. Nuclei were labeled with Hoechst.

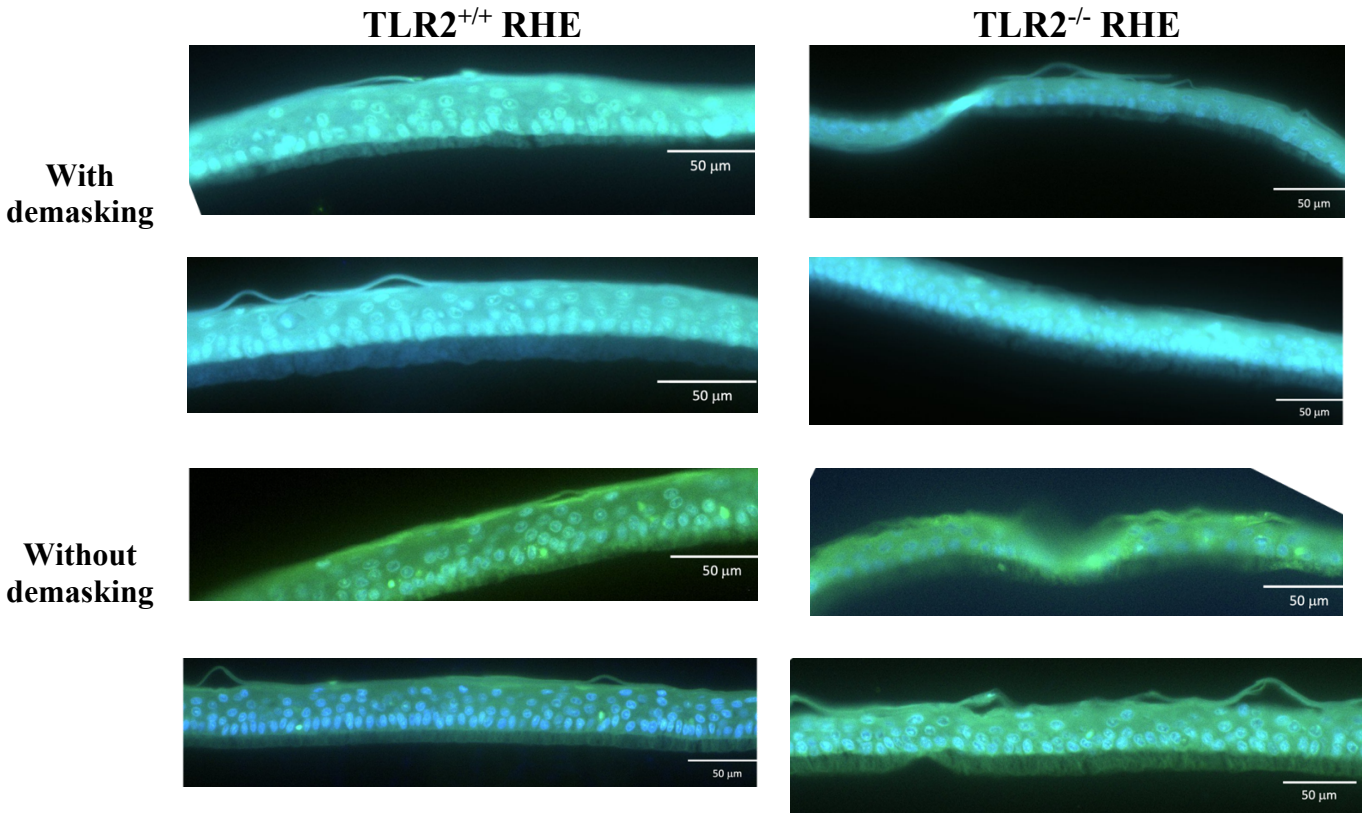

Bibliography

[1] H. Yousef, M. Alhajj, et S. Sharma, « Anatomy, Skin (Integument), Epidermis », in *StatPearls*, Treasure Island (FL): StatPearls Publishing, 2023. Consulté le: 28 août 2023. [En ligne]. Disponible sur: http://www.ncbi.nlm.nih.gov/books/NBK470464/

[2] B. Dréno, « Anatomie et physiologie de la peau et de ses annexes », *Ann. Dermatol. Vénéréologie*, vol. 136, p. S247-S251, oct. 2009, doi: 10.1016/S0151-9638(09)72527-X.

[3] « Human skin | Definition, Layers, Types, & Facts | Britannica ». Consulté le: 29 août 2023. [En ligne]. Disponible sur: https://www.britannica.com/science/human-skin

[4] A. V. Nguyen et A. M. Soulika, « The Dynamics of the Skin's Immune System », *Int. J. Mol. Sci.*, vol. 20, nº 8, p. 1811, avr. 2019, doi: 10.3390/ijms20081811.

[5] R. Wong, S. Geyer, W. Weninger, J.-C. Guimberteau, et J. K. Wong, « The dynamic anatomy and patterning of skin », *Exp. Dermatol.*, vol. 25, nº 2, p. 92-98, 2016, doi: 10.1111/exd.12832.

[6] « 12-fonction-sudorale.pdf ». Consulté le: 15 octobre 2023. [En ligne]. Disponible sur: https://www.sfdermato.org/media/pdf/formation-en-dpc/formation/12-fonction-sudorale.pdf

[7] I. M. Braverman, « The role of blood vessels and lymphatics in cutaneous inflammatory processes: an overview », *Br. J. Dermatol.*, vol. 109 Suppl 25, p. 89-98, juill. 1983.

[8] J. Khavkin et D. A. F. Ellis, « Aging Skin: Histology, Physiology, and Pathology », *Facial Plast. Surg. Clin. N. Am.*, vol. 19, nº 2, p. 229-234, mai 2011, doi: 10.1016/j.fsc.2011.04.003.

[9] C. Evrard, C. Lambert de Rouvroit, et Y. Poumay, « Epidermal Hyaluronan in Barrier Alteration-Related Disease », *Cells*, vol. 10, nº 11, p. 3096, nov. 2021, doi: 10.3390/cells10113096.

[10] G. Solanas et S. A. Benitah, « Regenerating the skin: a task for the heterogeneous stem cell pool and surrounding niche », *Nat. Rev. Mol. Cell Biol.*, vol. 14, nº 11, Art. nº 11, nov. 2013, doi: 10.1038/nrm3675.

[11] E. Goleva, E. Berdyshev, et D. Y. M. Leung, « Epithelial barrier repair and prevention of allergy », *J. Clin. Invest.*, vol. 129, nº 4, p. 1463-1474, doi: 10.1172/JCI124608.

[12] J. M. Anderson et C. M. Van Itallie, « Physiology and Function of the Tight Junction », *Cold Spring Harb. Perspect. Biol.*, vol. 1, nº 2, p. a002584, août 2009, doi: 10.1101/cshperspect.a002584.

[13] « Keratinization amy ». Consulté le: 22 octobre 2023. [En ligne]. Disponible sur: https://www.slideshare.net/AmyJoseph15/keratinization-amy

[14] M. Peschen *et al.*, « Changes of cytokeratin expression in the epidermis with chronic venous insufficiency », *VASA Z. Gefasskrankheiten*, vol. 26, nº 2, p. 76-80, mai 1997.

[15] M. Furue, « Regulation of Filaggrin, Loricrin, and Involucrin by IL-4, IL-13, IL-17A, IL-22, AHR, and NRF2: Pathogenic Implications in Atopic Dermatitis », *Int. J. Mol. Sci.*, vol. 21, nº 15, p. 5382, juill. 2020, doi: 10.3390/ijms21155382.

[16] J. Valladeau, « Les cellules de Langerhans », *médecine/sciences*, vol. 22, nº 2, p. 144-148, févr. 2006, doi: 10.1051/medsci/2006222144.

[17] G. K. Menon, G. W. Cleary, et M. E. Lane, « The structure and function of the stratum corneum », *Int. J. Pharm.*, vol. 435, nº 1, p. 3-9, oct. 2012, doi: 10.1016/j.ijpharm.2012.06.005.

[18] K. C. Madison, « Barrier Function of the Skin: "La Raison d'Être" of the Epidermis », *J. Invest. Dermatol.*, vol. 121, nº 2, p. 231-241, août 2003, doi: 10.1046/j.1523-1747.2003.12359.x.

[19] A. Kubo *et al.*, « The stratum corneum comprises three layers with distinct metal-ion barrier properties », *Sci. Rep.*, vol. 3, p. 1731, avr. 2013, doi: 10.1038/srep01731.

[20] A. F. Nikkels, N. Nikkels-Tassoudji, J. Arrese-Estrada, T. Ben Mosbah, C. Piérard-Franchimont, et G. E. Piérard, « [The cutaneous immune system and photo-aging] », *Rev. Med.*

Liege, vol. 46, nº 3, p. 158-163, mars 1991.
[21] J. van Smeden, M. Janssens, G. S. Gooris, et J. A. Bouwstra, « The important role of stratum corneum lipids for the cutaneous barrier function », *Biochim. Biophys. Acta BBA - Mol. Cell Biol. Lipids*, vol. 1841, nº 3, p. 295-313, mars 2014, doi: 10.1016/j.bbalip.2013.11.006.
[22] M. Boer, E. Duchnik, R. Maleszka, et M. Marchlewicz, « Structural and biophysical characteristics of human skin in maintaining proper epidermal barrier function », *Adv. Dermatol. Allergol. Dermatol. Alergol.*, vol. 33, nº 1, p. 1-5, févr. 2016, doi: 10.5114/pdia.2015.48037.
[23] Z. Gao, G. I. Perez-Perez, Y. Chen, et M. J. Blaser, « Quantitation of Major Human Cutaneous Bacterial and Fungal Populations », *J. Clin. Microbiol.*, vol. 48, nº 10, p. 3575-3581, oct. 2010, doi: 10.1128/JCM.00597-10.
[24] S. H. Vijaya Chandra, R. Srinivas, T. L. Dawson, et J. E. Common, « Cutaneous Malassezia: Commensal, Pathogen, or Protector? », *Front. Cell. Infect. Microbiol.*, vol. 10, p. 614446, janv. 2021, doi: 10.3389/fcimb.2020.614446.
[25] D. Zheng, T. Liwinski, et E. Elinav, « Interaction between microbiota and immunity in health and disease », *Cell Res.*, vol. 30, nº 6, p. 492-506, juin 2020, doi: 10.1038/s41422-020-0332-7.
[26] S. Hobi, C. Cafarchia, V. Romano, et V. R. Barrs, « Malassezia: Zoonotic Implications, Parallels and Differences in Colonization and Disease in Humans and Animals », *J. Fungi*, vol. 8, nº 7, p. 708, juill. 2022, doi: 10.3390/jof8070708.
[27] G. Gaitanis, P. Magiatis, M. Hantschke, I. D. Bassukas, et A. Velegraki, « The Malassezia Genus in Skin and Systemic Diseases », *Clin. Microbiol. Rev.*, vol. 25, nº 1, p. 106-141, janv. 2012, doi: 10.1128/CMR.00021-11.
[28] M. Tuor et S. LeibundGut-Landmann, « The skin mycobiome and intermicrobial interactions in the cutaneous niche », *Curr. Opin. Microbiol.*, vol. 76, p. 102381, sept. 2023, doi: 10.1016/j.mib.2023.102381.
[29] S.-H. Kim, H.-C. Ko, M.-B. Kim, K.-S. Kwon, et C.-K. Oh, « The Effect of Detergents on the Morphology and Immunomodulatory Activity of Malassezia furfur », *Ann. Dermatol.*, vol. 21, nº 2, p. 130-135, mai 2009, doi: 10.5021/ad.2009.21.2.130.
[30] T. Stalhberger *et al.*, « Chemical Organization of the Cell Wall Polysaccharide Core of Malassezia restricta », *J. Biol. Chem.*, vol. 289, nº 18, p. 12647-12656, mai 2014, doi: 10.1074/jbc.M113.547034.
[31] E. Thompson et J. R. Colvin, « Composition of the cell wall of Pityrosporum ovale (Bizzozero) Castellani and Chalmers », *Can. J. Microbiol.*, vol. 16, nº 4, p. 263-265, avr. 1970, doi: 10.1139/m70-048.
[32] L. Angiolella, S. Carradori, C. Maccallini, G. Giusiano, et C. T. Supuran, « Targeting Malassezia species for Novel Synthetic and Natural Antidandruff Agents », *Curr. Med. Chem.*, vol. 24, nº 22, p. 2392-2412, 2017, doi: 10.2174/0929867324666170404110631.
[33] H. R. Ashbee et E. G. V. Evans, « Immunology of Diseases Associated with Malassezia Species », *Clin. Microbiol. Rev.*, vol. 15, nº 1, p. 21-57, janv. 2002, doi: 10.1128/CMR.15.1.21-57.2002.
[34] I. F. Salkin et M. A. Gordon, « Polymorphism of Malassezia furfur », *Can. J. Microbiol.*, vol. 23, nº 4, p. 471-475, avr. 1977, doi: 10.1139/m77-069.
[35] I. Kurniadi, W. Hendra Wijaya, et K. H. Timotius, « Malassezia virulence factors and their role in dermatological disorders », *Acta Dermatovenerol. Alp. Pannonica Adriat.*, vol. 31, nº 2, p. 65-70, juin 2022.
[36] G. Ianiri, S. LeibundGut-Landmann, et T. L. Dawson, « Malassezia: A Commensal, Pathogen, and Mutualist of Human and Animal Skin », *Annu. Rev. Microbiol.*, vol. 76, nº 1, p. 757-782, 2022, doi: 10.1146/annurev-micro-040820-010114.
[37] F. Sparber et S. LeibundGut-Landmann, « Host Responses to Malassezia spp. in the

Mammalian Skin », *Front. Immunol.*, vol. 8, p. 1614, nov. 2017, doi: 10.3389/fimmu.2017.01614.
[38] B. Theelen, C. Cafarchia, G. Gaitanis, I. D. Bassukas, T. Boekhout, et T. L. Dawson Jr, « Malassezia ecology, pathophysiology, and treatment », *Med. Mycol.*, vol. 56, nº suppl_1, p. S10-S25, avr. 2018, doi: 10.1093/mmy/myx134.
[39] E. A. Grice et T. L. Dawson, « Host-microbe interactions: Malassezia and human skin », *Curr. Opin. Microbiol.*, vol. 40, p. 81-87, déc. 2017, doi: 10.1016/j.mib.2017.10.024.
[40] M. Glatz, P. P. Bosshard, W. Hoetzenecker, et P. Schmid-Grendelmeier, « The Role of Malassezia spp. in Atopic Dermatitis », *J. Clin. Med.*, vol. 4, nº 6, p. 1217-1228, mai 2015, doi: 10.3390/jcm4061217.
[41] G. Ianiri et J. Heitman, « Approaches for Genetic Discoveries in the Skin Commensal and Pathogenic Malassezia Yeasts », *Front. Cell. Infect. Microbiol.*, vol. 10, p. 393, août 2020, doi: 10.3389/fcimb.2020.00393.
[42] A. K. Gupta, R. Bluhm, et R. Summerbell, « Pityriasis versicolor », *J. Eur. Acad. Dermatol. Venereol. JEADV*, vol. 16, nº 1, p. 19-33, janv. 2002, doi: 10.1046/j.1468-3083.2002.00378.x.
[43] A. D. Silverio, C. Zeccara, F. Serra, S. Ubezio, et M. Mosca, « Pityriasis versicolor in a newborn Pityriasis versicolor bei einem Neugeborenen », *Mycoses*, vol. 38, nº 5-6, p. 227-228, 1995, doi: 10.1111/j.1439-0507.1995.tb00055.x.
[44] A. Di Silverio, M. Mosca, G. Brandozzi, et M. Gatti, « Pityriasis versicolor in the aged: a clinical investigation and epidemiological survey in 190 elderly hospitalized patients », *Mycopathologia*, vol. 105, nº 3, p. 187-190, mars 1989, doi: 10.1007/BF00437253.
[45] H. el-Hefnawi, Z. el-Gothamy, et M. Refai, « Studies on pityriasis versicolor in Egypt. I. Incidence », *Mykosen*, vol. 14, nº 5, p. 225-231, mai 1971, doi: 10.1111/j.1439-0507.1971.tb03041.x.
[46] D. M. L. Saunte, G. Gaitanis, et R. J. Hay, « Malassezia-Associated Skin Diseases, the Use of Diagnostics and Treatment », *Front. Cell. Infect. Microbiol.*, vol. 10, p. 112, mars 2020, doi: 10.3389/fcimb.2020.00112.
[47] R. Tao, R. Li, et R. Wang, « Skin microbiome alterations in seborrheic dermatitis and dandruff: A systematic review », *Exp. Dermatol.*, vol. 30, nº 10, p. 1546-1553, oct. 2021, doi: 10.1111/exd.14450.
[48] T. L. Dawson, « Malassezia globosa and restricta: Breakthrough Understanding of the Etiology and Treatment of Dandruff and Seborrheic Dermatitis through Whole-Genome Analysis », *J. Investig. Dermatol. Symp. Proc.*, vol. 12, nº 2, p. 15-19, déc. 2007, doi: 10.1038/sj.jidsymp.5650049.
[49] J. L. Burton et R. J. Pye, « Seborrhoea is not a feature of seborrhoeic dermatitis. », *Br. Med. J. Clin. Res. Ed*, vol. 286, nº 6372, p. 1169-1170, avr. 1983.
[50] J. A. COTTERILL, W. J. CUNLIFFE, B. WILLIAMSON, et L. BULUSU, « AGE AND SEX VARIATION IN SKIN SURFACE LIPID COMPOSITION AND SEBUM EXCRETION RATE », *Br. J. Dermatol.*, vol. 87, nº 4, p. 333-340, oct. 1972, doi: 10.1111/j.1365-2133.1972.tb07419.x.
[51] X. Hou, Z. Wei, C. C. Zouboulis, et Q. Ju, « Aging in the sebaceous gland », *Front. Cell Dev. Biol.*, vol. 10, p. 909694, août 2022, doi: 10.3389/fcell.2022.909694.
[52] G. W. Clark, S. M. Pope, et K. A. Jaboori, « Diagnosis and Treatment of Seborrheic Dermatitis », *Am. Fam. Physician*, vol. 91, nº 3, p. 185-190, févr. 2015.
[53] T. L. Dawson, « Malassezia globosa and restricta: breakthrough understanding of the etiology and treatment of dandruff and seborrheic dermatitis through whole-genome analysis », *J. Investig. Dermatol. Symp. Proc.*, vol. 12, nº 2, p. 15-19, déc. 2007, doi: 10.1038/sj.jidsymp.5650049.
[54] J. P. Z. Goh *et al.*, « The human pathobiont Malassezia furfur secreted protease Mfsap1

regulates cell dispersal and exacerbates skin inflammation », *Proc. Natl. Acad. Sci. U. S. A.*, vol. 119, nº 49, p. e2212533119, doi: 10.1073/pnas.2212533119.
[55] R. M. Rubenstein et S. A. Malerich, « Malassezia (Pityrosporum) Folliculitis », *J. Clin. Aesthetic Dermatol.*, vol. 7, nº 3, p. 37-41, mars 2014.
[56] B. S. Potter, C. F. Burgoon, et W. C. Johnson, « Pityrosporum folliculitis. Report of seven cases and review of the Pityrosporum organism relative to cutaneous disease », *Arch. Dermatol.*, vol. 107, nº 3, p. 388-391, mars 1973, doi: 10.1001/archderm.107.3.388.
[57] S. Nutten, « Atopic dermatitis: global epidemiology and risk factors », *Ann. Nutr. Metab.*, vol. 66 Suppl 1, p. 8-16, 2015, doi: 10.1159/000370220.
[58] S. Weidinger et N. Novak, « Atopic dermatitis », *The Lancet*, vol. 387, nº 10023, p. 1109-1122, mars 2016, doi: 10.1016/S0140-6736(15)00149-X.
[59] P. Pavel *et al.*, « Peroxisomal Fatty Acid Oxidation and Glycolysis Are Triggered in Mouse Models of Lesional Atopic Dermatitis », *JID Innov.*, vol. 1, nº 3, p. 100033, juin 2021, doi: 10.1016/j.xjidi.2021.100033.
[60] A. De Benedetto, A. Kubo, et L. A. Beck, « Skin Barrier Disruption - A Requirement for Allergen Sensitization? », *J. Invest. Dermatol.*, vol. 132, nº 3 0 2, p. 949-963, mars 2012, doi: 10.1038/jid.2011.435.
[61] B. S. Baker, « The role of microorganisms in atopic dermatitis », *Clin. Exp. Immunol.*, vol. 144, nº 1, p. 1-9, avr. 2006, doi: 10.1111/j.1365-2249.2005.02980.x.
[62] T. C. White *et al.*, « Fungi on the Skin: Dermatophytes and Malassezia », *Cold Spring Harb. Perspect. Med.*, vol. 4, nº 8, p. a019802, août 2014, doi: 10.1101/cshperspect.a019802.
[63] I. Weitzman et R. C. Summerbell, « The dermatophytes. », *Clin. Microbiol. Rev.*, vol. 8, nº 2, p. 240-259, avr. 1995.
[64] L. Brescini, S. Fioriti, G. Morroni, et F. Barchiesi, « Antifungal Combinations in Dermatophytes », *J. Fungi*, vol. 7, nº 9, p. 727, sept. 2021, doi: 10.3390/jof7090727.
[65] Y. Gräser *et al.*, « New insights in dermatophyte research », *Med. Mycol.*, vol. 56, nº suppl_1, p. 2-9, avr. 2018, doi: 10.1093/mmy/myx141.
[66] É. Faway, C. Lambert de Rouvroit, et Y. Poumay, « In vitro models of dermatophyte infection to investigate epidermal barrier alterations », *Exp. Dermatol.*, vol. 27, nº 8, p. 915-922, août 2018, doi: 10.1111/exd.13726.
[67] J. W. Deacon, *Fungal Biology*. John Wiley & Sons, 2005.
[68] « 16_IMAGES ». Consulté le: 19 octobre 2023. [En ligne]. Disponible sur: http://archive.bio.ed.ac.uk/jdeacon/FungalBiology/chap16_i.htm
[69] P. Zhan et W. Liu, « The Changing Face of Dermatophytic Infections Worldwide », *Mycopathologia*, vol. 182, nº 1-2, p. 77-86, févr. 2017, doi: 10.1007/s11046-016-0082-8.
[70] P. Nenoff, C. Krüger, J. Schaller, G. Ginter-Hanselmayer, R. Schulte-Beerbühl, et H.-J. Tietz, « Mycology - an update part 2: dermatomycoses: clinical picture and diagnostics », *J. Dtsch. Dermatol. Ges. J. Ger. Soc. Dermatol. JDDG*, vol. 12, nº 9, p. 749-777, sept. 2014, doi: 10.1111/ddg.12420.
[71] M. M. Pippin, M. L. Madden, et M. Das, « Tinea Cruris », in *StatPearls*, Treasure Island (FL): StatPearls Publishing, 2023. Consulté le: 17 novembre 2023. [En ligne]. Disponible sur: http://www.ncbi.nlm.nih.gov/books/NBK554602/
[72] M. J. Chamorro et S. A. House, « Tinea Manuum », in *StatPearls*, Treasure Island (FL): StatPearls Publishing, 2023. Consulté le: 17 novembre 2023. [En ligne]. Disponible sur: http://www.ncbi.nlm.nih.gov/books/NBK559048/
[73] J. W. Ely, S. Rosenfeld, et M. S. Stone, « Diagnosis and Management of Tinea Infections », *Am. Fam. Physician*, vol. 90, nº 10, p. 702-711, nov. 2014.
[74] D. Asz-Sigall, A. Tosti, et R. Arenas, « Tinea Unguium: Diagnosis and Treatment in Practice », *Mycopathologia*, vol. 182, nº 1, p. 95-100, févr. 2017, doi: 10.1007/s11046-016-0078-4.

[75] A. Zagnoli, B. Chevalier, et B. Sassolas, « Dermatophyties et dermatophytes », *EMC - Pédiatrie*, vol. 2, nº 1, p. 96-115, févr. 2005, doi: 10.1016/j.emcped.2004.05.001.
[76] R. Bellmann et P. Smuszkiewicz, « Pharmacokinetics of antifungal drugs: practical implications for optimized treatment of patients », *Infection*, vol. 45, nº 6, p. 737-779, 2017, doi: 10.1007/s15010-017-1042-z.
[77] R. Sacheli et M.-P. Hayette, « Antifungal Resistance in Dermatophytes: Genetic Considerations, Clinical Presentations and Alternative Therapies », *J. Fungi*, vol. 7, nº 11, p. 983, nov. 2021, doi: 10.3390/jof7110983.
[78] R. Iatta, L. A. Figueredo, M. T. Montagna, D. Otranto, et C. Cafarchia, « In vitro antifungal susceptibility of Malassezia furfur from bloodstream infections », *J. Med. Microbiol.*, vol. 63, nº Pt 11, p. 1467-1473, nov. 2014, doi: 10.1099/jmm.0.078709-0.
[79] A. Khurana, K. Sardana, et A. Chowdhary, « Antifungal resistance in dermatophytes: Recent trends and therapeutic implications », *Fungal Genet. Biol. FG B*, vol. 132, p. 103255, nov. 2019, doi: 10.1016/j.fgb.2019.103255.
[80] D. S. Perlin, E. Shor, et Y. Zhao, « Update on Antifungal Drug Resistance », *Curr. Clin. Microbiol. Rep.*, vol. 2, nº 2, p. 84-95, juin 2015, doi: 10.1007/s40588-015-0015-1.
[81] N. M. Martinez-Rossi *et al.*, « Dermatophyte Resistance to Antifungal Drugs: Mechanisms and Prospectus », *Front. Microbiol.*, vol. 9, p. 1108, mai 2018, doi: 10.3389/fmicb.2018.01108.
[82] A. k. Gupta *et al.*, « Onychomycosis: a review », *J. Eur. Acad. Dermatol. Venereol.*, vol. 34, nº 9, p. 1972-1990, 2020, doi: 10.1111/jdv.16394.
[83] E. T. Băguţ *et al.*, « Subtilisin Sub3 is involved in adherence of Microsporum canis to human and animal epidermis », *Vet. Microbiol.*, vol. 160, nº 3, p. 413-419, déc. 2012, doi: 10.1016/j.vetmic.2012.06.011.
[84] T. A. Bitencourt *et al.*, « Extracellular Vesicles From the Dermatophyte Trichophyton interdigitale Modulate Macrophage and Keratinocyte Functions », *Front. Immunol.*, vol. 9, p. 2343, oct. 2018, doi: 10.3389/fimmu.2018.02343.
[85] Y.-J. Zhang *et al.*, « Extracellular vesicles derived from Malassezia furfur stimulate IL-6 production in keratinocytes as demonstrated in in vitro and in vivo models », *J. Dermatol. Sci.*, vol. 93, nº 3, p. 168-175, mars 2019, doi: 10.1016/j.jdermsci.2019.03.001.
[86] F. Sparber, F. Ruchti, et S. LeibundGut-Landmann, « Host Immunity to Malassezia in Health and Disease », *Front. Cell. Infect. Microbiol.*, vol. 10, p. 198, mai 2020, doi: 10.3389/fcimb.2020.00198.
[87] F. Ruchti et S. LeibundGut-Landmann, « New insights into immunity to skin fungi shape our understanding of health and disease », *Parasite Immunol.*, vol. 45, nº 2, p. e12948, févr. 2023, doi: 10.1111/pim.12948.
[88] A. Baroni *et al.*, « Toll-like receptor 2 (TLR2) mediates intracellular signalling in human keratinocytes in response to Malassezia furfur », *Arch. Dermatol. Res.*, vol. 297, nº 7, p. 280-288, janv. 2006, doi: 10.1007/s00403-005-0594-4.
[89] B. M. Henrick, X.-D. Yao, A. Y. Taha, J. B. German, et K. L. Rosenthal, « Insights into Soluble Toll-Like Receptor 2 as a Downregulator of Virally Induced Inflammation », *Front. Immunol.*, vol. 7, p. 291, août 2016, doi: 10.3389/fimmu.2016.00291.
[90] G. A. Celestrino, A. P. C. Reis, P. R. Criado, G. Benard, et M. G. T. Sousa, « Trichophyton rubrum Elicits Phagocytic and Pro-inflammatory Responses in Human Monocytes Through Toll-Like Receptor 2 », *Front. Microbiol.*, vol. 10, p. 2589, nov. 2019, doi: 10.3389/fmicb.2019.02589.
[91] H. S. Goodridge et D. M. Underhill, « Fungal Recognition by TLR2 and Dectin-1 », in *Toll-Like Receptors (TLRs) and Innate Immunity*, S. Bauer et G. Hartmann, Éd., in Handbook of Experimental Pharmacology. , Berlin, Heidelberg: Springer, 2008, p. 87-109. doi: 10.1007/978-3-540-72167-3_5.

[92] P. V. Borges *et al.*, « Protective effect of gedunin on TLR-mediated inflammation by modulation of inflammasome activation and cytokine production: Evidence of a multitarget compound », *Pharmacol. Res.*, vol. 115, p. 65-77, janv. 2017, doi: 10.1016/j.phrs.2016.09.015.
[93] C. B. de Oliveira *et al.*, « TOLL-LIKE RECEPTORS (TLR) 2 AND 4 EXPRESSION OF KERATINOCYTES FROM PATIENTS WITH LOCALIZED AND DISSEMINATED DERMATOPHYTOSIS », *Rev. Inst. Med. Trop. São Paulo*, vol. 57, nº 1, p. 57-61, 2015, doi: 10.1590/S0036-46652015000100008.
[94] W. Hu et H. P. Spaink, « The Role of TLR2 in Infectious Diseases Caused by Mycobacteria: From Cell Biology to Therapeutic Target », *Biology*, vol. 11, nº 2, p. 246, févr. 2022, doi: 10.3390/biology11020246.
[95] M. Essakalli, O. Atouf, N. Bennani, N. Benseffaj, S. Ouadghiri, et C. Brick, « Toll-like récepteurs », *Pathol. Biol.*, vol. 57, nº 5, p. 430-438, juill. 2009, doi: 10.1016/j.patbio.2008.04.003.
[96] A. Gopalakrishnan et P. Salgame, « "Toll-like receptor 2 in host defense against Mycobacterium tuberculosis: To be or not to be-that is the question" », *Curr. Opin. Immunol.*, vol. 42, p. 76-82, oct. 2016, doi: 10.1016/j.coi.2016.06.003.
[97] A. Piermattei *et al.*, « Toll-Like Receptor 2 Mediates In Vivo Pro- and Anti-inflammatory Effects of Mycobacterium Tuberculosis and Modulates Autoimmune Encephalomyelitis », *Front. Immunol.*, vol. 7, p. 191, mai 2016, doi: 10.3389/fimmu.2016.00191.
[98] A. Tjärnlund, E. Guirado, E. Julián, P.-J. Cardona, et C. Fernández, « Determinant role for Toll-like receptor signalling in acute mycobacterial infection in the respiratory tract », *Microbes Infect.*, vol. 8, nº 7, p. 1790-1800, juin 2006, doi: 10.1016/j.micinf.2006.02.017.
[99] S. Thoma-Uszynski *et al.*, « Induction of Direct Antimicrobial Activity Through Mammalian Toll-Like Receptors », *Science*, vol. 291, nº 5508, p. 1544-1547, févr. 2001, doi: 10.1126/science.291.5508.1544.
[100] L. Chen et L. A. DiPietro, « Toll-Like Receptor Function in Acute Wounds », *Adv. Wound Care*, vol. 6, nº 10, p. 344-355, oct. 2017, doi: 10.1089/wound.2017.0734.
[101] S.-Q. Ma, H.-L. Wei, et X. Zhang, « TLR2 regulates allergic airway inflammation through NF-κB and MAPK signaling pathways in asthmatic mice », *Eur. Rev. Med. Pharmacol. Sci.*, vol. 22, nº 10, p. 3138-3146, mai 2018, doi: 10.26355/eurrev_201805_15073.
[102] Z. Su, W. Deng, S. Zhan, M. Li, S. Yin, et J. Chen, « Human and mouse TLR2 results in different activation of p38 and JNK signal pathway in HaCaT infected by Trichophyton rubrum and Microsporum canis », *Front. Immunol.*, vol. 13, p. 1063443, janv. 2023, doi: 10.3389/fimmu.2022.1063443.
[103] D. de F. Almeida *et al.*, « TLR2−/− Mice Display Increased Clearance of Dermatophyte Trichophyton mentagrophytes in the Setting of Hyperglycemia », *Front. Cell. Infect. Microbiol.*, vol. 7, p. 8, janv. 2017, doi: 10.3389/fcimb.2017.00008.
[104] E. De Vuyst, C. Charlier, S. Giltaire, V. De Glas, C. L. de Rouvroit, et Y. Poumay, « Reconstruction of Normal and Pathological Human Epidermis on Polycarbonate Filter », in *Epidermal Cells: Methods and Protocols*, K. Turksen, Éd., in Methods in Molecular Biology. , New York, NY: Springer, 2014, p. 191-201. doi: 10.1007/7651_2013_40.
[105] Y. Poumay, F. Dupont, S. Marcoux, M. Leclercq-Smekens, M. Hérin, et A. Coquette, « A simple reconstructed human epidermis: preparation of the culture model and utilization in in vitro studies », *Arch. Dermatol. Res.*, vol. 296, nº 5, p. 203-211, oct. 2004, doi: 10.1007/s00403-004-0507-y.
[106] M. Meyer, « Processing of collagen based biomaterials and the resulting materials properties », *Biomed. Eng. OnLine*, vol. 18, p. 24, mars 2019, doi: 10.1186/s12938-019-0647-0.
[107] E. Faway *et al.*, « Responses of Reconstructed Human Epidermis to Trichophyton

rubrum Infection and Impairment of Infection by the Inhibitor PD169316 », *J. Invest. Dermatol.*, vol. 139, nº 10, p. 2080-2089.e6, oct. 2019, doi: 10.1016/j.jid.2019.03.1147.
[108] É. Faway, L. Cambier, B. Mignon, Y. Poumay, et C. Lambert de Rouvroit, « Modeling dermatophytosis in reconstructed human epidermis: A new tool to study infection mechanisms and to test antifungal agents », *Med. Mycol.*, vol. 55, nº 5, p. 485-494, juill. 2017, doi: 10.1093/mmy/myw111.
[109] M. A. Dickson *et al.*, « Human Keratinocytes That Express hTERT and Also Bypass a p16INK4a-Enforced Mechanism That Limits Life Span Become Immortal yet Retain Normal Growth and Differentiation Characteristics », *Mol. Cell. Biol.*, vol. 20, nº 4, p. 1436-1447, févr. 2000.
[110] M. C. Moran, R. P. Pandya, K. A. Leffler, T. Yoshida, L. A. Beck, et M. G. Brewer, « Characterization of Human Keratinocyte Cell Lines for Barrier Studies », *JID Innov.*, vol. 1, nº 2, p. 100018, avr. 2021, doi: 10.1016/j.xjidi.2021.100018.
[111] J. P. H. Smits *et al.*, « Immortalized N/TERT keratinocytes as an alternative cell source in 3D human epidermal models », *Sci. Rep.*, vol. 7, p. 11838, sept. 2017, doi: 10.1038/s41598-017-12041-y.
[112] E. Faway *et al.*, « Towards a Standardized Procedure for the Production of Infective Spores to Study the Pathogenesis of Dermatophytosis », *J. Fungi*, vol. 7, nº 12, p. 1029, nov. 2021, doi: 10.3390/jof7121029.
[113] A. Progneaux *et al.*, « Keratinocytes activated by IL-4/IL-13 express IL-2Rγ with consequences on epidermal barrier function », *Exp. Dermatol.*, vol. 32, nº 5, p. 660-670, mai 2023, doi: 10.1111/exd.14749.
[114] B. Raut, L.-J. Chen, T. Hori, et H. Kaji, « An Open-Source Add-On EVOM® Device for Real-Time Transepithelial/Endothelial Electrical Resistance Measurements in Multiple Transwell Samples », *Micromachines*, vol. 12, nº 3, p. 282, mars 2021, doi: 10.3390/mi12030282.
[115] L. S. Miller, « Toll-like receptors in skin », *Adv. Dermatol.*, vol. 24, p. 71-87, 2008, doi: 10.1016/j.yadr.2008.09.004.
[116] B. N. Gantner, R. M. Simmons, S. J. Canavera, S. Akira, et D. M. Underhill, « Collaborative Induction of Inflammatory Responses by Dectin-1 and Toll-like Receptor 2 », *J. Exp. Med.*, vol. 197, nº 9, p. 1107-1117, mai 2003, doi: 10.1084/jem.20021787.